Journal of the
OPTICAL SOCIETY
of AMERICA

VOLUME 29 SEPTEMBER, 1939 NUMBER 9

The Dispersion Due to Weak Absorption Bands

KARL F. HERZFELD
Catholic University of America, Washington, D. C.
(Received July 21, 1939)

The evaluation of the transition probability or the electron number from absorption measurements is difficult for weak bands with background absorption. Here the formulae are developed to evaluate this quantity from the difference in height of maximum and minimum of the dispersion curve.

INTRODUCTION

An absorption or emission band is characterized not only by its wave-length, but also by the transition probability, from which we can get valuable information about the type of transition. For the infra-red, however, few data exist.[1] Most of them have been found from a measurement of the total absorption in the band, which is connected with the transition probability (for absorption) b by

$$b=\frac{1}{hN}\frac{4\pi}{c}\int\alpha_\nu d\nu, \qquad (1)$$

where N is the number of particles in 1 cc, h Planck's constant, ν the frequency, and the absorption index α defined by

$$\ln\frac{I_0}{I}=\frac{4\pi\nu\alpha_\nu}{c}x.$$

Classically one can express the transition probability by an "electron number" f,

$$b=(\pi e^2/3m'h\nu)f, \qquad (2)$$

where m' is the "reduced mass" of the absorbing oscillator (see below) and f signifies the electron number such that an oscillator with charge ef and mass $m'f$ would give an absorption equal to the observed one.[2]

It is rather difficult to evaluate (1), because of the background absorption, particularly if we investigate a weak band not very far from a strong one.

There is, however, a close connection between absorption and dispersion. Pfund has developed experimental methods, which Pittman has applied in the following paper, to measure the dispersion curve right through a weak band.

THEORY

The purpose of the present paper is to give formulae for the evaluation of the dispersion curve in the neighborhood of a weak band, so weak, that the greater part of the refractive index is due to other, much stronger bands lying

[1] For literature, see the following paper by Pittman.

[2] It seems to me that at least for the infra-red, where the absorption is due to the oscillation of known masses the quantity b would have more physical meaning if we take the effective charge as $e\sqrt{f}$ and leave m' unchanged.

BOSTON UNIVERSITY
COLLEGE OF LIBERAL ARTS
LIBRARY

at some distance. We have then

$$n^2-1=A\frac{\nu_0^2-\nu^2}{(\nu_0^2-\nu^2)^2+k^2}+F(\nu^2). \tag{3}$$

Here it is assumed that the band we consider is so weak that the absorption over the distance of one wave-length is negligible.

In (3), ν_0 is the proper frequency of the absorption band, k measures its width or the damping. It does not matter for the following whether k depends slightly on ν (usually $k=\nu'\nu$ where ν' is equal to the half-width). A is the quantity we are most interested in.

$$A=\frac{e^2N}{\pi m'}f=\frac{3N}{\pi^2}h\nu b. \tag{4}$$

Here, N is the number of molecules in 1 cc, m' the "relative mass" of the oscillator, f a dimensionless quantity, the "electron number," best used to characterize the strength of the band. If we call ρ the density, M the molecular weight of the molecule and M' the "relative molecular weight" of the oscillator (i.e., $M'=m'\times$Avogadro's number) we can write

$$A=\frac{\rho}{MM'}2.961\times10^{+7}fc^2. \tag{4'}$$

If ν is measured in wave numbers, c^2 is left out. Our purpose is to evaluate ν_0, A (or f), and k from the measurements. We do that by calculating the position and height of the maximum and minimum of the dispersion curve.

Abbreviate

$$\nu_0^2-\nu^2 \text{ by } x.$$

Then

$$n^2-1=A\frac{x}{x^2+k^2}+F(\nu_0^2-x). \tag{5}$$

The extreme values are given by

$$0=\frac{dn^2}{dx}=-A\frac{x^2-k^2}{(x^2+k^2)^2}-F'$$

or

$$x^4+x^2(2k^2+A/F')=-k^4+(A/F')k^2$$

or

$$x^2=-\left(k^2+\frac{A}{2F'}\right)\pm\left(\frac{A}{2F'}\left(\frac{A}{2F'}+4k^2\right)\right)^{\frac{1}{2}}. \tag{6}$$

As F usually increases with ν, i.e., $F'>0$, the positive sign must be taken to avoid a negative x^2, i.e., a nonreal frequency. But that is not enough. One finds in addition:

$$A>F'k^2. \tag{6'}$$

If the band is weaker than (6') expresses, the steepness of the general dispersion curves prevents the wriggle from the weak band from appearing.

If we have a well-developed maximum, we can use a power series

$$x_{1,\,2}=\mp k(1-2k^2F'/A) \tag{7}$$

or
$$x_1+x_2=0,\quad (\nu_1^2+\nu_2^2)/2=\nu_0^2, \tag{7'}$$

which expresses the fact that the frequency of the band lies midway between that of the maximum and minimum. (With the accuracy used here, we can say the same thing about the wave-length.) We will denote the maximum with the index 1, the minimum with 2.

Then

$$x_2-x_1=2k(1-2k^2F'/A) \tag{8}$$

or, by replacing x_1-x_2 approximately by $2\nu_0(\nu_1-\nu_2)$ and making another corresponding simplification

$$k=\nu_0(\nu_2-\nu_1)\{1+\nu_0(\nu_2-\nu_1)(\nu_2^2-\nu_1^2)F'/A\}. \tag{8'}$$

If we assume as before that the part of the dispersion curve which is due to the other distant absorption bands can be replaced by a straight line within our narrow weak absorption band, we find

$$(\nu_2^2-\nu_1^2)F'=F_2-F_1. \tag{9}$$

Here, F_1 and F_2 are the values of F at the place of the maximum and minimum of the dispersion curve, i.e., those values of n^2-1, which one finds by extrapolating in a straight line through the band coming from higher frequencies. They shall be denoted by $n_1^{02}-1$; $n_2^{02}-1$.

Therefore

$$k/\nu_0=(\nu_2-\nu_1)\{1+\nu_0(\nu_2-\nu_1)(F_2-F_1)/A\}. \tag{10}$$

If our band were alone present, the distance between maximum and minimum would be k/ν_0. As usually $F_1<F_2$, this distance is diminished.

The maximum and minimum values of the refractive index are found by inserting (7) into (5).

$$n_1^2-1=A/2k+F_1,$$
$$n_2^2-1=-A/2k+F_2.$$

(Apart from F_1 these are the usual formulae, but k is now not $\nu_0(\nu_2-\nu_1)$.) Therefore

$$n_1^2-n_2^2=A/k+F_1-F_2.$$

Using (10)

$$n_1^2-n_2^2=\frac{A}{\nu_0(\nu_2-\nu_1)}\left\{1-\nu_0(\nu_2-\nu_1)\frac{F_2-F_1}{A}\right\}$$
$$+(F_1-F_2)=A/\nu_0(\nu_2-\nu_1)+2(F_1-F_2). \quad (11)$$

This can be rewritten, by calling n the average value of the refractive index, and using

$$F_1-F_2=n_1^{02}-n_2^{02}=2n(n_1^0-n_2^0),$$
$$n_1^2-n_2^2=2n(n_1-n_2)$$

in the following form:

$$2n\nu_0(\nu_2-\nu_1)\{n_1-n_2-2(n_1^0-n_2^0)\}=A$$
$$=\frac{\rho}{MM'}2.961\cdot10^7 f, \quad (12)$$

using wave numbers for ν. Using wave-lengths λ

$$2n\frac{\lambda_1-\lambda_2}{\lambda_0^3}\{n_1-n_2-2(n_1^0-n_2^0)\}=A$$
$$=\frac{\rho}{MM'}0.2961f \quad (12')$$

if λ is measured in μ.

We have assumed in our development that (6′) is fulfilled with a good margin. If it is just barely fulfilled, i.e., if the band is so weak and broad that maximum and minimum only just appear, one has to use a different approximation. If one writes $A/F'=k^2+\delta$ one finds

$$x_{1,2}=\pm(\delta/3)^{\frac{1}{2}}.$$

Again ν_0 lies in the middle between maximum and minimum,

$$\nu_0(\nu_1-\nu_2)=(\delta/3)^{\frac{1}{2}}$$

gives the distance between maximum and minimum.

The refractive index in those places turns out to be

$$n^2-1=\pm\left(\frac{\delta}{3}\right)^{\frac{1}{2}}\frac{\frac{2}{3}\delta F'}{A/F'-\frac{2}{3}\delta}+F$$

or

$$n_1-n_2=\frac{2n_0^2(n_1^0-n_2^0)^2\nu_0(\nu_1-\nu_2)}{A-2n_0(n_1^0-n_2^0)\nu_0(\nu_1-\nu_2)}$$

or

$$A=2n_0(n_1^0-n_2^0)\nu_0(\nu_1-\nu_2)\left\{1+\frac{n_0(n_1^0-n_2^0)}{n_1-n_2}\right\}.$$

Infra-Red Dispersion of $CHCl_3$ and $CHBr_3$

M. A. PITTMAN*
Rowland Hall, Johns Hopkins University, Baltimore, Maryland
(Received July 21, 1939)

THE classical dispersion theories of Sellmeier, Helmholtz and Drude were based on the concepts of forced vibrations and resonance; the modern, quantum-mechanical theory of Heisenberg and Kramers, on the other hand, involves the concept of transition probabilities. Herzfeld** has elaborated on this theory and has shown how such transition probabilities may be calculated from dispersion curves. It is the purpose of this work to present numerical data on the dispersion of $CHCl_3$ and $CHBr_3$ and to make the calculation suggested by Herzfeld. From an experimental standpoint the work was difficult, since it was demanded that the dispersion be followed continuously through absorption bands. This could be accomplished only upon resorting to radiometric devices of very high sensitivity.

The apparatus consists essentially of two infra-red spectrometers in series: the first serving as a monochromator for the second with which the dispersion measurements were carried out. Since both spectrometers are of the conventional design (involving the use of Wadsworth mirrors) a description is omitted. Certain details, however, must be mentioned: from 0.5μ to 4μ a street-series tungsten lamp was employed as the source while a Nernst lamp served in the regions of greater wave-length; energies were measured with a single-junction (Pfund) vacuum thermopile connected to a low resistance Leeds and Northrup galvanometer; the concave mirrors in both spectrometers had focal lengths of about 30 cm; under all conditions the three† slits were adjusted to the same width; the slit widths varied from 0.25 mm in regions of great energy, to 1.0 mm around 8μ when the energy was feeble.

Dispersion measurements were carried out by means of hollow prisms equipped with rocksalt plates which were attached to the brass skeleton with a nitrocellulose cement. From the visible spectrum to about 4μ a prism having an angle of 60° 20′ 10″ was used; in the regions where absorption was great, a thinner prism having an angle 15° 7′ 50″ was employed. A double-walled cylindrical housing, for purposes of water-cooling, surrounded the prism; openings in the housing were covered with films of nitrocellulose so thin as to show Newton's colors.

The problem in hand demanded that the spectrometer table bearing the hollow prism be rotatable through relatively large angles and that spectrometer settings be read to 1″ of arc. Since the graduations on the spectrometer table were far too coarse, a meter (steel) scale graduated in mm. was mounted 4.8 m away from the spectrometer table and formed into an arc of the above radius. Light from this brilliantly illuminated scale proceeded to a vertical mirror mounted rigidly on the spectrometer table, thence to a fixed mirror which returned the light at a small angle to the first mirror. The light, thus twice reflected from the moving mirror, entered a telescope. Calculations showed that a motion of 1 mm on the steel scale corresponded to 10″ of arc. Since readings of 0.1 mm could be made, the desired sensitivity of 1″ of arc was realized.

As for the amplification of galvanometer deflections, it may be stated that the galvanometer connected to the thermopile was mounted on a vibration-free support of unusual stability. The deflections of this (first) galvanometer were amplified by a device due, originally, to Moll and Burger. In place of the thermopile employed by them, a Weston Photronic cell connected to a (second) high resistance galvanometer was used. Defining "absolute amplification" as the ratio of the angles through which the mirrors of the second and first galvanometer moved, and "working amplification" as the ratio of the actual deflections occasioned by the second and first galvanometers, it may be stated that, while the absolute amplification was 375, the working amplification was 1500.

* Now at Madison College, Harrisonburg, Virginia.
** Professor Herzfeld's discussion appears in this issue of the J. Opt. Soc. Am.
† The exit slit of the monochromator served as the entrance slit for the spectrometer.

To obtain measurements on the dispersion of a liquid, the procedure was briefly the following: the purity of the liquid was established by making refractive index measurements at 20°C with an Abbe refractometer and by comparing the result obtained with accepted values. A hollow rocksalt prism was then filled with the same liquid and was mounted on the table of a precision spectrometer by means of which the angle of minimum deviation for the sodium lines was determined. From this value together with the angle of minimum deviation, the prism angle was calculated—care having been taken to correct for the slightly prismatic form of the rocksalt plates. This filled prism was then remounted in the infra-red spectrometer again at minimum deviation for the Na lines. Having mounted the thermocouple at the exit slit of the spectrometer, the monochromator was adjusted so that radiation of a known wave-length was transmitted. By rotating slowly the spectrometer table bearing the liquid prism, the monochromatic beam was caused to sweep across the exit slit of this spectrometer—a situation recognized by noting galvanometer deflections. Since it was not possible to determine exactly the position of the prism corresponding to maximum galvanometer deflection, the prism was rotated slowly until the maximum has been slightly but definitely overshot and the reading on the steel scale was recorded; the rotation of the prism was then reversed so that the maximum is overshot in the opposite direction. The (steel) scale reading so found was averaged with the first for the final reading.

The liquids studied: bromoform $CHBr_3$ and

TABLE I. $CHCl_3$ *at 20°C.*

WAVE-LENGTH μ	INDEX OF REFRACTION n	WAVE-LENGTH μ	INDEX OF REFRACTION n	WAVE-LENGTH μ	INDEX OF REFRACTION n	WAVE-LENGTH μ	INDEX OF REFRACTION n
0.589	1.44621	1.54	1.43452	4.20	1.43022	8.25	1.39298
.59	1.44617	1.56	1.43445	4.26	1.42940	8.28	1.39209
.62	1.44510	1.59	1.43439	4.33	1.42900	8.30	1.43531
.63	1.44467	1.62	1.43431	4.40	1.42858	8.32	1.43829
.65	1.44417	1.63	1.43422	4.55	1.42806	8.35	1.43575
.66	1.44360	1.65	1.43429	4.70	1.42768	8.39	1.43470
.675	1.44314	1.66	1.43432	4.82	1.42768	8.42	1.43380
.69	1.44255	1.68	1.43416	4.96	1.42693	8.50	1.43186
.71	1.44207	1.70	1.43412	5.06	1.42625	8.65	1.42663
.73	1.44155	1.72	1.43405	5.17	1.42603	8.78	1.42296
.74	1.44106	1.75	1.43398	5.26	1.42543	8.95	1.41908
.76	1.44046	1.80	1.43390	5.36	1.42439	9.10	1.41579
.775	1.43994	1.88	1.43383	5.45	1.42319	9.22	1.41108
.80	1.43941	1.90	1.43376	5.50	1.42312	9.35	1.40756
.84	1.43886	1.97	1.43367	5.55	1.42252	9.45	1.40479
.855	1.43854	2.13	1.43357	5.60	1.42259	9.58	1.40345
.87	1.43820	2.25	1.43333	5.65	1.42259	9.70	1.40263
.91	1.43798	2.37	1.43308	5.70	1.42259	9.72	1.40659
.95	1.43767	2.40	1.43275	5.75	1.42259	9.75	1.40412
1.00	1.43746	2.48	1.43298	5.85	1.42185	9.77	1.40622
1.02	1.43729	2.51	1.43248	5.94	1.42828	9.80	1.40524
1.025	1.43719	2.72	1.43197	6.02	1.41855	9.95	1.40255
1.035	1.43716	2.90	1.43157	6.20	1.41609	10.00	1.40090
1.07	1.43689	3.05	1.43113	6.28	1.41522	10.18	1.39739
1.11	1.43653	3.15	1.43095	6.37	1.41436	10.30	1.39350
1.15	1.43623	3.23	1.43075	6.42	1.41250	10.42	1.38976
1.18	1.43604	3.26	1.43113	6.50	1.41250	10.55	1.38647
1.19	1.43607	3.30	1.43155	6.52	1.41243	10.65	1.38355
1.22	1.43597	3.32	1.43173	6.55	1.41227	10.75	1.37989
1.26	1.43567	3.33	1.43162	6.65	1.41205	10.88	1.37659
1.34	1.43538	3.34	1.43150	6.75	1.41900	11.00	1.37195
1.40	1.43511	3.36	1.43142	6.80	1.41916	11.10	1.36702
1.43	1.43489	3.45	1.43120	6.92	1.41834	11.20	1.36394
1.435	1.43492	3.53	1.43102	7.15	1.41571	11.32	1.36125
1.45	1.43486	3.67	1.43063	7.32	1.41123	11.42	1.35445
1.46	1.43480	3.95	1.42987	7.50	1.40697	11.55	1.35047
1.50	1.43473	4.12	1.43000	7.72	1.40352	11.65	1.34718
1.50[5]	1.43466			7.95	1.40060	11.75	1.33685
1.51	1.43456			8.15	1.39649	11.85	1.33198
1.52	1.43456			8.20	1.39649	11.95	1.32374

TABLE II. $CHBr_3$ *at 20°C.*

WAVE-LENGTH μ	INDEX OF REFRACTION n	WAVE-LENGTH μ	INDEX OF REFRACTION n
0.589	1.58900	2.40	1.56438
.59	1.58858	2.48	1.56411
.60	1.58785	2.57	1.56397
.62	1.58681	2.64	1.56372
.63	1.58576	2.72	1.56347
.65	1.58469	2.90	1.56295
.66	1.58371	2.98	1.56271
.675	1.58276	3.07	1.56247
.69	1.58168	3.14	1.56228
.71	1.58068	3.20	1.56213
.73	1.57917	3.23	1.56193
.74	1.57854	3.25	1.56204
.76	1.57756	3.315	1.56386
.775	1.57654	3.32	1.56392
.80	1.57550	3.34	1.56367
.82	1.57500	3.36	1.56353
.84	1.57449	3.45	1.56334
.855	1.57397	3.53	1.56318
.87	1.57344	3.67	1.56285
.91	1.57298	3.81	1.56241
.95	1.57252	3.95	1.56207
.975	1.57223	4.03	1.56178
1.00	1.57195	4.12	1.56148
1.02	1.57172	4.20	1.56127
1.025	1.57159	4.26	1.56142
1.03	1.57160	4.35	1.56178
1.035	1.57152	4.40	1.56163
1.05	1.57127	4.50	1.56142
1.07	1.57101	4.55	1.56112
1.11	1.57050	4.70	1.56082
1.15	1.56993	4.77	1.56051
1.19	1.56961	4.82	1.56037
1.20	1.56961	4.90	1.56030
1.22	1.56947	4.96	1.56007
1.26	1.56899	5.00	1.56015
1.30	1.56870	5.06	1.56030
1.32	1.56863	5.09	1.56044
1.34	1.56848	5.12	1.56030
1.37	1.56827	5.17	1.55962
1.40	1.56805	5.22	1.55952
1.43	1.56775	5.26	1.55952
1.435	1.56773	5.31	1.55918
1.45	1.56768	5.36	1.55880
1.46	1.56768	5.40	1.55880
1.50	1.56748	5.45	1.55873
1.505	1.56727	5.55	1.55835
1.51	1.56716	5.60	1.55827
1.52	1.56716	5.65	1.55798
1.54	1.56695	5.75	1.55768
1.56	1.56688	5.80	1.55765
1.59	1.56678	5.85	1.55730
1.62	1.56655	5.88	1.55716
1.63	1.56648	5.94	1.55716
1.66	1.56660	5.97	1.55701
1.68	1.56640	6.02	1.55671
1.70	1.56623	6.10	1.55641
1.72	1.56607	6.20	1.55582
1.75	1.56602	6.37	1.55506
1.80	1.56596	6.55	1.55417
1.88	1.56587	6.70	1.55172
1.90	1.56577	6.75	1.55200
1.97	1.56555	6.80	1.55333
2.05	1.56533	6.92	1.55223
2.13	1.56495	7.03	1.55198
2.25	1.56457	7.15	1.55174
2.30	1.56442	7.32	1.54917
2.37	1.56422	7.50	1.54754

chloroform $CHCl_3$ were obtained from the Eastman Kodak Company. As a check on the purity of these liquids, the indices of refraction, at a temperature of 20°C, were measured for sodium light by means of a hollow prism and also with the Abbe refractometer. The indices so obtained agreed with those recorded by Landolt and Börnstein.[1] These values are:

n_D 1.44621 chloroform
n_D 1.58900 bromoform.

The results obtained are presented in Tables I and II and are plotted in Figs. 1 and 2.

DISCUSSION

If one develops the classical theory of dispersion from the equation

$$m\ddot{x}+b\dot{x}+ax=eE_0e^{i\omega t} \qquad (1)$$

TABLE II (*Continued*).

WAVE-LENGTH μ	INDEX OF REFRACTION n	WAVE-LENGTH μ	INDEX OF REFRACTION n
7.55	1.54732	10.30	1.55305
7.62	1.54841	10.42	1.55216
7.67	1.54694	10.55	1.55044
7.72	1.54657	10.65	1.54925
7.78	1.54745	10.75	1.54732
7.85	1.54463	10.88	1.54575
7.95	1.54343	11.00	1.54448
8.05	1.54284	11.10	1.54320
8.10	1.54269	11.20	1.54292
8.15	1.54172	11.32	1.54119
8.35	1.53739	11.42	1.54007
8.50	1.53246	11.55	1.53814
8.55	1.53246	11.65	1.53679
8.60	1.52918	11.70	1.53545
8.65	1.51926	11.75	1.53523
8.70	1.52156	11.80	1.53433
8.78	1.51708	11.85	1.53276
8.82	1.51753	11.90	1.53254
8.87	1.55701	11.95	1.53202
8.92	1.55873	12.05	1.53008
8.95	1.57662	12.12	1.52769
8.98	1.58632	12.22	1.52582
9.02	1.59988	12.32	1.52328
9.10	1.58826	12.40	1.52209
9.22	1.57744	12.47	1.52037
9.35	1.57237	12.55	1.51806
9.45	1.56895	12.60	1.51537
9.58	1.56656	12.70	1.51186
9.70	1.56469	12.75	1.50910
9.80	1.56127	12.82	1.50633
9.95	1.55850	12.90	1.50440
10.05	1.55730	13.00	1.50149
10.18	1.55462		

[1] Landolt-Börnstein, Meyerhofen. Phys. Chem. Tab. (1905).

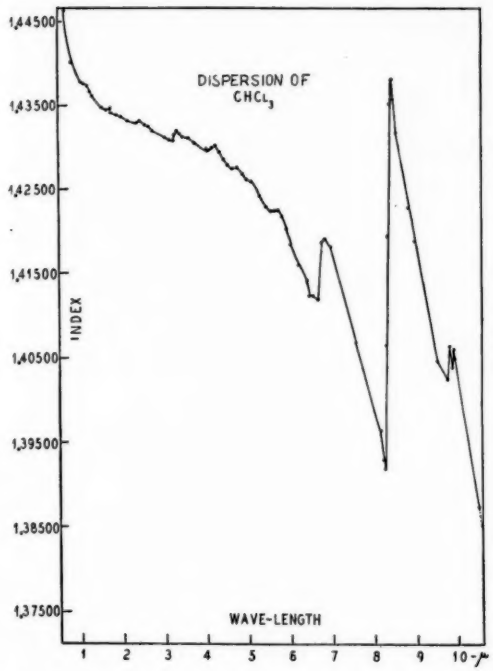

FIG. 1.

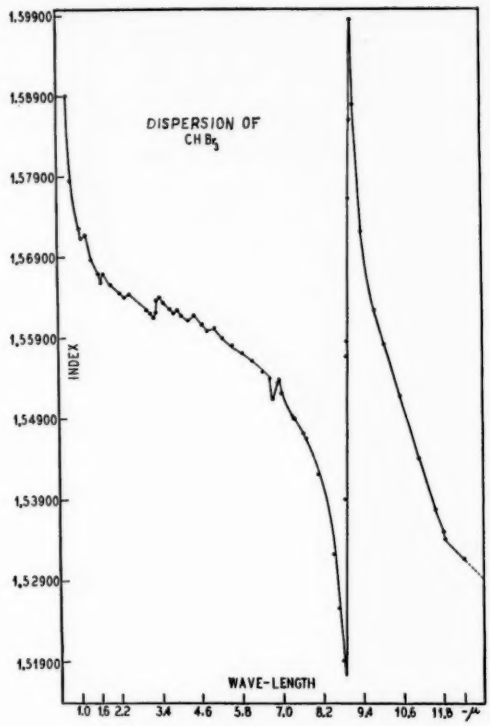

FIG. 2.

the value of the index of refraction obtained is

$$n^2=1+\sum_k \frac{(N_k e^2/\pi m)(\nu_k^2-\nu^2)}{(\nu_k^2-\nu^2)^2+(\nu b_k/2\pi m)^2}. \qquad (2)$$

If there are many absorption bands, there is a summation sign prefixed on the second term as is written. Here the symbols have meanings which are suggested in the previous equation and N_k is the number of oscillators per cm³ with a natural frequency ν_k. Since at any time we will be considering only one band, the second term in the denominator will change very slowly in the region of anomalous dispersion and will always be negligible outside. It may therefore be replaced by a constant K. Furthermore N_k can be replaced by $f_k N_0$ where the interpretation of f_k depends upon the type of band considered. If the band under consideration is due to an electronic oscillation (or transition speaking quantum-mechanically), f_k becomes the number of electrons per atom with frequency ν_k and N_0 the number of atoms per cm³. If the band is due to a vibration of an atom or group of atoms, f_k becomes the number of atoms per molecule of frequency ν_k and N_0 the number of molecules per cm³. Rewriting Eq. (2) then and focusing our attention on some individual infra-red band, the expression becomes

$$n^2=1+\frac{(N_0 e^2 f_k/\pi m')(\nu_k^2-\nu^2)}{(\nu_k^2-\nu^2)^2+K^2}+F(\nu^2), \qquad (3)$$

where $F(\nu^2)$* represents the contribution to n of all other bands far removed from the one in question. Here now m' will not be simply the mass of the atom, but will be a "reduced mass." Unlike the electronic case, infra-red bands are due to the oscillation not of a single atom, but some group of atoms for now all masses become of comparable magnitude, hence participate more evenly in a given excitation.

An equation developed from the standpoint of Eq. (1) suggests dispersion in gases. It is

* Using Herzfeld's notation.

however, well known[2] that if one considers the polarizing forces due to the surrounding atoms, a solution of exactly the same type is obtained for liquids and solids except that the ν_k of the gas is replaced by a ν_k of the liquid or solid (the latter being of smaller magnitude). It is the dispersion of liquids that shall concern us here.

To then obtain the oscillator strengths of the various bands in question it is first necessary to consider the type of a vibration responsible for them. In the case of the two molecules to be considered (chloroform and bromoform) we have a molecule of the type ZYX_3, as suggested by Dennison.[3] The addition of the Z atom (H atom) to the tetrahedral molecule creates an additional two degrees of freedom, one of which corresponds to the motion of the Z atom along the axis of symmetry and the other a bending of the Z atom with respect to the lower part of the molecule (CCl_3 or CBr_3). During these vibrations, the lower part of the molecule remains relatively undisturbed, for their absorptions lie in other regions of the spectrum. m' is then replaced by the reduced mass in which one component is the mass of the hydrogen atom and the other the mass of the remaining tetrahedral molecule. The bands at 3.28μ in chloroform and bromoform[4] and the bands at 8.4μ in chloroform and 8.8[2] in bromoform, are then associated with these vibrations. No attempt was made to evaluate the oscillator strength of the bands occurring at 6.7μ in both compounds, for their origin was not definitely known.

To then evaluate the oscillator strengths of the two bands for each compound, one proceeds as suggested in the enlarged drawing of the 3.28μ band of $CHBr_3$ (Fig. 3). If we first transpose all the components of A in Herzfeld's Eq. (12′) except the f to the opposite side of the equation, it can be written in the form

$$= 10^8 \frac{MM'}{\rho} \frac{\pi c^2}{N_L{}^2 e^2} \frac{2n(\lambda_1-\lambda_2)}{\lambda_0{}^3} \times \{n_1 = n_2 - 2(n_1{}^0 - n_2{}^0)\}, \quad (4)$$

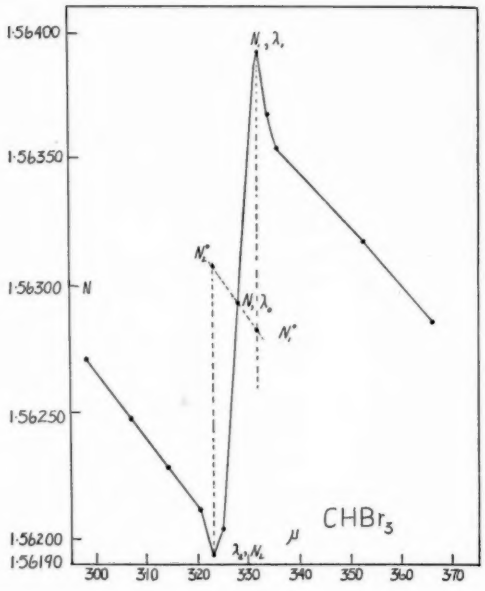

FIG. 3.

where now λ is in microns (μ). Putting in the numerical values of the constant terms, we find

$$f = 3.380 \frac{MM'}{\rho} \frac{2n(\lambda_1-\lambda_2)}{\lambda_0{}^3} \times \{n_1 - n_2 - 2(n_1{}^0 - n_2{}^0)\}, \quad (5)$$

where ρ is the density of the liquid, M its molecular weight, N_L is Avogadro's number and $M' = m'N_L$, m' is the reduced mass and is equal to $mm_H/m + m_H$ where m_H is the mass of the hydrogen atom and m the mass of the remaining tetrahedral part which can be looked upon as a unit (both m's in grams). For all practical purposes, this will be found to be very nearly equal to the mass of the hydrogen atom itself. Referring then to Fig. 3, we can find the various values of λ and n required. λ_1 and λ_2 are the wave-lengths at which the index of refraction assumes minimum and maximum values, while λ_0 is the wave-length in the middle of the region corresponding of course to the maximum of absorption. n_1, n_2, and n are, respectively, the values of the refractive indices corresponding to these three wave-lengths. $n_1{}^0$ and $n_2{}^0$ are the contributions to n_1 and n_2 from other absorption

[2] J. C. Slater and N. H. Frank, *Introduction to Theoretical Physics* (McGraw-Hill, 1933), p. 280.
[3] D. M. Dennison, Rev. Mod. Phys. **3**, 302 (1931).
[4] W. W. Coblentz, *Investigations of Infra-Red Spectra* (Carnegie Institution of Washington, 1905).
[5] J. Lecomte, *Traite de Chemie Organique* (Grignard, 1936), Vol. II, p. 197.

bands far removed from the one in question. These, as are indicated, are evaluated by extrapolating the background dispersion through the band in question and noting the value of the index of refraction at λ_1 and λ_2.

Results

From Fig. 3 then these values for the 3.28μ band of $CHBr_3$ are

$$\lambda_1=3.32\mu, \quad n_1=1.56392, \quad n_1^\circ=1.56282,$$
$$\lambda_2=3.23\mu, \quad n_2=1.56193, \quad n_2^\circ=1.56307.$$
$$\lambda_0=3.28\mu, \quad n=1.56293,$$

These when substituted in Eq. (5) yield an f value of 2.21×10^{-3}. Proceeding in a like manner we find the various oscillator strengths to be

$CHBr_3$	3.28μ	2.21×10^{-3}
$CHBr_3$	8.8μ	5.46×10^{-3}
$CHCl_3$	3.28μ	1.27×10^{-3}
$CHCl_3$	8.4μ	2.87×10^{-3}

Classically the above calculated f's represent the number of independent, linear, harmonic oscillators (atoms) per molecule contributing to the absorption band in question. When these values (as they usually are) are far from whole numbers, the interpretation usually suggested[6] is that the oscillators are anharmonic so that equivalent oscillators may vibrate at any number of given frequencies, the number depending upon the degree of anharmonicity. In either case however, should one sum the f's over all the infra-red bands for a given molecule, the resulting sum should on the basis of the above simple picture be equal to the sum of the atoms in the molecule. That the above sum rule should hold for the electronic case (approximately) is not surprising for there the electrons possess an individuality and act independently (relatively) of each other. Those interactions which do exist are small and result in fine structures of the lines. In the case of vibration spectra, the system is a much more complex one. The atom loses its individuality and becomes part of an oscillating system with many degrees of freedom of oscillation. In such a highly coupled oscillating system, the classical interpretation of the f and the f sum rule are of little value. Independently of this however, the f still maintains its quality of being a measure of the strength of absorption. For a given molecule therefore, the ratios of the f values will give the ratios of the strengths of the absorption bands.

[6] Max Born, *Optics*, p. 471.

A Mechanical Integrator for Evaluating the Integral of the Product of Two Functions and its Application to the Computation of I.C.I. Color Specifications from Spectrophotometric Curves

J. A. VAN DEN AKKER
The Institute of Paper Chemistry, Appleton, Wisconsin

(Received July 14, 1939)

INTRODUCTION

IN the spectrophotometric or "indirect" method of colorimetry, tristimulus values are obtained from spectral reflectance* of the colored sample by evaluation of the integrals,

$$X=\int_{\lambda_1}^{\lambda_2} E\bar{x}Rd\lambda, \quad Y=\int_{\lambda_1}^{\lambda_2} E\bar{y}Rd\lambda,$$

$$Z=\int_{\lambda_1}^{\lambda_2} E\bar{z}Rd\lambda, \qquad (1)$$

where X, Y, and Z are the tristimulus values, E is the spectral energy distribution of the illuminant used in viewing, $\bar{x}$, $\bar{y}$, and $\bar{z}$ are the tristimulus values of the spectrum colors as seen by the I.C.I. standard observer, R is the spectral reflectance of the sample, λ is wave-length, and λ_1 and λ_2 are the limits of the visible spectrum. Tables for $E\bar{x}$, $E\bar{y}$, and $E\bar{z}$ for the three I.C.I. standard illuminants A, B, and C are available[1,2] and hence these products in the integrals above may be replaced by the respective variables, U, V, and W. Thus the computation of colorimetric data involves the problem of integrating the product of two functions of the same independent variable. The integrals may be evaluated by the weighted ordinate method, in which the tabular values of U, V, and W at wave-lengths separated by a definite interval (e.g., 10 mμ) are multiplied into the corresponding values of R. The three columns of figures thus obtained are summed on an adding machine, and the sums become tristimulus values upon multiplication by a certain constant. This method requires too much time where data for many samples must be obtained. The time required for computation of tristimulus values and the probability of personal error have been greatly reduced by the well-known and widely used method of selected ordinates described by Hardy in 1935.[3] Three integrating mechanisms based on this method have been described,[3–5] although, as ordinarily used, the method of selected ordinates requires no equipment more elaborate than a simple adding machine. An electrical integrator designed to operate in connection with a recording spectrophotometer has been described by Razek.[6]

The determination of a tristimulus value by the selected ordinate method involves the addition of reflectances at ten, thirty, or one hundred selected wave-lengths, the choice of the number of selected ordinates depending upon the shape of the spectral reflectance curve. Hence, to obtain the three tristimulus values, thirty, ninety, or three hundred figures must be summed, and the time required for the determination naturally depends upon the complexity of the spectral reflectance curve. Where the intermediate or largest number of ordinates must be used, the method of selected ordinates leaves much room for improvement in speed. The chance for personal error is not small, and, where a recording spectrophotometer is employed, errors due to change in dimensions of the chart paper may not be negligible.*

In view of the advantages of continuous integration, it was felt desirable to design and construct a mechanical integrator which would continuously multiply two functions of the same independent variable and integrate their product.

* In this discussion "spectral reflectance" may be replaced by "spectral transmittance."

[1] D. B. Judd, J. Opt. Soc. Am. **23**, 359 (1933).

[2] A. C. Hardy, *Handbook of Colorimetry* (Cambridge, The Technology Press, 1936).

[3] A. C. Hardy, J. Opt. Soc. Am. **25**, 305 (1935). An earlier method of integration is described by this author in J. Opt. Soc. Am. **18**, 96 (1929).

[4] H. W. Swank and M. G. Mellon, J. Opt. Soc. Am. **27**, 414 (1937).

[5] F. W. Sears, J. Opt. Soc. Am. **29**, 77 (1939).

[6] J. Razek, J. Opt. Soc. Am. **24**, 54 (1934).

* Incorrect scale dimensions during recording will cause error where readings are subsequently read from the chart; however, no error due to expansion or contraction of the chart paper will enter if a suitably designed integrating mechanism is used immediately after the recording, because the scale markings are not then involved.

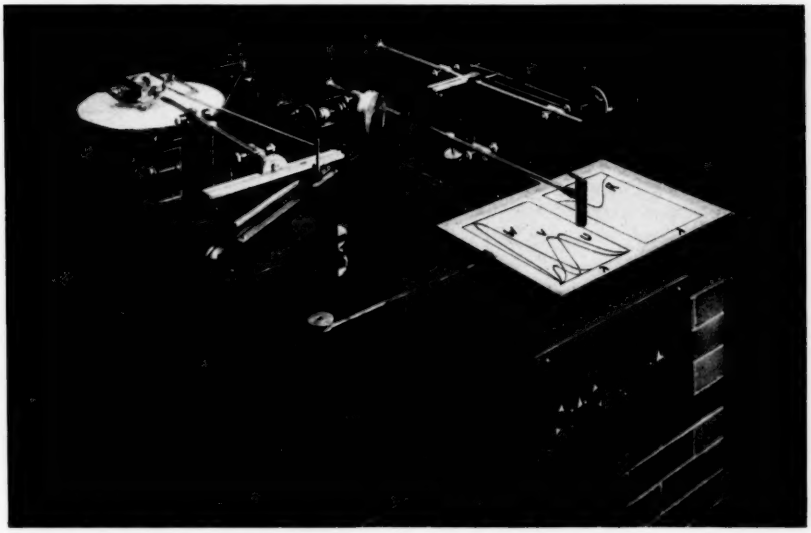

FIG. 1. Photograph of the I.P.C. mechanical integrator. This instrument is situated conveniently near a G. E. recording spectrophotometer.

Accordingly, an integrator for this purpose was designed and constructed at The Institute of Paper Chemistry. It has been used for the determination of tristimulus values from several hundred spectral-reflectance curves. Its speed, accuracy, and convenience in use have been such that a description might be of interest to the reader.

DESCRIPTION OF THE I.P.C. MECHANICAL INTEGRATOR

A photograph of the integrator, which is conveniently situated within a few feet of a General Electric Recording Spectrophotometer, is reproduced in Fig. 1. The principles of operation may be explained by reference to Fig. 2, in which a schematic drawing is presented. The chart giving U, V, and W (only U is shown) and the chart giving R *versus* wave-length are placed on a chart carrier H. This carrier is mounted on linear ball bearing races and may move parallel to the wave-length axis; its position depends upon the angular position of the disk D of an integrating unit (comprised of an integrating wheel K and the disk D). Below this disk is a drum, around which a thin metal ribbon T winds. This drum is connected to the shaft carrying the disk through a simple train of gears. The disk is driven by a small variable speed, reversible motor (shown in Fig. 1). As the disk rotates, the chart carrier is moved, and the distance x through which the carrier moves is accurately proportional to the angle θ through which the disk rotates. A clock spring at S provides a pull of nearly constant tension, which permits movement of the chart carrier from left to right.

The members A and B are follower rods which are constrained to move parallel to the y axis. A beam EOC is rotatable about an axis

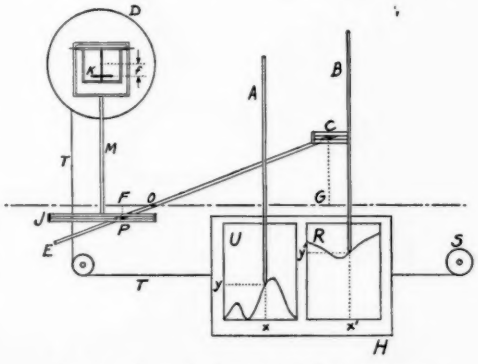

FIG. 2. Schematic drawing of the integrator.

through O and links the rod B through a roller at C, which engages a slotted member connected rigidly to B. When the rod B is moved to follow the curve R, the beam EOC rotates and, at all times, the distance CG is equal to the distance y'. A roller at P is mounted on a sliding member, so that P may move along the line EO. The sliding member is so connected to the follower rod A by a thin metal ribbon (described later) that the distance OP is at all times equal to y. A slotted member J rigidly connected to a slideable rod M engages the roller at P. The rod M connects with the frame holding the integrating wheel K, and thus the distance f between the point of contact of this wheel on the integrating disk and the center of the disk is equal at all instants to FP.

Since the right triangles OFP and OGC are similar,

$$(FP)/(OP) = (GC)/(OC). \tag{2}$$

Substituting $f = FP$, $y = OP$, $y' = GC$, and $L = OC$ = adjustable constant of the apparatus,

$$f = yy'/L. \tag{3}$$

When D rotates through an infinitesimal angle $d\theta$, the integrating wheel K rotates through $d\theta'$, and the charts move a common distance dx. If the radius of the integrating wheel is r,

$$d\theta' = (f/r)d\theta. \tag{4}$$

If k is the gear ratio of the train of gears connecting D and the drum around which T winds, and the radius of the drum is b,

$$dx = bkd\theta. \tag{5}$$

Combining Eqs. (3), (4), and (5),

$$d\theta' = (yy'/Lrbk)dx. \tag{6}$$

Now y, y', and x are actual distances (e.g., inches), so that scale factors must be introduced to relate $d\theta'$ with U, R, and λ. Let $U = hy$, $R = iy'$, and $\lambda = jx$; making these substitutions in Eq. (6), and integrating,

$$\theta' = (1/Lrbkhij)\int_{\lambda_1}^{\lambda_2} URd\lambda. \tag{7}$$

This equation states that the total angle turned through by the integrating wheel is equal to the desired integral multiplied by a constant. Since recording dials are most simply arranged to read in revolutions, n, the desired integral may be put equal to $2\pi(Lrbkhij)n$.

For maximum convenience in use, the various constants were assigned such numerical values as to make the dial readings for n numerically equal to the tristimulus values. The curves for U, V, and W were very carefully drawn with a wave-length scale of length equal to that involved in the G.E. Recording Spectrophotometer. The tabular data for U, V, and W (I.C.I. illuminant C) were adjusted so that the curve for W had a maximum value of 100.0 at 10.00 inches. With spectral reflectance at a maximum value of 100.0 at 10.00 inches (assumed reflectance of magnesium oxide), the numerical values of the integrals of UR, VR, and WR are, respectively, 473,000, 482,900, and 570,500 (with wave-length in millimicrons). The constants were so chosen that, with $R = 100.0$, the dial readings of the integrator would read $n_x = X = 98.0$, $n_y = Y = 100.0$, and $n_z = Z = 118.1$. The scale factors h, i, and j were determined from linear measurements; there was, of course, much latitude in the assignment of numerical values to the four apparatus constants, L, r, b, and k. Consideration of accuracy of integration indicates that the integrating wheel K should have large peripheral speed relative to its speed of slide toward or away from the center of the integrating disk D. This requires that the gear ratio k should be small; it was given the value 1/160 (one 80 : 1 worm and a 2 : 1 pair of spur gears). The other constants were given the values, $L = 20$ inches (adjustable), $r = 1.00$ inch, and $b = 1.414$ inches.

Mechanical Features

Reference will be made to the photograph of Fig. 1, the schematic drawing of Fig. 2, and the detailed drawing of the beam assembly given in Fig. 3. The curves are followed by means of small spot lights attached to the ends of the follower rods. These project small disks of light upon the charts and, in operation, the rods are adjusted to keep the centers of the two spots of light on the respective curves. In this way, errors due to parallax, involved where pointers are used, are avoided, and rapid operation is

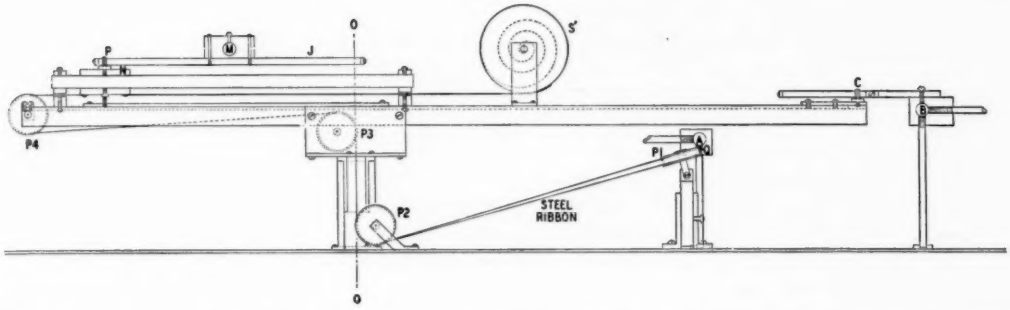

FIG. 3. Detailed drawing of the beam system showing the path taken by the steel ribbon connecting the follower rod *A* and the sliding member *N*.

made possible. (The eye can detect surprisingly small displacements of a point or line from the center of a circle.) The follower rod *B* is moved by means of a hand wheel. The other follower rod, *A*, is moved by a small variable speed, reversible motor, although this rod could also be moved by means of a hand wheel. At present the motor is so connected through a circular rheostat that, by simply rotating the rheostat, the speed of the motor may be adjusted from maximum in one direction through zero to maximum in the opposite direction. Relatively little experience is required for an operator to follow a curve accurately by this means. Both rods are equipped with mechanical stops (*see* Fig. 1) which force the rods to stop at their respective zero positions. When the rods are in their zero positions, the spot lights are quickly adjusted (if necessary) to the origins of the two charts.

The follower rod *A* moves the sliding member *N* carrying the roller *P* by means of a thin steel ribbon which connects to the rod through a hook *Q* arranged below the rod (Fig. 3). From that point, the ribbon runs along a line under and parallel to the rod to a pulley *P1*. It runs around the pulley *P1* to go in a downward path to a pulley *P2*; between these two pulleys the ribbon experiences a mild 90-degree twist. The pulley *P2* is tangent to the axis of rotation of the beam. The bearing which carries the beam is hollow, and it is through this hollow bearing that the ribbon proceeds to the beam system; after passing around pulley *P2*, the ribbon goes vertically upward through the hollow bearing, along the bearing axis. At a point approximately four inches above pulley *P2*, the ribbon meets a third pulley, *P3*, which is connected to the beam system, at a point below the beam, and so positioned that, like pulley *P2*, it is tangent to the axis of rotation of the beam. Between these two pulleys the ribbon is twisted through an angle dependent upon the instantaneous position of the beam; this twist at maximun causes no appreciable change in length of the ribbon. After a 90-degree turn about the pulley *P3*, the ribbon proceeds under the beam to the last pulley, *P4*, about which it makes a half-turn and runs to the sliding member *N*, to which it is connected. A wire proceeds from the sliding member *N* to a drum *S'*, which is mounted on the beam and contains a clock spring. This spring provides a nearly constant tension in the metal ribbon and permits motion of the sliding member toward the axis of rotation when the follower rod moves toward its zero position. (In the present design, the rod is pulled away from its zero position by the motor, and the spring *S'* provides the force required to return the rod to its zero position.) This system ensures that the displacement of the roller *P* from its zero position at *O* is at all times equal to the displacement of the follower rod *A* from its zero position.

After long continued use, sufficient play might develop in the bearing of the roller *P* and between the roller and the slotted member *J* in which it runs to cause appreciable error. Projecting below the sliding member *N* is a small roller which runs in a slotted member mounted on the beam; this constrains the sliding member

to move without rotation, and play may also develop at this roller. The spring S'' (Fig. 1) effectively eliminates play at both rollers.

The integrating disk is covered with vegetable parchment paper, which is held in place by means of several small tabs of "Scotch Tape" applied around the periphery of the paper disk. When the paper is worn through at the center, it is easily replaced by a fresh disk.

The result of an integration is read from two dials, which are connected to the integrating wheel in conventional fashion. A large dial graduated in 100 divisions gives the number of revolutions, and a drum carried by the shaft of the integrating wheel is graduated to read directly in tenths of a revolution.

Operation and Performance

With the chart carrier in its starting position (at wave-length slightly less than 400 mμ) and the dials of the integrating unit both set at zero, the rheostat controlling the integrating disk motor is set at normal speed. (When the W curve is involved the speed is set at approximately half-normal, because of the large slope of this curve, but the time required for integration is normal because only about half of the spectrum must be covered.) On starting, one operator follows the U, V, or W curve, and a second operator follows the spectrophotometric curve. The time required for one integration is approximately 55 seconds, and the three tristimulus values may be obtained in about three minutes. It has been our practice, however, to perform two integrations for each tristimulus value. This is most simply accomplished by the following procedure. First, an integration is made in the direction of increasing wave-length, and the result is recorded. Second, the integration is carried out in the opposite sense, i.e., the curves are retraced. Half of the final dial reading subtracted from the result of the first integration gives at once the average of the two determinations. The final dial reading provides a good indication of the accuracy of tracing of the curves, and this combined with a rule that both operators read the dials independently eliminates error due to blunders. Operating on this basis, the average time required to obtain the three mean tristimulus values is between five and six minutes.

The instrumental error is estimated from comparisons with the weighted ordinate and selected ordinate methods to be somewhat less than 0.2 percent. Careful integrations of U, V, and W (with R held constant at 100.0), performed at reduced speed, yield results agreeing with the ideal values to within about 0.1 percent. The personal error at normal speed of operation is surprisingly small, being of the order of 0.1 tristimulus unit (maximum reading for Y, 100 units). In a thesis work it was necessary to obtain colorimetric data for more than five hundred samples, and the student used the integrator for this purpose; he computed the mean deviations for the first 125 determinations, and found these to be 0.09, 0.08, and 0.08 tristimulus unit for the respective U, V, and W curves.

Where unusually close comparison of colorimetric data are required (as in a study of color tolerance), a special procedure is followed. The tristimulus values for one of the samples are obtained. If these are X, Y, and Z, the tristimulus values for another sample may be written as $X+\delta X$, $Y+\delta Y$, and $Z+\delta Z$. The differences δX and δY are then measured on the integrator in the following way. The differences between the two spectrophotometric curves, which are recorded on the same chart, are mentally multiplied by ten and the augmented differences are roughly plotted on the chart. A minus sign is placed in those regions corresponding to negative difference between the spectrophotometric curves, and the remaining regions are designated with the plus sign. When the integration proceeds from shorter to longer wave-lengths, the curve is followed where the difference is positive and the follower rod is kept at zero in the negative regions; during the return integration the follower rod is kept at zero in the positive regions and the curve is followed in the negative regions. The dials are read after the return integration. (A more general application of this procedure is described in the following section.) The difference curve is followed with the U and V curves only; the respective readings after division by ten are δX and δY. The color difference may then be stated in terms of δY (difference in visual efficiency), and the differences in trichromatic coefficients,

$\delta x = \delta X/(X+Y+Z)$ and $\delta y = \delta Y/(X+Y+Z)$. The differences in trichromatic coefficients are plotted on the I.C.I. mixture diagram in the usual way to obtain the differences in dominant wave-length and purity.

Heretofore, the curves for U, V, and W were drawn on chart paper. Hence the dimensions of the chart were subject to small variations occasioned by changes in relative humidity. The dimensions of the similar charts on which the spectrophotometric curves are recorded suffer similar but not exactly equal changes, and it has been necessary to make changes in L with the season of the year. A more serious consequence of change in size of the chart paper is the failure of the scale markings to be correct during the recording of the spectrophotometric curve, which causes the recorded curve to bear incorrect relationship with these markings. If, on the other hand, the U, V, and W curves are drawn upon a metal plate, and the integrator is used shortly after a recording, the result of the integration will be free of error originating in hygroexpansivity* of the paper; it is then only necessary that the chart be properly oriented on the chart carrier, namely, with the origin at the proper point and the wave-length axis coincident with the x axis of the chart carrier. The U, V, and W curves are now drawn upon an electrolytically oxidized aluminum plate, the surface of which takes ink very well and diffusely reflects light to provide good visibility.

Extension of Applicability of the Integrator

The present integrator was designed specifically for an application which involves functions having only positive values. By a simple change in design, the integrator may be used for the evaluation of definite integrals of products of two functions, either one or both of which may take on both positive and negative values. With reference to Fig. 2, it is only necessary to provide for motion of the roller P on both sides of the axis of rotation through O, and to shift M and the integrating system to the right, so that M lies over the point O. However, the integrator described herein may now be used where the functions take on both signs, if the following procedure is carried out: The absolute values of the two functions are plotted, and the regions in which the functions have the same sign are designated "plus" and the remaining regions are designated "minus." During the forward integration the curves are followed in the "plus" regions and the followers are kept at zero in the "minus" regions, but during the return integration the curves are followed in the "minus" regions and the followers are kept at zero in the "plus" regions. The dial reading after a "round trip" will then be proportional to the desired integral.

A curve giving the product of the two functions may be traced by connecting a pen to the slidable rod M of Fig. 2 and providing a means for moving the chart with the carrier H.

* A newly coined term which refers to the property some hygroscopic materials have of exhibiting change in dimensions when moisture content changes.

Acknowledgments

The writer expresses his appreciation to Mr. Carleton Root for his care in constructing the integrator and to Dr. William Foote for his kindness in checking the accuracy and reproducibility of integrations performed with the instrument.

Rectangular Uniform-Chromaticity-Scale Coordinates

F. C. Breckenridge and W. R. Schaub*
National Bureau of Standards, Washington, D. C.

(Received June 5, 1939)

The advantages and limitations of the I.C.I. coordinate system and the trilinear coordinate system yielding uniform chromaticity scales as proposed by Judd are compared. The advantages for engineering applications of a system combining rectangular coordinates with the uniform chromaticity scale (U.C.S.) are pointed out. The U.C.S. triangle is transformed to give such a system. A slight modification of the constants and a simple translation give a system of coordinates in which the first quadrant contains only greens, the second blues, the third purples and the fourth reds and yellows. The resulting diagram is compared with that obtained by MacAdam. Transformation equations for obtaining the rectangular uniform-chromaticity-scale coordinates from the I.C.I. coordinates and for the reverse transformation, the distribution coefficients for an equal-energy spectrum and for the spectrum of the Planckian radiator at 2355°K and at 2842°K, and also the ordinates to be used in computing rectangular uniform-chromaticity-scale coordinates by the Hardy selected ordinate method for a source at 2842°K are included.

I. Introduction

TRISTIMULUS specifications for colors serve in the main three purposes: they provide a means for recording color stimuli so that the corresponding colors may be reproduced at some other time or place; they afford a medium for specifying colors and color tolerances in regulations and commercial transactions; and they make it possible to visualize the relationship of colors, thus facilitating the solution of color problems. Any tristimulus coordinate system which is not ambiguous will satisfy the first of these purposes. For the second and third purposes it is highly desirable that the coordinate system be such that equal lengths on its Maxwell triangle correspond to equal chromaticity steps for an observer with normal eyes, that is, the chromaticity scale should be uniform for all colors.

The standard observer and coordinate system adopted by the International Commission on Illumination at its Cambridge meeting in 1931[1] is quite satisfactory as a means of recording color stimuli for identification. The Maxwell triangles associated with this coordinate system, however, do not have uniform chromaticity scales. The coordinates can be transformed, however, so as to yield uniform chromaticity scales without altering the characteristics of the standard observer.

Judd has published equations for transforming the I.C.I. (C.I.E. and I.B.K. in French and German, respectively) coordinate system into one yielding uniform chromaticity scales.[2] This system, sometimes called the U.C.S. system, is expressed in triangular coordinates, which for most purposes are less convenient than rectangular coordinates. In addition, the tables required for computing these coordinates directly from spectral transmission or reflection data are not available.

It is the purpose of this paper to present a coordinate system which is consistent with the I.C.I. observer, meets the requirement of uniform chromaticity scales within the limits of available criteria and is particularly adapted for the visualization of chromaticity relations. This system will be called the rectangular uniform-chromaticity-scale (R.U.C.S.) coordinate system.

II. Transformation Equations

The equations for the projective transformation of the I.C.I. coordinate system have been discussed by MacAdam.[3] The essential requirement is that any new system be obtainable from

* Deceased.

[1] D. B. Judd, "The 1931 I.C.I. Standard Observer and Coordinate System for Colorimetry," J. Opt. Soc. Am. **23**, 359 (1933).

[2] D. B. Judd, "A Maxwell Triangle Yielding Uniform Chromaticity Scales," J. Opt. Soc. Am. **25**, 24 (1935).

[3] D. L. MacAdam, "Projective Transformations of I.C.I. Color Specifications," J. Opt. Soc. Am. **27**, 294 (1937).

the I.C.I. system by the equations:

$$x'=\frac{K_{xx}x+K_{xy}y+K_{xz}}{K_xx+K_yy+K_z},$$
$$y'=\frac{K_{yx}x+K_{yy}y+K_{yz}}{K_xx+K_yy+K_z}, \qquad (1)$$
$$x'+y'+z'=1.$$

In these equations, and throughout this paper, x, y, z are trilinear coordinates in the I.C.I. system and x', y', z' are corresponding coordinates in the transformed system. The K's are arbitrary constants. The equations contain nine of these constants but by multiplying the numerators and denominators by the same factors we may make any one of the constants equal to any convenient value, such as unity, without changing the transformation. Eight degrees of freedom are, therefore, possible in the transformation from the I.C.I. to any other system representing the same standard observer. We may accordingly choose eight values of trilinear coordinates of colors specified in the I.C.I. system and adjust the K's so that the corresponding coordinates take any desired values in the new system, provided we do not choose trilinear coordinates for more than two points in any straight line.

The fixing of two points, involving the assignment of values to four coordinates, is sufficient to determine the location, orientation and scale of any given figure in a plane. The other four degrees of freedom are available to expand or contract areas of the I.C.I. Maxwell triangle or mixture diagram to obtain the desired uniform chromaticity scales. This stretching and shrinking of the I.C.I. trilinear coordinates must be such as to produce a spectrum locus of approximately the same form as obtained by Judd's transformations but it is permissible to vary the constants somewhat because all the experimental data which furnish criteria of uniform chromaticity are uncertain.

If trilinear coordinates are to be computed initially in a uniform-chromaticity-scale system, it is desirable to make the straight portion of the spectrum locus at the long-wave end coincide with one of the axes. By this alinement many of the factors in the computation take the value zero and this considerably reduces the labor of computing the coordinates. For the I.C.I. system the value of $\bar{z}$ is less than 0.00005 for all values of λ greater than 635 mμ. Simplicity of representation is gained by making the long-wave portion coincide with the y' axis, that is, we will set $x'=0$ for $z=0$.

The denominators of (1) cannot vanish for any case that is of interest. Hence, substituting in (1) and using the relation $x+y+z=1$, we have for $z=0$

$$(K_{xx}-K_{xy})x+K_{xy}+K_{xz}=0.$$

But this is true for all values of x, and consequently

$$K_{xz}=K_{xy} \quad \text{and} \quad K_{xy}=-K_{xz}. \qquad (2)$$

These two relations, therefore, make sure that the coordinate system will yield values of distribution coefficients having the largest possible proportion of zero values with consequent convenience in computation. They reduce the number of degrees of freedom from eight to six but they do not at all interfere with our purpose to obtain a uniform-chromaticity-scale system. Table I lists the fixed points selected for the evaluation of the transformation coefficients, the coordinates representing these points in the I.C.I. system, and the corresponding values chosen for the R.U.C.S. system. For comparison, the table also shows the coordinates obtained for these points by transforming Judd's U.C.S. coordinates into rectangular coordinates, without any deformation of the spectrum locus.

By substituting the coordinate values from Table I into the equations of (1) and solving for the K's we may obtain the following numerical values for them:

$$K_{xx}=+0.82303 \quad K_{yx}=+3.69700 \quad K_x=+1.00000,$$
$$K_{xy}=+0.82303 \quad K_{yy}=-5.07713 \quad K_y=-7.05336,$$
$$K_{xz}=-0.82303 \quad K_{yz}=-1.36896 \quad K_z=+1.64023.$$

TABLE I. *Fixed coordinates used for determination of transformation coefficients.*

	I.C.I.		R.U.C.S.		JUDD	
FIXED POINTS	x	y	x'	y'	x'	y'
$\lambda=780$ mμ	0.73467	0.26533	(0.000)*	0.000	0.000	0.000
Equal Energy	0.33333	0.33333	0.075	0.500	0.072	0.500
$\lambda=500$ mμ	0.00820	0.53840	(0.069)*	0.750	0.066	0.747
$\lambda=380$ mμ	0.17410	0.00500	0.450	0.500	0.423	0.488

* These values were not used in determining the transformation coefficients, but are given for comparison with the corresponding values under "Judd."

The transformation equations for obtaining trilinear coordinates in the R.U.C.S. system from trilinear coordinates expressed in the I.C.I. system is given as formula (c) in an appendix to this paper.

For the transformation of the distribution functions MacAdam gives equations in the following form:

$$\begin{aligned}\bar{x}' &= k_{xx}\bar{x}+k_{xy}\bar{y}+k_{xz}\bar{z},\\ \bar{y}' &= k_{yx}\bar{x}+k_{yy}\bar{y}+k_{yz}\bar{z},\\ \bar{z}' &= k_{zx}\bar{x}+k_{zy}\bar{y}+k_{zz}\bar{z}.\end{aligned} \tag{3}$$

The k's of (3) are related to the K's of (1) as follows:

$$\begin{aligned}k_{xx} &= K_{xx}+K_{xz}, & k_{yx} &= K_{yx}+K_{yz},\\ k_{xy} &= K_{xy}+K_{xz}, & k_{yy} &= K_{yy}+K_{yz},\\ k_{xz} &= K_{xz}, & k_{yz} &= K_{yz},\\ k_{zx} &= -K_{xx}-K_{yx}+K_x+k_{zz},\\ k_{zy} &= -K_{xy}-K_{yy}+K_y+k_{zz},\\ k_{zz} &= -K_{xz}-K_{yz}+K_z.\end{aligned} \tag{4}$$

Substituting the numerical values of the K's in (4) we get for the k's

$$\begin{aligned}k_{xx} &= 0.00000, & k_{yx} &= +2.32804, & k_{zx} &= +2.96827,\\ k_{xy} &= 0.00000, & k_{yy} &= -6.44609, & k_{zy} &= -2.24750,\\ k_{xz} &= 0.82303, & k_{yz} &= -1.36896, & k_{zz} &= +0.55176.\end{aligned}$$

The corresponding transformation equations are given by (a) in the appendix. Following the procedure given by Judd[4] we may solve these equations for $\bar{x}$, $\bar{y}$, $\bar{z}$ in terms of $\bar{x}'$, $\bar{y}'$, $\bar{z}'$ and obtain the equations for the reverse transformation given by (b) in the appendix. By the relations given in (4) we obtain the equations for transforming R.U.C.S. coordinates into I.C.I. coordinates which are given by (d) in the appendix.

In the I.C.I. system the luminosity coefficients are 0, 1, 0 and the luminous energy corresponding to a sample of radiant energy is given by the expression $\Sigma\bar{y}_\lambda E_\lambda \Delta\lambda$, in which $\bar{y}_\lambda$ is the relative luminosity of radiant energy at wave-length λ and E_λ is the radiant energy of the sample within the interval $\Delta\lambda$ multiplied by a factor to make the summation result in the desired units. But $\Sigma\bar{y}_\lambda E_\lambda \Delta\lambda \equiv \bar{y}$ and $\bar{y}$ together with $\bar{x}$ and $\bar{z}$ constitute a tristimulus specification. Hence $\bar{y}$ may be evaluated by Eq. (b) in the appendix. As a definition of the luminosity coefficients $L_{x'}$, $L_{y'}$ and $L_{z'}$ we may write

$$\bar{y} = L_{x'}\bar{x}'+L_{y'}\bar{y}'+L_{z'}\bar{z}'. \tag{5}$$

Both (5) and (b) are true for all values of $\bar{x}'$, $\bar{y}'$ and $\bar{z}'$. We may therefore identify the $L_{x'}$, $L_{y'}$ and $L_{z'}$ with the numerical coefficients of (b) as indicated by (e) in the appendix.

If the products $\bar{y}_\lambda E_\lambda$ have been multiplied by appropriate factors to make $\bar{y}$ equal the luminous energy, the reflection factor, or the transmission of a sample, the luminosity coefficients operating as in Eq. (5) will also give them. Otherwise the luminosity coefficients have only relative significance. Some labor may be saved in the computation of such quantities by making one of the luminosity coefficients equal to unity. This is accomplished by multiplying all the luminosity coefficients by the proper factor and dividing all the distribution coefficients by this same factor.

III. Explanation of Tables

The distribution functions of the I.C.I. system as given in the *Handbook of Colorimetry*[5] were adopted as a basis for the R.U.C.S. system. The application of transformation (a) to these functions yielded the distribution functions for the R.U.C.S. system which are given in the appendix. The trilinear coordinates for the spectrum locus, the weighted ordinates for light sources at 2355°K and 2842°K, and the selected ordinates for a light source at 2842°K were computed as described in the *Handbook of Colorimetry*, but with the additional adjustment to make $L_{y'}=1$. The coordinates for the Planckian locus, the equal energy spectrum, and I.C.I. illuminants B and C were computed by means of formulae (a) from the values given in the Handbook supplemented by values taken from Judd's tables.[1] All of the trilinear coordinates have been subjected to the translation described in Section IV following.

IV. The Mixture Diagram

The spectrum locus as derived from the transformation equations is located in the quadrant for which both x and y are positive with the extreme red end of the locus at $x'=0$, $y'=0$. This is

[4] D. B. Judd, "Reduction of Data on Mixture of Color Stimuli," Nat. Bur. Stand. J. Research **4**, 523 (1930); RP163.

[5] A. C. Hardy, *Handbook of Colorimetry* (Technology Press, Cambridge, Mass., 1936).

desirable for computation because it avoids negative numbers. It does not, however, give the most convenient representation of the colors. The translations,

$$x''=0.0750-x',$$
$$y''=y'-0.5000,$$

accomplish three useful results. The equal-energy point, representing a nominally achromatic stimulus, is placed at the center of the coordinate system, $x''=0$, $y''=0$; the diagram is inverted bringing the spectrum colors into the same order as has become customary through the

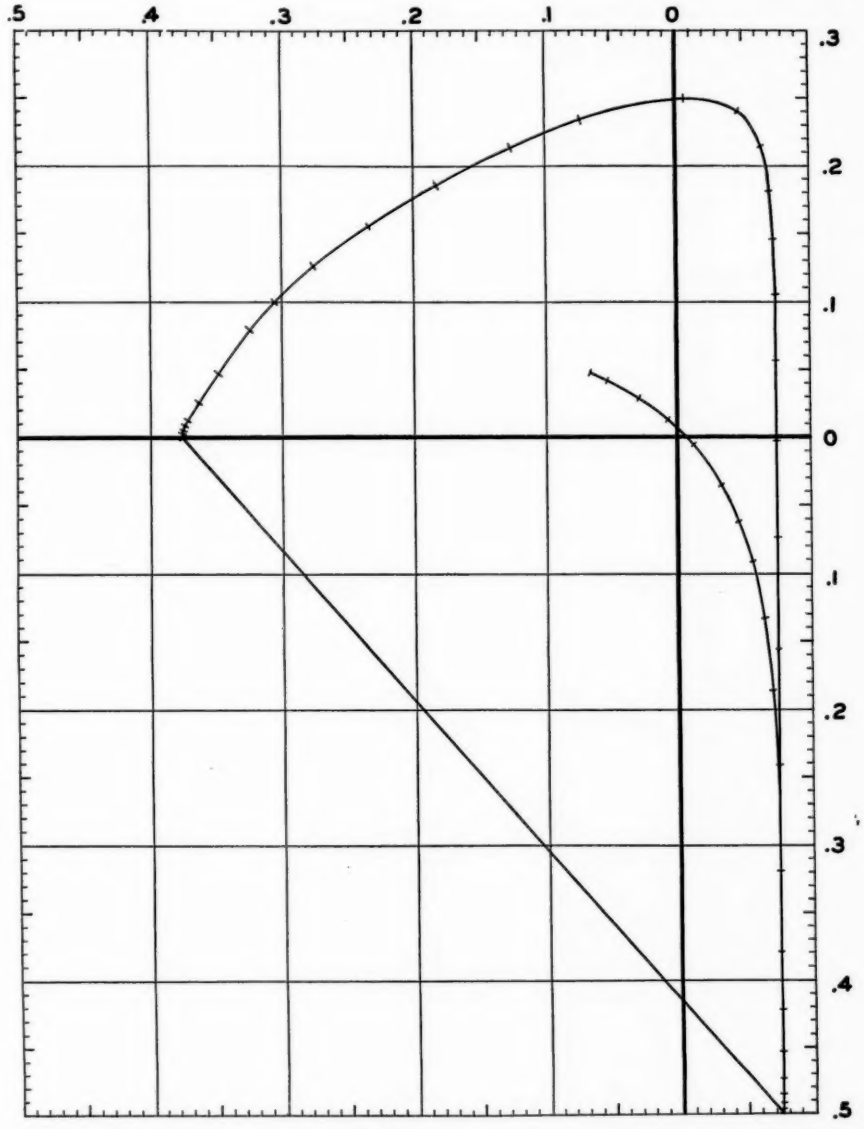

FIG. 1. The spectrum locus and Planckian locus plotted in rectangular uniform-chromaticity-scale coordinates. Nomenclature has been omitted to permit reproduction with any nomenclature desired.

use of the I.C.I. diagram; and the quadrants become significant with respect to the usual names of colors. Fig. 1 shows the R.U.C.S. diagram in this form.

The regions occupied by the several spectrum colors are indicated in the diagram by the names and arrows around the edge of Fig. 4. The segregation of the colors by quadrants is notable. The blue-green and yellow-green boundaries fall so close to the axes that we may make them coincide with the axes and keep well within a reasonable allowance for experimental uncertainty. Thus we have for an average observer normally adapted:

x'' positive, y'' negative, hue is red, orange or yellow,
x'' positive, y'' positive, hue is green,
x'' negative, y'' positive, hue is blue,
x'' negative, y'' negative, hue is purple.

Similarly the following definitions appear satisfactory:

x'' positive, $y'' < -4.444x''$, hue is red,
x'' positive, $-4.444x'' < y'' < -2.222x''$, hue is orange,
x'' positive, $-2.222x'' < y'' < 0.000$, hue is yellow.

TABLE II.

Authority	Date	Boundaries λ in mμ			
		Red Orange	Orange Yellow	Yellow Green	Green Blue
Helmholtz[a]	1866	656			
Bezold[b]	1874	656	589	558	502
Rood[c]	1890	621	588		502
Weld[d]	1932	622	597	577	492
Gage[e]	1933	625	600		
Ornstein[f]	1934	593	586	565	494
Verbeek[g]	1935	605	587	569	496
Terpstra[h]	1935	603	587	562	488
Van de Werfhorst I[i]	1935	607	590	570	
Van de Werfhorst II	1935	608	590	570	495
Average, all		619.6	590.4	567.3	495.6
Average, since 1930		609.0	591.0	568.8	493.0
Fig. 4		612	591	570	499

[a] H. v. Helmholtz, *Handbuch der Physiol. Optik* (1866), p. 236.
[b] W. v. Bezold, *Die Farbenlehre* (1874), pp. 24–27.
[c] O. N. Rood, *Modern Chromatics* (1890), p. 26.
[d] LeRoy D. Weld, "Some Observations on Spectral Color Discrimination," Iowa Acad. Sci. **39**, 209 (1932).
[e] H. P. Gage, "Report of Limits of Hue, Preliminary Draft by the Committee on Color Names" (unpublished), Inter Society Color Council (1933).
[f] L. S. Ornstein, Frl. J. G. Eymers and D. Vermeulen, "Farbenerkennungsprüfungen mit Rücksicht auf die Brauchbarkeit von Signalgläsern," Proc. Kon. Akad. v W. Amst. **37**, 385 (1934).
[g] H. P. J. Verbeek and M. L. Bazen, "Distribution of the Chief Colors in the Spectrum," Physica II, **4**, 380 (1935).
[h] J. Terpstra, quoted by J. F. Schouten, "Grundlagen einer quantitative Vierfarbentheorie I," Proc. Kon. Akad. v W. Amst. **38**, 600 (1935).
[i] G. B. van de Werfhorst, *Kleurwaardeering, Voordrachten betreffende Verlichtingskunde* ('s Gravenhage, 1937), Editor Martinus Nijhoff; p. 107–109. This paper contains data for I and II.

The intercepts of the above equations on the spectrum locus are

$$y'' = -0.3333 \quad \text{and} \quad y'' = -0.1667.$$

The extent to which these boundaries agree with the classification of spectrum colors by average observers under usual experimental conditions may be judged from Table II.

These boundary relations did not enter explicitly into the coordinates assigned for the fundamental stimuli which were used to determine the constants of the transformation equations. The coordinates were determined from the values for the selected stimuli derived from Judd's "Uniform Chromaticity Scale Triangle"[2] by adjusting the values to give integral relations. Thus, disregarding signs, the maximum negative value of y'' is twice the maximum positive value of y''; the total height of the diagram parallel to the y'' axis is ten times the maximum positive value of x'' and two times the maximum negative value of x''. While these relations have no scientific significance they are of great practical assistance in recalling the dimensions of the diagram and the limits of hues. How little adjustment was required to obtain these multiple relationships may be seen from Table I and Fig. 2.

In Fig. 2 the I.C.I. diagram, Judd's U.C.S. diagram, and the two variations of Judd's diagram proposed by MacAdam and by the present paper, respectively, are all shown. To facilitate comparison of the relative positions of the different colors the point of the spectrum locus corresponding to $\lambda = 780$ mμ has in each case been placed at $x'' = 0.075$, $y'' = -0.500$, and that line in each diagram which corresponds to $z = 0$ in the I.C.I. diagram has been made coincident with the line $x'' = 0.075$. The diagrams have been contracted or expanded as required to make them all approximately equal in height.

The translations, rotations, and changes in scale used in placing the diagrams in Fig. 2 involve no distortion of the diagrams, so that distance ratios are unaltered. The transformations (3) by which the three U.C.S. diagrams are derived from the I.C.I. diagram do involve distortions, but since the transformations are both linear and homogeneous, these distortions are such as not to violate the characteristics of the I.C.I. Standard Observer. Nevertheless the dis-

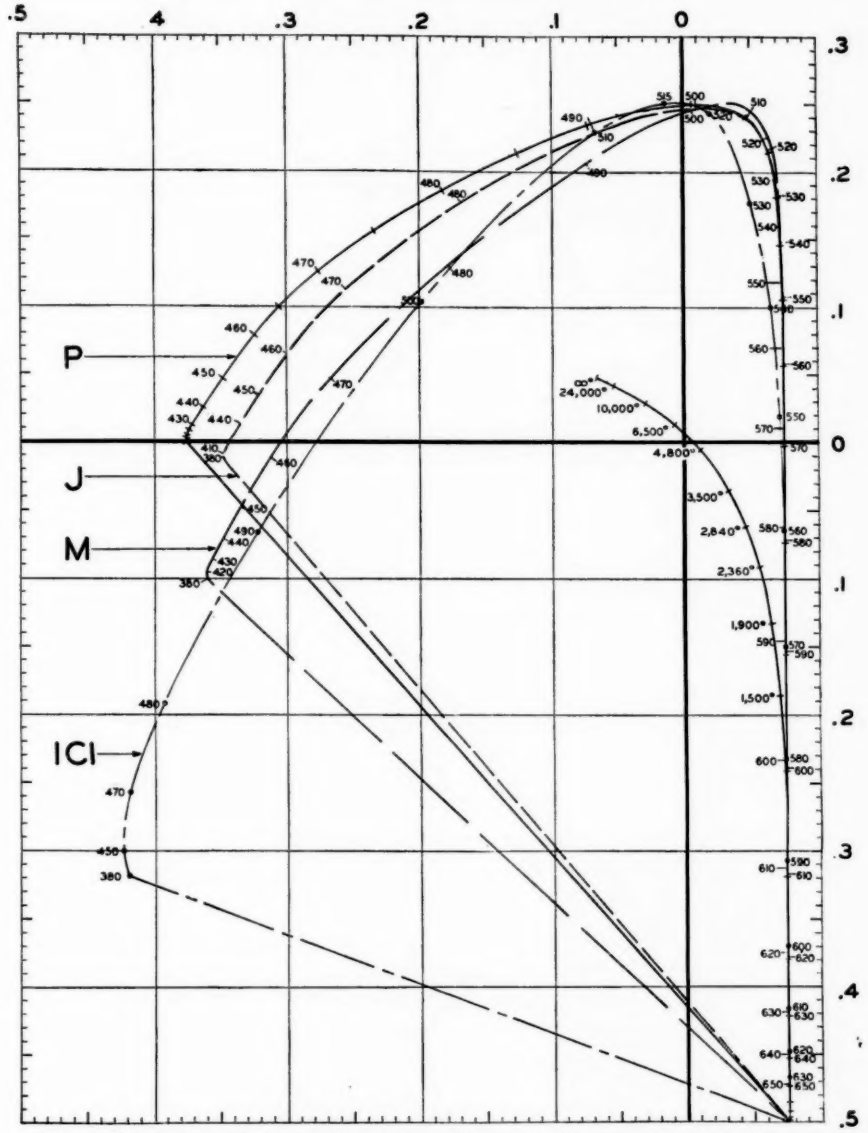

FIG. 2. Comparison of three uniform-chromaticity-scale diagrams with I.C.I. diagram. *J*, Judd's diagram; *M*, MacAdam's modification; *P*, modification proposed in this paper. Planckian locus is in accordance with *P*. The diagrams have been rotated and contracted to facilitate comparison of spacing of spectrum colors.

tortions affect the spacing of the wave-lengths along the spectrum locus and this effect is in part independent of the shape of the spectrum locus. This is readily evident along the red end of the loci where the curves coincide but the wave-lengths represented by the same point in the three uniform-chromaticity-scale diagrams differ as much as 20 mμ.

Figure 3 shows an application of the R.U.C.S. diagram. At its session in 1935, the International Commission on Illumination adopted three sets of definitions for signal colors to be used in

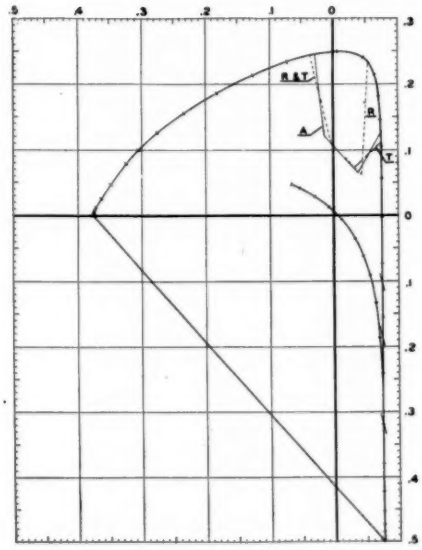

FIG. 3. I.C.I. signal color definitions in proposed R.U.C.S. coordinates. *A*, aviation green; *R*, railway green; *T*, traffic signal green. Yellow and red limits are for aviation signals only.

aviation, traffic regulation, and railway signaling. These definitions were expressed by equations in terms of the I.C.I. trilinear coordinates. In Fig. 3 the corresponding boundaries for the three greens and aviation red and yellow are shown graphically on an R.U.C.S. diagram.

V. SELECTION OF DIAGRAMS

The selection of a rectangular, uniform-chromaticity-scale diagram for international standardization must be determined primarily by the experimental data for sensibility to stimulus differences in respect to chromaticity. These data are at present so inaccurate as not to afford a satisfactory basis for choosing even among the three uniform-scale diagrams shown in Fig. 2. It is understood that new data are soon to be published and it is hoped that these data may afford a basis for consideration and discussion during the interim between the 1939 Session of the I.C.I. and the next following session.

The uniformity of a chromaticity scale depends upon the conditions governing the observations. These include the state of the observer's eyes as well as the angular area subtended by the observed sample, its brightness, and the chromaticity and brightness of the background. For such an extreme condition as the observation of point sources against a black background by a "dark adapted" observer, the conditions that are of greatest importance in signal practice, the uniform-chromaticity diagram may be quite different from any of the diagrams considered in this paper. As pointed out by MacAdam[3] several different diagrams will be required to meet the needs of different conditions.

To facilitate comparisons between color specifications expressed in terms of different mixture diagrams, it will be advantageous to recognize one system of coordinates as primary. It does not follow, however, that the present I.C.I. system should always remain as the primary system. It would, in the long run, be more economical of time to select as the primary system the particular rectangular uniform-chromaticity-scale coordinate system which represents the most common conditions.

In considering the properties to be desired in tristimulus systems for color specification we should differentiate between primary and secondary systems. For a primary, rectangular, uniform-chromaticity-scale coordinate system it is desirable (1) that it be compatible with the I.C.I. Standard Observer, (2) that it be uniform within the experimental uncertainty under the standard conditions, (3) that the labor required for computing the coordinates and transmission or reflection factor of a sample be a minimum, (4) that the origin of the final coordinates represent an acceptable achromatic point, and (5) that the dimensions of the spectrum locus and the boundaries between colors be expressible in terms of easily remembered numerical values. The extent to which all these properties can be combined in one system cannot be determined until there are available satisfactory experimental results on sensibility to stimulus differences associated with variations of chromaticity.

For a secondary system the uniformity of the chromaticity scales must, of course, be judged with reference to the conditions which the system is intended to represent. For such a system the other properties desirable in a primary system are desirable and in addition it is desirable that transformations between the primary and secondary systems be accomplished with as little labor as

possible. It should not be taken for granted, however, that all computations will be made in the primary system and transformed into the secondary system. Some laboratories may find the reverse procedure advantageous and it is equally satisfactory.

Too much emphasis should not be placed upon making the luminosity coefficients 0, 1, 0. For the selected-ordinate system of computation such simple coefficients represent a minimum of labor in computing transmission and reflection factors. For the weighted ordinate system this conclusion is not necessarily true. In the case of the R.U.C.S. system presented in this paper there are so many more zero factors among the distribution coefficients that more time is saved in computing coordinates than is required for the computation of transmission or reflection factors.

For practical applications a simple relation between colors and coordinates is of great value in making it possible to visualize the approximate hue and saturation of a color from the coordinates of its stimulus. The simple relations obtained with the proposed R.U.C.S. system are indicated in Fig. 4. In the same figure the spectrum locus resulting from the transformation given in Eq. (8) of MacAdam's paper[3] is also shown.

Evaluated in accordance with the properties listed above, the R.U.C.S. system of coordinates presented in this paper is equal or superior to the present I.C.I coordinate system on every count. Nevertheless no proposal to substitute the new system is suggested. The replacement of the present standard system by any other should await the compilation of more experimental information on chromaticity differences and should not be considered until the proposed new diagram has been in use for several years as a secondary system. When it is in order to consider a standard rectangular uniform-chromaticity-scale coordinate system, the diagram proposed in this paper may be of some interest as a guide to a simple relation between the coordinates and the colors.

VI. Acknowledgments

It is a pleasure to acknowledge our indebtedness to many colleagues who have generously assisted in the preparation of this paper. Especially the authors thank Dr. Deane B. Judd for the numerous suggestions he has contributed and Messrs. B. H. Napier, M. K. Laufer and A. H. Mason and Mrs. A. B. Wallin for their cooperation in carrying out a considerable part of the laborious computations required.

Appendix

Formulae and tables

General transformation equations for transforming tristimulus coefficients.—

(a) I.C.I. into R.U.C.S.

$$\begin{aligned}\bar{x}' &= +0.00000\bar{x}+0.00000\bar{y}+0.82303\bar{z},\\ \bar{y}' &= -2.32804\bar{x}+6.44609\bar{y}+1.36896\bar{z},\\ \bar{z}' &= +2.96827\bar{x}+2.24750\bar{y}-0.55176\bar{z}.\end{aligned} \quad \text{(a)}$$

(b) R.U.C.S. into I.C.I.

$$\begin{aligned}\bar{x} &= +0.33078\bar{x}'-0.09224\bar{y}'+0.26455\bar{z}',\\ \bar{y} &= -0.13857\bar{x}'+0.12182\bar{y}'+0.09554\bar{z}',\\ \bar{z} &= +1.21502\bar{x}'+0.00000\bar{y}'+0.00000\bar{z}'.\end{aligned} \quad \text{(b)}$$

Transformation equations for transforming trilinear coordinates.—

(c) I.C.I. into R.U.C.S.

$$x' = \frac{0.82303x+0.82303y-0.82303}{1.00000x-7.05336y-1.64023},$$

$$y' = \frac{3.69700x-5.07713y-1.36896}{1.00000x-7.05336y-1.64023}. \quad \text{(c)}$$

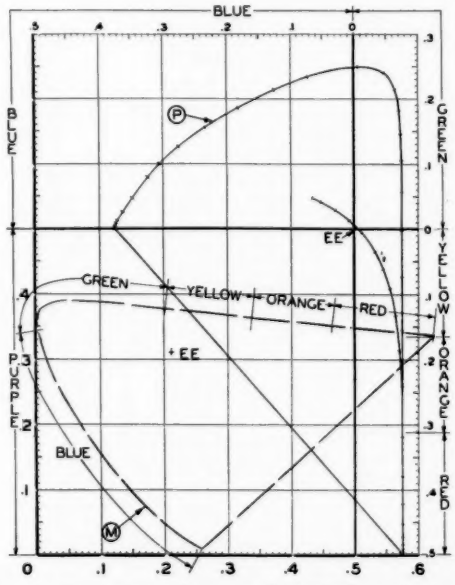

Fig. 4. Comparison of proposed R.U.C.S. system with MacAdam's proposal each in normal scale and orientation.

TABLE A. *Tristimulus distribution coefficients for computing R. U. C. S. coordinates* $\lambda=770\ m\mu$ *at* $x'=0$, $y'=0$

EQUAL ENERGY SOURCE			WAVE-LENGTH (mμ)	PLANCKIAN SOURCE* AT 2355°K			WAVE-LENGTH (mμ)	PLANCKIAN SOURCE* AT 2842°K		
$\bar{x}'$	$\bar{y}'$	$\bar{z}'$		$\bar{x}'E$	$\bar{y}'E$	$\bar{z}'E$		$\bar{x}'E$	$\bar{y}'E$	$\bar{z}'E$
540	601	60	380	2	3		380	6	7	1
1,655	1,840	180	390	10	11	1	390	23	25	2
5,637	6,272	598	400	43	48	5	400	94	104	10
16,926	18,881	1,731	410	165	184	17	410	338	377	35
53,158	59,701	5,164	420	652	732	63	420	1,260	1,415	122
114,040	131,058	10,437	430	1,741	2,001	159	430	3,175	3,649	291
143,224	172,292	12,121	440	2,689	3,234	228	440	4,641	5,584	393
145,898	188,900	10,524	450	3,328	4,309	240	450	5,450	7,056	393
137,388	199,471	7,729	460	3,765	5,466	212	460	5,865	8,515	330
106,008	189,497	7,379	470	3,456	6,178	241	470	5,131	9,173	357
66,899	178,611	14,777	480	2,570	6,861	568	480	3,644	9,728	805
38,277	190,293	30,589	490	1,718	8,543	1,373	490	2,330	11,583	1,862
22,387	244,300	59,046	500	1,164	12,704	3,070	500	1,513	16,512	3,991
13,018	343,721	107,089	510	778	20,546	6,401	510	971	25,637	7,987
6,441	453,656	174,035	520	439	30,953	11,874	520	527	37,135	14,246
3,469	522,900	240,525	530	268	40,441	18,602	530	310	46,719	21,490
1,676	550,141	299,483	540	146	47,927	26,091	540	163	53,387	29,063
722	541,672	351,809	550	70	52,833	34,314	550	76	56,824	36,906
317	503,519	399,868	560	34	54,679	43,423	560	36	56,849	45,146
170	436,510	440,085	570	20	52,501	52,931	570	21	52,829	53,262
126	347,718	467,410	580	17	46,076	61,936	580	16	44,926	60,391
95	249,134	474,790	590	14	36,198	68,984	590	13	34,240	65,253
63	159,622	456,996	600	10	25,323	72,501	600	9	23,254	66,576
31	90,825	410,697	610	5	15,661	70,819	610	5	13,982	63,223
16	46,704	339,243	620	3	8,719	63,333	620	3	7,573	55,007
7	21,271	250,248	630	1	4,283	50,394	630	1	3,622	42,613
3	8,548	172,265	640	1	1,850	37,283	640	1	1,525	30,726
0	2,969	108,205	650		688	25,082	650		553	20,161
	926	62,664	660		229	15,508	660		180	12,167
	283	33,136	670		74	8,728	670		57	6,688
	71	17,702	680		20	4,948	680		15	3,706
	7	8,573	690		2	2,536	690		1	1,858
	0	4,291	700			1,340	700			961
		2,198	710			723	710			507
		1,099	720			379	720			261
		544	730			197	730			133
		262	740			99	740			66
		125	750			50	750			32
		63	760			26	760			17
		31	770			13	770			8
878,191	5,861,914	4,983,771	Totals	23,109	489,277	684,691	Totals	35,622	533,036	647,046
x' 0.074906	y' 0.499998	z' 0.425096	Source	x' 0.019305	y' 0.408726	z' 0.571969	Source	x' 0.029302	y' 0.438459	z' 0.532240

Let $X'=\Sigma\bar{x}'ET_\lambda$ or $\Sigma\bar{x}'ER_\lambda$, $Y'=\Sigma\bar{y}'ET_\lambda$ or $\Sigma\bar{y}'ER_\lambda$, $Z'=\Sigma\bar{z}'ET_\lambda$ or $\Sigma\bar{z}'ER_\lambda$, $S'=X'+Y'+Z'$
$x'=X'/S'$, $y'=Y'/S'$, $z'=Z'/S'$, $x''=0.0750-x'$, $y''=y'-0.5000$,
T or $R=(-1.13751\ X'+1.00000\ Y'+0.78431\ Z')10^{-6}$.

* Temperatures correspond to values of C_2 as follows:

cm deg.	deg. K	deg. K
1.432	2355	2842
1.433	2357	2844
1.434	2358	2846
1.435	2360	2848
1.436	2362	2850

TABLE B. *Trilinear coordinates of spectrum locus.*

$\lambda=770$ mμ AT $x'=0$, $y'=0$			WAVE-LENGTH (mμ)	$\lambda=770$ mμ AT $x''=0.0750$, $y''=-0.5000$		
x'	y'	z'		x''	y''	z''
0.4500	0.5000	0.0500	380	−0.3750	0.0000	1.3750
.4503	.5005	.0491	390	− .3753	.0005	1.3748
.4507	.5015	.0478	400	− .3757	.0015	1.3742
.4509	.5030	.0461	410	− .3759	.0030	1.3729
.4504	.5058	.0438	420	− .3754	.0058	1.3696
.4463	.5129	.0408	430	− .3713	.0129	1.3584
.4371	.5259	.0370	440	− .3621	.0259	1.3362
.4225	.5470	.0305	450	− .3475	.0470	1.3005
.3987	.5789	.0224	460	− .3237	.0789	1.2448
.3500	.6256	.0244	470	− .2750	.1256	1.1494
.2570	.6862	.0568	480	− .1820	.1862	.9958
.1477	.7343	.1180	490	− .0727	.2343	.8384
.0687	.7500	.1813	500	.0063	.2500	.7437
.0281	.7411	.2309	510	.0469	.2411	.7121
.0102	.7154	.2744	520	.0648	.2154	.7298
.0045	.6818	.3136	530	.0705	.1818	.7477
.0020	.6462	.3518	540	.0730	.1462	.7808
.0008	.6058	.3934	550	.0742	.1058	.8200
.0004	.5572	.4425	560	.0746	.0572	.8682
.0002	.4979	.5019	570	.0748	−.0021	.9273
.0002	.4265	.5733	580	.0748	−.0735	.9987
.0001	.3441	.6558	590	.0749	−.1559	1.0810
.0001	.2588	.7411	600	.0749	−.2412	1.1663
.0001	.1811	.8189	610	.0749	−.3189	1.2440
	.1211	.8790	620	.0750	−.3790	1.3040
	.0783	.9216	630	.0750	−.4217	1.3467
	.0473	.9527	640	.0750	−.4527	1.3777
	.0267	.9733	650	.0750	−.4733	1.3983
	.0146	.9854	660	.0750	−.4854	1.4104
	.0084	.9916	670	.0750	−.4916	1.4166
	.0040	.9960	680	.0750	−.4960	1.4210
	.0009	.9991	690	.0750	−.4991	1.4241
		1.0000	700	.0750	−.5000	1.4250
		1.0000	710	.0750	−.5000	1.4250
		1.0000	720	.0750	−.5000	1.4250
		1.0000	730	.0750	−.5000	1.4250
		1.0000	740	.0750	−.5000	1.4250
		1.0000	750	.0750	−.5000	1.4250
		1.0000	760	.0750	−.5000	1.4250
		1.0000	770	.0750	−.5000	1.4250

(d) R.U.C.S. into I.C.I.

$$x=\frac{+0.06325x'-0.34073y'+0.25264}{+1.00000x'-0.31564y'+0.34389},$$

$$y=\frac{-0.22358x'+0.02509y'+0.09124}{+1.00000x'-0.31564y'+0.34389}. \qquad (d)$$

(e) Luminosity coefficients for R.U.C.S. system.

$L_{x'}=0.13857$, $L_{y'}=-0.12182$, $L_{z'}=-0.09554$.

(f) Luminosity coefficients adjusted to make $L_{y'}$ equal unity.

TABLE C. *Thirty selected ordinates for computing R.U.C.S. coordinates Planckian source at 2842°K ($C_2=1.432$ cm deg.).*

ORDINATE NO.	$\lambda\overline{x'}$	$\lambda\overline{y'}$	$\lambda\overline{z'}$
1	415.429	440.155	507.166
*2	423.874	463.850	524.684
3	428.419	482.711	534.516
4	431.931	497.275	542.072
*5	434.970	506.632	548.431
6	437.725	513.280	554.001
7	440.287	518.569	559.009
*8	442.712	523.116	563.595
9	445.040	527.217	567.853
10	447.300	531.014	572.402
*11	449.498	534.598	575.650
12	451.635	538.022	579.282
13	453.724	541.331	582.783
*14	455.782	544.555	586.186
15	457.818	547.719	589.514
16	459.844	550.844	592.787
*17	461.872	553.948	596.029
18	463.922	557.051	599.266
19	466.038	560.174	602.517
*20	468.250	563.339	605.812
21	470.591	566.573	609.181
22	473.103	569.911	612.660
*23	475.844	573.390	616.298
24	478.900	577.072	620.166
25	482.393	581.033	624.376
*26	486.543	585.404	629.118
27	491.662	590.415	634.631
28	498.277	596.490	641.398
*29	507.391	604.693	650.722
30	525.695	619.580	668.621
Factors	$F_{x'}$	$F_{y'}$	$F_{z'}$
30 ordinates	0.0011887	0.0177684	0.0215693
*10 ordinates	0.0035660	0.0533053	0.0647080

Let $X'=F_{x'}\Sigma T_\lambda$, $Y'=F_{y'}\Sigma T_\lambda$, $Z'=F_{z'}\Sigma T_\lambda$

$S'=X'+Y'+Z'$, $x'=X'/S'$, $y'=Y'/S'$, $z'=Z'/S'$

$x''=0.0750-x'$, $y''=y'-0.5000$

T or $R=(-1.13751\ X'+1.00000\ Y'+0.78431\ Z')10^{-6}$

$L_{x'}=-1.13751$, $L_{y'}=1.00000$, $L_{z'}=0.78431$.

(g) Trilinear coordinates of important illuminants.

SOURCE BLACKBODY AT:*	x''	y''
1000°K	0.0743	−0.2931
1500°	0.0704	−0.1859
1900°	0.0644	−0.1325
2360°	0.0557	−0.0912
2848°	0.0457	−0.0616
3500°	0.0328	−0.0351
4800°	0.0115	−0.0053
6500°	−0.0078	0.0135
10,000°	−0.0296	0.0291
24,000°	−0.0530	0.0416
∞	−0.0668	0.0475
* $C_2=1.435$ cm deg.		
Equal Energy	0.0000	0.0000
I.C.I. Illuminant *A*	0.0457	−0.0616
I.C.I. Illuminant *B*	0.0096	−0.0053
I.C.I. Illuminant *C*	−0.0113	0.0134

(h) Equations for Signal Color Limits as Defined by I.C.I. in 1931:

Aviation Signal Limits

Red $y'' \leqq 0.003 - 4.27x''$,
$x'' \geqq 0.0747 + 0.0005y''$.

Yellow $y'' \leqq 0.194 - 4.01x''$,
$y'' \geqq 0.118 - 4.12x''$,
$x'' \geqq 0.0739 + 0.0019y''$.

Green $x'' \geqq -0.119y''$,
$y'' \geqq 1.71x''$,
$y'' \geqq 0.106 - 1.09x''$.

Traffic Signal Limits

Red $y'' \leqq -0.017 - 4.30x''$,
$x'' \geqq 0.0748 + 0.0003y''$.

Yellow $y'' \leqq 0.172 - 4.04x''$,
$y'' \geqq 0.082 - 4.16x''$,
$x'' \geqq 0.0734 + 0.0027y''$.

Green $y'' \geqq 0.045 + 0.910x''$,
$y'' \geqq 0.106 - 1.09x''$,
$x'' \geqq 0.022 - 0.241y''$.

Railway Signal Limits

Red $y'' \leqq -0.028 - 4.31x''$,
$x'' \geqq 0.0739 + 0.0019y''$.

Yellow $y'' \leqq 0.156 - 4.07x''$,
$y'' \geqq 0.094 - 4.15x''$,
$x'' \geqq 0.0691 - 0.0197y''$.

Green $x'' \geqq 0.022 - 0.241y''$,
$y'' \geqq 0.105 - 1.02x''$,
$x'' \leqq 0.039 + 0.060y''$.

Errors in Spectrophotometry Due to Imperfect Collimation and to the Finite Size of the Light Source

G. O. LANGSTROTH
George Eastman Research Laboratories of Physics, Massachusetts Institute of Technology, Cambridge, Massachusetts
(Received July 10, 1939)

IT is common practice in absorption spectrophotometry to collimate the light beam passing through the solution, and to calculate the extinction coefficient by application of the Lambert-Beer formula to observed transmission data. The path length of the light within the solution is taken to be equal to the internal depth of the absorption cell. This procedure involves the assumption that every light ray passes through the solution along a normal to the cell surface—a condition which is attainable only when an infinitely small light source is accurately placed at the principal focus of the collimating lens. There appears to be no readily available discussion in the literature concerning the errors introduced in such extinction or transmission measurements by the use of a light source of finite size, and by variations in its distance from the principal focus of the collimating lens. The present article deals with an analysis of the problem for a commonly used optical system, *viz.* a line source of light (e.g. a slit), a "collimating" lens, and an absorption cell containing the solution.

The relation between the optical density and the transmission of a solution is found to differ from the Lambert-Beer relation by a multiplicative factor. This factor is a function of the absorption coefficient and refractive index of the solution, the cell depth, the distance of the source from the principal focus of the lens, the dimensions of the source, and factors determined by the portion of the lens through which light is permitted to pass. It does not reduce to unity when the source is placed at the principal focus of the lens.

In general, only small errors are introduced in determined absorption coefficients by the assumption that every light ray passes through the solution along a normal to the cell surface; the errors introduced in determined specific transmissions are somewhat greater. Perhaps the most striking point brought out by the analysis is that for most purposes it is unnecessary to use a collimated light beam in making absorption coefficient determinations. The source may be placed at a considerable distance from the principal focus of even a fast (e.g. f: 2.5) lens without introducing serious errors on interpreting the data with the aid of the Lambert-Beer formula. Furthermore, there is an optimum source-to-lens distance which does not coincide with the focal length of the lens. These features are of interest with respect to instrument design, since they suggest simplifications and advantages which must be sacrificed if a collimated beam is used.

1. Analysis of the Problem

The optical system is represented diagrammatically in Fig. 1. A vertical line source of length $2H$ situated at a distance p from a lens of focal length f, is bisected by the optic axis of the lens. The absorption cell, of internal depth l, contains a solution of absorption coefficient μ and refractive index n for the particular wave-length considered; the optic axis of the lens is normal to the cell surface.

Part (*a*) of this section is devoted to the development of expressions for the transmission ratio of the solution, and of allied equations. Part (*b*) is concerned with a discussion of the mathematical approximations, and part (*c*) deals with the physical assumptions on which the analysis is based.

(a) Development of equations

In the following treatment reflection and absorption by the lens are neglected, as are any effects introduced by the windows of the absorption cell (cf. Part *c*). Consider a ray which comes from an element dh of the source situated at a distance h above the optic axis, and which passes through the lens at a point (r, α), where r is the distance from the lens center, and α is the angle made by the radius vector with the vertical

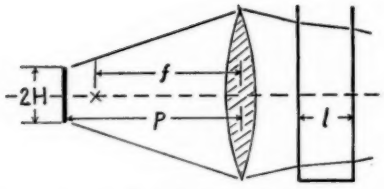

FIG. 1. Diagram of the investigated optical system.

(Fig. 2a). When $p>f$, the path length of this ray within a solution of unit refractive index can be shown from the geometry of the figure and application of the simple lens formula, to be,

$$t=l\left[1+\frac{h^2}{p^2}+\frac{r^2(p-f)^2}{p^2f^2}+\frac{2rh(p-f)}{p^2f}\cos\alpha\right]^{\frac{1}{2}}. \quad (1)$$

If the solution has a refractive index n, the ray has a path length t_n, related to t by (Fig. 2b),

$$l/t=\cos i, \quad l/t_n=\cos\rho, \quad \sin i/\sin\rho=n,$$

where i and ρ are the angles of incidence and refraction at the solution surface. Hence,

$$t_n=l\Big/\left[1-\frac{t^2-l^2}{n^2t^2}\right]^{\frac{1}{2}}. \quad (2)$$

If each element of the source radiates equally, and if the intensity due to each element is uniform over the lens surface (cf. Part *c*), the energy of the ray after passing through the solution is

$$\Delta E=C\cdot e^{-\mu t_n}\cdot r\,dh\cdot d\alpha\cdot dr$$

where C is a constant depending on source conditions. The ratio of the light transmitted through the solution to that incident on it is therefore given by,

$$T=\frac{\int_0^H\int_{\alpha_1}^{\alpha_2}\int_{R_1}^{R_2} r\cdot e^{-\mu t_n}\cdot dh\cdot d\alpha\cdot dr}{\int_0^H\int_{\alpha_1}^{\alpha_2}\int_{R_1}^{R_2} r\cdot dh\cdot d\alpha\cdot dr}. \quad (3)$$

In this equation R_1 and R_2 define the radial limits, and α_1 and α_2 the angular limits of the portion of the lens through which light is permitted to pass.

In order to integrate the numerator of (3) it is desirable to express t_n as a rapidly converging series. This may be done by expanding (2) in a Maclaurin's series in powers of $(t^2-l^2)/l^2$, i.e.,

$$t_n=l\left[1+\frac{1}{2n^2}\cdot\frac{t^2-l^2}{l^2}-\frac{4n^2-3}{8n^4}\cdot\left(\frac{t^2-l^2}{l^2}\right)^2+\cdots\right]. \quad (4)$$

A first-order approximation of t_n is ample for the present purpose (cf. Part *b*). With the aid of (4) and (1), the numerator of (3) may be written,

$$e^{-\mu l}\int_0^H\int_{\alpha_1}^{\alpha_2}\int_{R_1}^{R_2} r\cdot\exp\left[-\frac{\mu l}{2n^2}\left\{\frac{h^2}{p^2}+\frac{r^2(p-f)^2}{p^2f^2}+\frac{2rh(p-f)}{p^2f}\cos\alpha\right\}\right]\cdot dh\cdot d\alpha\cdot dr. \quad (5a)$$

Expanding the exponential and retaining second-order terms (cf. Part *b*), this becomes,

$$e^{-\mu l}\int_0^H\int_{\alpha_1}^{\alpha_2}\int_{R_1}^{R_2} r\left\{1-\frac{\mu l}{2n^2}\left[\frac{h^2}{p^2}+\frac{r^2(p-f)^2}{p^2f^2}+\frac{2rh(p-f)}{p^2f}\cos\alpha\right]+\frac{\mu^2l^2}{8n^4}\left[\frac{h^2}{p^2}+\frac{r^2(p-f)^2}{p^2f^2}+\frac{2rh(p-f)}{p^2f}\cos\alpha\right]^2\cdots\right\}dh\cdot d\alpha\cdot dr. \quad (5)$$

Substitution of (5) in (3) and integration of numerator and denominator leads to the second-

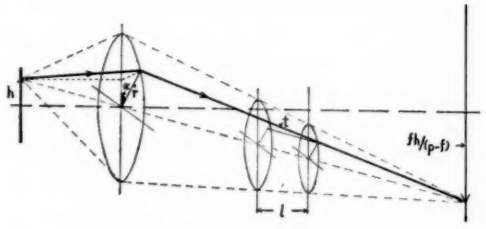

FIG. 2a. A three-dimensional representation of the optical system, indicating the geometrical construction necessary for evaluation of the path length of the ray (h, r, α) through a solution of unit refractive index.

order approximation equation for the transmission. It is,

$$T=e^{-\mu l}\left\{1-\frac{\mu l}{2n^2p^2}\left[\frac{H^2}{3}+\frac{D^2R(4)}{2f^2}+\frac{2AHDR(3)}{3f}\right]+\frac{\mu^2l^2}{4n^4p^4}\left[\frac{H^4}{10}+\frac{D^4R(6)}{6f^4}+\frac{H^2D^2R(4)}{3f^2}+\frac{AH^3DR(3)}{3f}+\frac{2AHD^3R(5)}{5f^3}+\frac{BH^2D^2R(4)}{6f^2}\right]\cdots\right\}, \quad (6)$$

where,

$$D=(p-f), \qquad A=\frac{\sin\alpha_2-\sin\alpha_1}{\alpha_2-\alpha_1},$$

$$R(i)=\frac{R_2{}^i-R_1{}^i}{R_2{}^2-R_1{}^2}, \qquad B=\frac{\sin\alpha_2\cos\alpha_2-\sin\alpha_1\cos\alpha_1}{\alpha_2-\alpha_1}.$$

In the special case in which the full lens aperture of radius R (or a symmetrically placed circular diaphram of radius R) is used, Eq. (6) reduces to.

$$T=e^{-\mu l}\left\{1-\frac{\mu l}{2n^2p^2}\left[\frac{H^2}{3}+\frac{D^2R^2}{2f^2}\right]+\frac{\mu^2l^2}{4n^4p^4}\left[\frac{H^4}{10}+\frac{D^4R^4}{6f^4}+\frac{H^2D^2R^2}{3f^2}\right]\cdots\right\}. \quad (7)$$

The first-order approximations of (6) and (7) are sufficient for most purposes (cf. Part *b*). They may be written,

$$T=e^{-\mu l}\{1-\mu lK/n^2\} \quad (6a)$$

and

$$T=e^{-\mu l}\{1-\mu lk/n^2\}, \quad (7a)$$

where K and k are determined solely by the characteristics of the optical system employed.

The above equations become identical with the Lambert-Beer formula only when both $(p-f)$ and H are equal to zero. It is of some interest to ascertain the conditions for which they most closely approach the Lambert-Beer relation with a source of height $2H$. These conditions are obtained when the factor $\mu lk/n^2$ (or $\mu lK/n^2$) has a minimum value. Differentiating this factor in (7a) with respect to p and equating the result to zero, one obtains for the optimum source-to-lens distance,

$$P_0=f\{1+\tfrac{2}{3}H^2/R^2\}. \quad (8)$$

It is apparent from (7a) that a determined specific transmission will be in error by $100\cdot\mu lk/n^2$ percent, if the true value is taken to be that obtained when each ray passes through the sample along a normal to the surface. On the other hand, the error in an absorption coefficient determined with the aid of the Lambert-Beer formula will be only $100\cdot k/n^2$ percent. This

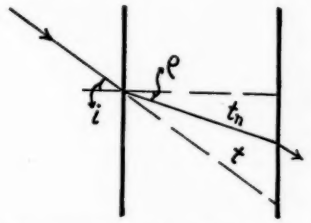

FIG. 2b. Diagram illustrating the relation between the path length of a ray through a solution of unit refractive index and that through a solution of refractive index n.

follows from (7a) since,

$$\ln T_{\text{obs}}=-\mu l+\ln\left(1-\frac{\mu l}{n^2}k\right)$$

$$=-\mu l-\left[\frac{\mu l}{n^2}k+\frac{1}{2}\left(\frac{\mu lk}{n^2}\right)^2+\cdots\right]\rightarrow-\mu l\left[1+\frac{k}{n^2}\right]$$

to a first approximation. Hence,

$$(\mu l)_{\text{obs}}=\mu l[1+k/n^2]. \quad (9)$$

The magnitudes of the errors in T and μl for a number of specific examples are given in Table I of the next section.

(b) The mathematical approximations

Second and higher powers of (l^2-l^2/l^2) were neglected in the Maclaurin's series expansion of t_n (Eq. (4)). The following figures illustrate the relative magnitudes of the terms in the alternating series of (4) for an extreme case ($f=10$ cm, $p=40$ cm, $r=2$ cm, $h=2$ cm, $\alpha=0$).

n	2	1	0.8	0.6
Second-order term/first-order term	0.032	0.010	0.0068	0.043
% change in t_n on inclusion of second-order term	0.016	0.020	0.020	0.23

These figures refer to the extreme ray; since the approximation is still better for other rays, the error introduced in the integrated expression for T is considerably smaller than that in t_n.

Third power and higher terms were neglected in the series expansion of the exponential in (5a). The suitability of this approximation may be judged from an examination of the relative magnitudes of first- and second-order terms in the integrated expression for T (Eq. (6)), e.g. for an extreme case ($f=10$ cm, $p=40$ cm, $R_1=1$ cm, $R_2=2$

cm, $\alpha_1 = 0$, $\alpha_2 = 0.66$ radians, $2H = 4$ cm, $\mu l = 4.6$)

n	2	1	0.8	0.6
Second-order terms/first-order terms	0.0065	0.026	0.041	0.072
% change in $T/e^{-\mu l}$ on inclusion of second-order terms	0.008	0.12	0.31	1.1

The figures indicate that the first-order approximation is sufficient for most purposes. When the full lens aperture is used the approximation is still better, i.e., for the example cited above, neglect of second-order terms introduces an error of 0.06 percent in $T/e^{-\mu l}$ when $n = 1$, and of 0.14 percent when $n = 0.8$.

Second- and higher-order terms were neglected in the expansion of $\ln [1 - \mu l k/n^2]$ in arriving at Eq. (9). Since $\mu l \cdot k/n^2$ attains a value of 0.05 only in extreme cases (cf. Table I), the expanded expression is given to better than 2.5 percent; the expression amounts to about 1 percent of $\ln T_{obs}$ when $\mu l = 4.6$, so that the error introduced in $\ln T_{obs}$ is less than 0.03 percent.

(c) Physical assumptions

It was assumed that equal amounts of energy were transmitted by each unit area of the "collimating" lens, i.e., departures from a uniform intensity distribution over the lens surface, and reflection and absorption losses at the lens, were neglected. In general, factors which increase the intensity of the rays passing through the outer parts of the lens accentuate the differences between the transmission—optical density relation and the Lambert-Beer formula; factors which increase the intensity of central rays on the other hand, have the opposite effect.

Owing to the operation of the inverse square law and to the difference in incidence angle of the light on different parts of the lens, the intensity distribution over the lens surface is not uniform. Correction for these factors, however, has only an insignificant effect on the equations developed. For example, a small source placed 20 cm away from a lens of 4 cm diameter illuminates the center only about 1 percent more intensely than the edges. Considerably greater departures from a uniform distribution may be encountered when the source corresponds, say, to the exit slit of a monochromator: the effect produced will depend on whether they favor the central or the outer parts of the lens.

Reflection losses are practically uniform over the lens surface, and therefore need not be considered. As calculated from Fresnel's formula, the amount of light reflected at the edge of a plano-convex lens of 4 cm diameter (refractive index 1.5) differs by less than 0.01 percent from that reflected at the center, when the source is 20 cm away.

In some wave-length regions the lens material may absorb strongly enough to alter appreciably the relative amounts of energy in the central and the extreme rays. In contrast to factors already discussed, the effect of such absorption is to accentuate the difference between the transmission-optical density relation and the Lambert-Beer formula. Absorption losses become important, however, only below about 3700A with crown glass, and below about 2200A with quartz.

Reflection losses at the windows of the absorption cell are practically identical for central and extreme rays, and therefore need not be considered. For example, when the source is placed 20 cm away from a lens of 10 cm focal length and 4 cm diameter (refractive index 1.5) the reflection loss of an extreme ray at the cell window differs by less than 0.01 percent from that for a ray incident normally. The differential absorption of extreme and central rays by the cell windows may also be neglected, since in general the absorption of the window is low compared to that of the solution, and since the effect enters for both solution and solvent cells

The deviations undergone by the rays in passing through the cell window were neglected. An extreme ray from a source placed 20 cm away from a lens of focal length 10 cm and diameter 4 cm makes an angle of about 6° with the cell window; if the window has a refractive index of 1.5 and the solution a refractive index of 1.3, the path length of the ray in the solution is about 0.1 percent shorter than the value given by Eq. (4). Insofar as this effect is concerned, therefore, the equations developed in this article differ from the Lambert-Beer relation somewhat more than they should.

2. Discussion

The calculated data of Table I indicate the magnitude of the errors introduced on interpreting observed data by application of the

Lambert-Beer formula. Extreme examples have been included, in order to show the maximum errors likely to be encountered in practice. The figures are given for three different values of the refractive index, since it is a well-known fact that this variable decreases in the neighborhood of an absorption band; it is improbable that it ever reaches a value as low as 0.8 under ordinary conditions.

Examples (*a*) show the magnitude of the errors introduced by the use of a source of finite size, while a comparison of examples (*a*) and (*b*) illustrates the improved accuracy obtained by placing a long source at the optimum lens-to-source distance. Comparison of (*c*) with either (*a*) or (*b*) illustrates the marked effect of diaphragming down the lens and placing it at the optimum source-to-lens distance. Examples (*d*) show the decreased accuracy obtained when only an outer portion of the lens is used. Examples (*e*), (*f*), and (*g*) present similar calculated results for a lens of greater focal length.

The figures indicate that it is unnecessary to use a collimated light beam in ordinary measurements of absorption coefficients. For example, noncollimation and the finite size of the source introduce an error of less than 0.2 percent when a 1-cm long source is placed 50 cm away from a lens of focal length 20 cm and diameter 4 cm ($\mu l = 4.6$). Furthermore, if the source is 4 cm long, the error is actually less when it is placed at 50 cm from the lens, than when it is placed at the principal focus (cf. Table I). These features are interesting from the viewpoint of instrument design.

This work was carried out under a grant from the Rockefeller Foundation to Professor G. R. Harrison.

Summary

The Lambert-Beer relation between the transmission and the optical density of a solution

TABLE I. *Examples of the percentage errors introduced in T and μl by assuming ideal photometric conditions. The calculations were made with the aid of Eqs. (6a), (7a), (8) and (9), for a μl value of 4.6 (i.e. T→0.01).*

	f CM	R_2 CM	R_1 CM	α_1 RADIANS	α_2 RADIANS	p CM	$2H$ CM	% ERROR IN T n 1.5	n 1.0	n 0.8	% ERROR IN μl n 1.5	n 1.0	n 0.8
(*a*)	10	2	0	0	2π	10	0.5	0.02	0.05	0.08	0.005	0.010	0.016
						10	1.0	0.09	0.19	0.30	0.018	0.041	0.065
						10	2.0	0.34	0.77	1.2	0.074	0.17	0.26
						10	4.0	1.4	3.1	4.8	0.30	0.67	1.0
(*b*)*	10	2	0	0	2π	10.1	0.5	0.02	0.05	0.07	0.005	0.010	0.016
						10.4	1.0	0.08	0.18	0.29	0.018	0.039	0.063
						11.7	2.0	0.29	0.66	1.0	0.063	0.14	0.22
						16.6	4.0	0.81	1.8	2.9	0.18	0.39	0.63
(*c*)*	10	.5	0	0	2π	11.6	0.5	0.02	0.04	0.06	0.004	0.009	0.014
						16.6	1.0	0.05	0.12	0.18	0.011	0.026	0.039
						36.4	2.0	0.09	0.21	0.33	0.020	0.046	0.072
						116	4.0	0.12	0.26	0.41	0.026	0.057	0.089
(*d*)	10	2	1	0	.66	20	1.0	0.85	1.9	3.0	0.18	0.41	0.65
						40	1.0	1.6	3.6	5.5	0.35	0.78	1.2
						20	4.0	1.7	3.9	6.0	0.37	0.85	1.3
						40	4.0	2.1	4.7	7.3	0.46	1.0	1.6
(*e*)	20	2	0	0	2π	20	1.0	0.02	0.05	0.08	0.005	0.010	0.016
						20	4.0	0.34	0.77	1.2	0.074	0.17	0.26
(*f*)	20	2	0	0	2π	30	1.0	0.07	0.15	0.23	0.014	0.033	0.050
						30	4.0	0.21	0.47	0.73	0.046	0.10	0.16
						50	1.0	0.19	0.43	0.67	0.041	0.093	0.15
						50	4.0	0.24	0.54	0.84	0.052	0.12	0.18
(*g*)	20	2	1	0	.66	30	1.0	0.12	0.27	0.43	0.026	0.059	0.093
						30	4.0	0.39	0.87	1.4	0.085	0.19	0.30
						50	1.0	0.28	0.63	0.98	0.061	0.14	0.21
						50	4.0	0.46	1.0	1.6	0.10	0.22	0.35

* These examples were calculated for the optimum lens-to-source distance as determined from Eq. (8).

holds rigidly only for an idealized optical system in which every light ray passes through the solution along a normal to cell surface. The corresponding relation for a system consisting of a line source of light (e.g. a slit), a "collimating" lens, and a cell containing the solution, is shown to be of the form,

$$T = e^{-\mu l}[1 - \mu l k/n^2]$$

where T, μ, and n, represent, respectively, the transmission, the absorption coefficient, and the refractive index of the solution, l denotes the cell depth, and k is a factor determined solely by the characteristics of the optical system. k does not vanish when a source of finite size is placed at the principal focus of the lens.

In general, interpretation of observed transmission data by application of the Lambert-Beer relation does not lead to serious errors in the absorption coefficients. The error introduced in this way is a minimum for a certain lens-to-source distance which does not coincide with the focal length of the lens. A striking point brought out by the analysis is that under most circumstances it is unnecessary to use a collimated light beam in absorption coefficient measurements. The analysis suggests several features which are of interest with respect to instrument design.

Luminescence of Sulphide and Silicate Phosphors

R. P. JOHNSON
Research Laboratory, General Electric Company, Schenectady, New York

(Received July 14, 1939)

Many features of the behavior of luminescent sulphides can be correlated by means of a mechanism based on the energy-band theory of the solid insulator. It is imagined that after excitation, which is essentially an ionization of an activator atom, the dissociated electron is highly likely to be trapped and held localized in a discrete energy level in the forbidden region, recombining with an ion and emitting the characteristic luminescence only after it has been freed from this trapped state by thermal excitation or other agencies. This picture, with appropriate modifications, is also useful in explaining the properties of silicate phosphors.

INTRODUCTION

THE purpose of this paper is to enquire whether simple models based on the energy-band theory of solids[1] can account for the properties of sulphide phosphors such as ZnS·Cu and of silicate phosphors such as Zn_2SiO_4·Mn. The theory, it will appear, predicts many of the salient qualitative observations and is capable of quantitative agreement with the data on particular samples. In support of the theory, recent experiments of the writer will be used to supplement the extensive published information.[2]

SULPHIDE MODEL

Figure 1(a) shows the spectrum of energy states accessible to valence electrons in the proposed model of a sulphide phosphor. In the forbidden region between the uppermost filled band of levels and the next-higher band, normally empty, are localized electron states of two kinds. The "impurity states," one of which is contributed by each activator atom, are supposed normally to contain each an electron. The "trapping states," associated with cracks, strains, and surfaces,[3] are supposed normally to be vacant. Absorption of a quantum of ultraviolet radiation raises an electron from the lower band to the corresponding level in the upper band ((b) in Fig. 1). This excited electron and the hole it has left rapidly drift to the bottom and the top of their respective bands (c) and thereafter their direct recombination is prohibited by the principle of conservation of the wave number vector. The hole captures an electron from an impurity level, and the excited electron falls into one of the trapping states (d). A quantum of the luminescence radiation is emitted when this electron drops into the vacated impurity level, having been freed from the trapping state to the upper band by temperature excitation or other means (e).

We next ask whether the behavior to be expected with this simple picture is in fact observed.

(1) The space-density of the trapping states and their distribution in energy-of-trapping (energy required for raising an electron from one of them to the upper conduction band) may be expected to vary widely among different samples, depending on the details of mixing, heating, and the like. A corresponding diversity in the observations is evident when one regards, for example, the multiform empirical laws proposed by different investigators to fit their data on decay.

(2) The color of the emitted light and the course of decay should be independent of the mode of excitation. Such independence is usually found.

(3) The efficiency should be high, since the model includes automatic transport of excitation

[1] For a nonmathematical discussion and references, see F. Seitz and R. P. Johnson, J. App. Phys. **8**, 84, 186, 246 (1937); also, N. F. Mott, Trans. Faraday Soc. **34**, 822 (1938).

[2] Summarized by E. L. Nichols and E. Merritt, *Studies in Luminescence* (Washington, 1912); P. Lenard, F. Schmidt and R. Tomaschek, *Handbuch der Experimentalphysik* XXIII/1 and 2 (Leipzig, 1928); P. Pringsheim, *Fluoreszenz und Phosphoreszenz* (Berlin, 3rd Ed., 1928); M. Curie, *Luminescence des Corps Solides* (Paris, 1934); L. Vanino, *Die Leuchtfarben* (Stuttgart, 1935); H. Rupp, *Die Leuchtmassen und ihre Verwendung* (Berlin, 1937).

[3] E. T. Goodwin, Proc. Camb. Phil. Soc. **35**, 205, 221, 232 (1939); W. Shockley, Phys. Rev. **56**, 317 (1939).

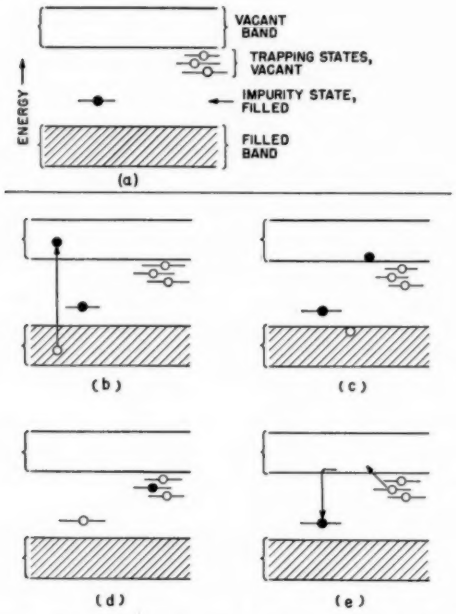

FIG. 1. (a) Scheme of energy levels for valence electrons in proposed sulphide phosphor model. (b)–(e) Course of decay after excitation by a quantum in the fundamental ultraviolet absorption region of the lattice.

energy from any point in the lattice to the neighborhood of an activator atom where it is available for luminescence.[4] The measured efficiencies, for comparison, are of the order of 50 percent (watts/watt) in ultraviolet excitation, of the order of 5 to 10 percent in electron bombardment at high voltages,[5] and 80 percent in one reported case of alpha-particle bombardment.[6]

(4) The detailed course of the decay curve (log brightness *vs.* time of decay) at room temperature will obviously depend on the detailed distribution of the trapping states, but its general shape can be found by a simple approximate analysis. This calculation shows that invariably the decay should begin at a finite rate from the level of brightness during excitation, that the semi-log plot should be concave upward, and that its initial steepness should be greater the greater the initial brightness. These are just the three generalizations that emerge from the vast data on decay of sulphides, when the variations among individual samples are overlooked.

(5) Suppose the decay curve of a sample which has been excited to equilibrium with a source of low intensity is taken as a standard, and is compared with the decay of the same sample brought to the same initial brightness by brief excitation with a more intense source. In this brief excitation the upper trapping states will have come more nearly to their equilibrium filling than the lower trapping states, and hence the decay curve will be initially steeper than the standard curve and will increasingly fall below the standard during decay. If, on the other hand, the standard low level of initial brightness is reached by decay after excitation to equilibrium with an intense source, during the decay before observation begins chiefly the upper trapping states will have been depleted while the lower trapping states retain nearly their initial complement of electrons. The remaining part of this decay curve will therefore be initially less steep than the standard curve and will increasingly lie above the standard during decay. These predictions are easily tested and are found to be true for sulphide phosphors as a group.[7]

(6) At elevated temperatures the decay should obviously be more rapid. This prediction is generally fulfilled.

(7) The sulphides should fluoresce at low temperatures. Whether or not they show a visible low temperature phosphorescence will depend on the density of trapping states near the upper conduction band. Actually the sulphides as a group fluoresce and phosphoresce brightly in liquid air. At low temperatures there should be a pronounced storage of light recoverable on heating—this is, of course, a well-known phenomenon. One experiment with this storage effect, out of many all of which gave results consistent with the proposed model, will be described: The sample in liquid air was excited to equilibrium with an intense source, then was removed from the bath and warmed up toward room temperature, glowing as it warmed. Just after its brightness had gone through a maximum it was put back into liquid air (which now

[4] See M. Schön, Zeits. f. tech. Physik **19**, 361 (1938).
[5] K. Scherer and R. Rübsaat, Archiv f. Elektrot. **31**, 821 (1937).
[6] P. M. Wolf and N. Riehl, Ann. d. Physik **11**, 108 (1931).
[7] See also A. Guntz, Ann. de Chimie **6**, 5 (1926).

rendered it entirely dark) and again was excited while in liquid air, this time to equilibrium with a weak source. As it again warmed up in the dark its brightness was at first low, corresponding to the low intensity of the second excitation, until the same temperature was reached which had been reached in the previous warming. Thereupon the brightness became much higher and continued during the subsequent warming to be high, corresponding to the intensity of the original excitation. The interpretation in terms of electrons trapped in levels of different energy is obvious.

(8) Photoconductivity, high during excitation and "phosphorescent" thereafter,[8] appears readily as a net drift of the loosely-trapped electrons in an applied electric field.

(9) The model is consistent with the existence of saturation effects,[9] commonly and plausibly attributed to the fact that as the intensity of excitation is increased the number of "centers" (here, impurity states) which are instantaneously excited and so are not available for excitation becomes comparable with the total number of centers.

(10) Excitation, in the model, is essentially a one-stage process, the time required for reaching the condition of Fig. 1(d) being supposed negligible in comparison with the time between (d) and (e). It follows that the brightness during excitation should increase smoothly from zero up toward its equilibrium value. This behavior appears in the few cases where build-up curves have been measured.[10] If the excitation were a two-stage process, the electrons being excited to an upper state, decaying to an intermediate state, and thence to the ground state with emission of luminescence, a simple analysis shows that the build-up curve should have a point of inflection, and that after a sufficiently brief excitaton the brightness should continue to increase for a time. Neither of these effects has been reported (the second could make sulphide screens useless for television purposes), so it is fair to say that the model is consistent with the observations on kinetics of excitation.

(11) The familiar effect of infra-red radiation in hastening the decay of sulphides is clearly due to the excitation, by infra-red quanta, of electrons from the low-lying trapping states to upper trapping states or to the upper band. This interpretation is supported by three easily-demonstrated facts: (a) The infra-red is relatively ineffective if the irradiation follows too closely after excitation. It is necessary to wait until the electrons in the upper trapping states, which are readily freed by temperature excitation, have become so few that the brightness is limited by the rate of excitation from the low-lying levels. (b) When irradiation with infra-red of constant intensity is begun, the brightness of the decaying sample rises *gradually* and goes through a maximum. This build-up period is to be expected, since the irradiation requires time to bring about a new quasi-equilibrium distribution of the trapped electrons in which the upper states are more densely populated than they should be in the absence of infra-red. (c) Correspondingly, after the irradiation is stopped time is required for the electrons to sink back toward a new quasi-equilibrium distribution, and during this period the sample remains abnormally bright—there is a "phosphorescence" of the accelerating action of infra-red.

Silicate Model

Silicate phosphors differ strikingly from sulphides in their decay characteristics.[11] During the first 10 to 100 milliseconds of decay the

Table I. (*From Johnson and Davis, reference 11.*)

Type of Silicate	Luminescent Color	Approximate Time Constant of Initial Decay (sec.)
$Zn_2SiO_4 \cdot Mn$	Green	13×10^{-3}
Zn Be Silicate	Yellow	9×10^{-3}
Zn Be Silicate	Rose	7×10^{-3}
Cd Silicate	Rose	30×10^{-3}
Soda-lime glass	Yellow	7×10^{-3}

[8] A. L. Reimann, Nature **140**, 501 (1937).

[9] W. B. Nottingham, J. App. Phys. **10**, 73 (1939); S. T. Martin and L. B. Headrick, J. App. Phys. **10**, 116 (1939); W. de Groot, Physica **6**, 393 (1939); N. Riehl, Zeits. f. tech. Physik **20**, 152 (1939).

[10] A. Schleede and B. Bartels, Zeits. f. tech. Physik **19**, 364 (1938); P. J. Mulder, J. Frank. Inst. **225**, 527 (1938); W. de Groot, Physica **6**, 275 (1939); R. B. Nelson, R. P. Johnson and W. B. Nottingham, J. App. Phys. **10**, 335 (1939).

[11] S. T. Martin and L. B. Headrick, J. App. Phys. **10**, 116 (1939); R. B. Nelson, R. P. Johnson and W. B. Nottingham, J. App. Phys. **10**, 335 (1939); G. R. Fonda, J. App. Phys. **10**, 408 (1939); R. P. Johnson and W. L. Davis, J. Opt. Soc. Am. **29**, 283 (1939).

brightness decreases exponentially at a rate which varies among the different types of silicates (Table I) but does not vary among different samples of the same type and does not depend on the nature, energy, or rate of arrival of the exciting particles, nor on the duration of the excitation, nor on the temperature if this is not too high. Later the brightness declines much less rapidly, and the shape of the curve in this later period varies from sample to sample and does depend on the other parameters listed—in short, the decay after the first exponential phase is like that of a typical sulphide.

In the proposed model of a silicate phosphor this basic difference is introduced by assuming that each activator atom (usually Mn) contributes *two* localized states in the forbidden region, the lower one being normally filled, the upper one empty (Fig. 2(a)). The gap between the two bands, as indicated by the long wavelength limit of the excitation spectra, is roughly 1 ev larger in the silicates than in the sulphides, and the assumption of two activator states instead of one is therefore not implausible. A quantum of luminescence light results from the transition of an electron from the upper to the lower of these two levels; this transition is assumed to be radioactive in character, little affected by external parameters, and to require an average time of the order of 10 milliseconds. Excitation and decay then proceed nearly as in the sulphides, with the essential difference that an excited electron has high probability of being captured by one of the upper impurity levels rather than by a trapping state (Fig. 2(d)). It is necessary to assume also that an upper impurity level is accessible to electrons only if the associated lower level is vacant. The decay rate will be limited at first by the rate of transition between the two impurity states (e), and later by the rate of excitation of trapped electrons up to the conduction band (f).

It is evident that this picture will account for a decay curve having the two phases described. The latter, slower decay should become relatively unimportant at high temperatures where the trapped electrons are freely re-excited and at low temperatures where they are semi-permanently bound. Experiment shows that this later component actually goes through a maximum of prominence, as compared with the exponential phase, at about room temperature.[12]

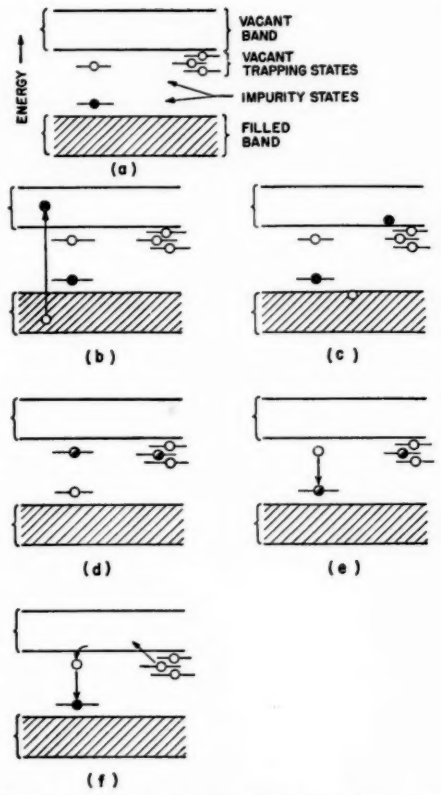

FIG. 2. (a) Scheme of energy levels for valence electrons in proposed silicate phosphor model. (b)–(f) Course of decay after excitation by a quantum in the fundamental ultraviolet absorption region of the lattice.

The silicates at liquid-air temperature do not exhibit the persistent component of decay, and after excitation in liquid air they have to be warmed to higher temperatures than do the sulphides before they yield their stored light at a comparable rate. Photoconductivity in the silicates is several orders of magnitude lower than in the sulphides.[13] These observations are consistent in indicating that with the silicates the trapping states in the region of energy just below the upper band are not so dense as with the sulphides.

The silicates, as compared with the sulphides, are only slightly affected by irradiation with a

[12] G. R. Fonda, J. App. Phys. **10**, 408 (1939).
[13] R. Hofstader, Phys. Rev. **54**, 864 (1938).

continuous spectrum of infra-red. As a silicate sample warms up after excitation in liquid air its brightness goes through a succession of maxima and minima; sulphides, in the same experiment, usually go through a single broad maximum of brightness. These facts indicate that the trapping states in the silicates are more closely bunched about particular energies-of-trapping than in the sulphides.

Conclusion

It appears that the proposed models are useful in correlating diverse properties of the sulphide and silicate phosphors, and that they offer in the variable distribution of trapping states approximately the latitude necessary for fitting quantitative observations on particular samples. Experiments on the build-up and decay of a sulphide at different temperatures, on its saturability at different temperatures, and on its infra-red absorption as a function of the several possible variables, should all yield the same distribution of trapping states. Data are at present lacking for such a test.

The picture is, of course, far too simplified. It is an *ad hoc* arrangement of concepts afforded by the energy-band theory of solids, and not a deduction from the theory. It leaves untouched such important topics as the width of the emission spectra, the specificity of certain activators and of certain poisoning additives,[14] the local balance of electric charge in the lattice, and the dependence of efficiency on temperature. The simple energy-band theory is itself known to be a poor approximation for the excited states of an insulator.[15] The writer would like to see these suggested models evaluated from a less naive viewpoint.

Readers acquainted with the literature will recognize that many of the elements of the present picture have been used since the earliest work in this field. Mechanisms specifically of the sort examined here have been the basis of several recent discussions of luminescence,[16] and their application to the decay characteristics of sulphides has been treated by Blochinzew[17] and by de Groot.[18]

It is a pleasure to acknowledge the advice and cooperation of Dr. G. R. Fonda, Dr. Frederick Seitz and Mr. C. G. Found.

[14] See, for example, J. W. Marden and G. Meister, Trans. I.E.S. **34**, 503 (1939).
[15] J. C. Slater, Trans. Faraday Soc. **34**, 828 (1938); A. von Hippel, Phys. Rev. **54**, 1096 (1938).
[16] For example, Trans. Faraday Soc. **35** (Discussion on Luminescence) (1939).
[17] D. Blochinzew, Phys. Zeits. Sowjetunion **12**, 587 (1937).
[18] W. de Groot, Physica **6**, 275 (1939).

Normal Systems With Two Caustic Lines*

M. HERZBERGER
Eastman Kodak Company, Rochester, New York
(Received June 24, 1939)

ACCORDING to the law of Malus, all the rays originating from a point in the object space form a normal system of rays in the image space. Therefore, a thorough investigation of normal systems is one of the most important problems of optical investigation.

Sturm's "conoid" is widely known. If we have an astigmatic bundle, we try to picture it in the following way: We take two line elements orthogonal to each other and to the principal ray. We put one in the first focus so that it is in the second meridional plane, and the other in the second focus, so that it is in the first meridional plane, and examine all the lines connecting any point of the first line element with any point of the second line element. If we intersect the bundle with a plane perpendicular to the principal ray, we get ellipses whose axes are proportional to the distances from the two focal points.

This conception of the Sturm conoid is simple, illuminating, and easily understood, and is therefore in every textbook of optics. It shares these advantages with the well-known theory of optical collineation. Unfortunately, it shares with it also a disadvantage, namely, that it is optically impossible. I shall show in a subsequent paper a simple way to replace these theories by others equally simple, but which give approximations which are not contradictory to optical laws. In this paper I shall answer only one problem connected with the Sturm conoid. The question arises: Does there not exist a normal system connecting two curved lines, and if so, can both curves become straight lines?

To investigate this question we shall consider two given curves $\mathbf{a}(u)$ and $\mathbf{b}(v)$, and connect every point of the first curve with every point of the second curve by a straight line. We ask what conditions must $\mathbf{a}$ and $\mathbf{b}$ fulfill if our system of straight lines is to be a normal system.

Let $\lambda(u, v)$ be the distance from point $\mathbf{a}(u)$ to point $\mathbf{b}(v)$, and let $\mathbf{s}(u, v)$ be the unit vector of the connecting line. Then we have

$$\mathbf{b}(v)-\mathbf{a}(u)=\lambda(u, v)\mathbf{s}(u, v). \tag{1}$$

The system is a normal system, if and only if

$$\mathbf{a}_u\mathbf{s}_v=\mathbf{a}_v\mathbf{s}_u, \text{ which equals zero} \tag{2}$$

since $\mathbf{a}$ does not depend on v. We now have from (1)

$$\mathbf{a}_u=-\lambda_u\mathbf{s}-\lambda\mathbf{s}_u, \tag{3}$$

$$\mathbf{a}_u\mathbf{s}_v=-\lambda\mathbf{s}_u\mathbf{s}_v=0. \tag{4}$$

From (3) we derive

$$\mathbf{a}_u\cdot\mathbf{s}=-\lambda_u, \tag{5}$$

or, differentiated,

$$\mathbf{a}_u\mathbf{s}_v=-\lambda_{uv}=0. \tag{6}$$

Integration of (6) means that there exist two functions ϕ and χ such that

$$\lambda=\phi(u)+\chi(v). \tag{7}$$

Our fundamental equation now takes the form

$$\mathbf{b}(v)-\mathbf{a}(u)=[\phi(u)+\chi(v)]\xi(u, v) \tag{8}$$

or, squared,

$$\mathbf{b}^2(v)+\mathbf{a}^2(u)-2\mathbf{b}(v)\mathbf{a}(u) =\phi^2(u)+\chi^2(v)+2\phi(u)\chi(v). \tag{9}$$

Differentiation according to u and v gives

$$\mathbf{b}_v\mathbf{a}_u=-\phi_u\chi_v. \tag{10}$$

We distinguish two cases. First, either χ or ϕ is zero. Let us assume $\chi=0$. Then we have

$$\mathbf{b}(v)-\mathbf{a}(u)=\phi(u)\mathbf{s}(u, v),\quad \mathbf{b}_v\cdot\mathbf{a}_u=0. \tag{11}$$

Let us take next a fixed point on our first curve. Then, all vectors tangential to the second curve must lie in a plane perpendicular to $\mathbf{a}_u$, and $\mathbf{b}(v)$ must be a plane curve. Now, let us reverse the picture. All vectors tangential to the first curve $\mathbf{a}(u)$ must be perpendicular to this

* Communication No. 734 from Kodak Research Laboratories.

plane. The second curve must therefore be a straight line.

Bringing our origin to the intersection point, let us choose a Cartesian coordinate system with the unit vectors, $\mathbf{i}, \mathbf{j}, \mathbf{k}$, such that k is the direction of our curves $\mathbf{a}(u)$. Then we have

$$\begin{aligned} \mathbf{a}(u) &= \alpha(u)\mathbf{k}, \\ \mathbf{b}(v) &= \beta_1(v)\mathbf{i} + \beta_2(v)\mathbf{j}. \end{aligned} \tag{12}$$

Substitution of (12) in (9) gives

$$\beta_1^2(v) + \beta_2^2(v) + \alpha^2(u) = \phi^2(u) \tag{13}$$

or

$$\begin{aligned} \beta_1^2(v) + \beta_2^2(v) &= \text{constant} = R^2, \\ \alpha^2(u) - \phi^2(u) &= R^2. \end{aligned} \tag{14}$$

Eq. (14) shows us that our curve $\mathbf{b}$ is a circle around the intersection point of the straight line with the plane of the circle. The system of normals is the normals of a toric system. Convenient variables are

$$\begin{aligned} \mathbf{a}(u) &= (-r \tan u)\mathbf{k}, \\ \mathbf{b}(v) &= (r \cos v)\mathbf{i} + (r \sin v)\mathbf{j}. \end{aligned} \tag{15}$$

The normals are given by the unit vectors $\mathbf{s}(u, v)$.

$$\mathbf{s}(u, v) = (\cos u \cos v)\mathbf{i} + (\cos u \sin v)\mathbf{j} + (\sin u)\mathbf{k}. \tag{16}$$

The wave surfaces are given by $\mathbf{a} + \lambda\mathbf{s}$ with $\lambda = -(r/\cos u) + C$, which means that

$$\mathbf{W}(u, v) = (r + C \cos u)(\cos v)\mathbf{i} + (r + C \cos u)(\sin v)\mathbf{j} + (C \sin u)\mathbf{k}, \tag{17}$$

or

$$\begin{aligned} x &= (r + C \cos u) \cos v, \\ y &= (r + C \cos u) \sin v, \\ z &= C \sin u. \end{aligned} \tag{18}$$

Elimination of u and v gives the equation of the toric surfaces belonging to our system, i.e.,

$$(x^2 + y^2 + z^2 - C^2 + r^2)^2 = 4r^2(x^2 + y^2). \tag{19}$$

We now deal with the second case, namely, that $\phi_u \chi_v \neq 0$. Let us divide (10) by ϕ_u and χ_v. We find that

$$\left(\frac{1}{\chi_v}\mathbf{b}_v\right)\left(\frac{1}{\phi_u}\mathbf{a}_u\right) = -1. \tag{20}$$

This means that the product of two vectors, of which one depends only on u, and the other depends only on v, must be constant. This is again impossible, unless one of the vector functions in brackets is constant, while the other lies in a plane, for this case not perpendicular to the first. We choose again a vector coordinate system $\mathbf{i}, \mathbf{j}, \mathbf{k}$, such that k is in the direction of our straight-line function for which we shall take again $\mathbf{a}(u)$. Then we have

$$\begin{aligned} \mathbf{a}(u) &= -\phi(u)\mathbf{k}, \\ \mathbf{b}(v) &= \beta_1(v)\mathbf{i} + \beta_2(v)\mathbf{j} + \psi(v)\mathbf{k}, \end{aligned} \tag{21}$$

if we choose our coordinate origin again at the point where the curve $\mathbf{a}(u)$ intersects our plane. We find that

$$(\mathbf{b}(v) - \mathbf{a}(u))^2 = \beta_1^2(v) + \beta_2^2(v) + (\phi(u) + \psi(v))^2 = (\phi(u) + \chi(v))^2, \tag{22}$$

or

$$\beta_1^2(v) + \beta_2^2(v) + \psi^2(v) - \chi^2(v) = 2\phi(u)(\chi(v) - \psi(v)). \tag{23}$$

For $\phi(u) \neq 0$, Eq. (13) leads to

$$\begin{aligned} \chi(v) &= \psi(v), \\ \beta_1(v) &= \beta_2(v) = 0. \end{aligned} \tag{24}$$

This is the degenerate case in which the two curves are parallel straight lines, and our system consists of all straight lines in the plane.

We have finally to investigate only the case in which one of the curves is infinite. In this case, all our rays must have a direction orthogonal to a given direction (unit vector $\mathbf{a}(u)$) and they can have all possible directions in this plane. We assume a curve $\mathbf{a}(u)$ and write

$$\begin{aligned} \mathbf{a}(u) &= \alpha_1(u)\mathbf{i} + \alpha_2(u)\mathbf{j} + \alpha_3(u)\mathbf{k}, \\ \mathbf{s}(v) &= (\cos v)\mathbf{i} + (\sin v)\mathbf{j}. \end{aligned} \tag{25}$$

The system is a normal system only if

$$\mathbf{a}_u \mathbf{s}_v = \mathbf{a}_v \mathbf{s}_u = 0,$$

or

$$\alpha_{1u} = \alpha_{2u} = 0, \tag{26}$$

or if we choose our origin conveniently,

$$\begin{aligned} \mathbf{a}(u) &= \alpha_3(u)\mathbf{k}, \\ \mathbf{s}(v) &= (\cos v)\mathbf{i} + (\sin v)\mathbf{j}. \end{aligned} \tag{27}$$

That means the second curve is a straight line perpendicular to the plane of the rays. The corresponding wave surfaces are given by $\mathbf{a}+\mu\mathbf{s}$ with

$$\mu = C \tag{28}$$

or

$$\mathbf{W}(u) = (C \cos v)\mathbf{i} + (C \sin v)\mathbf{j} + \alpha_3(u)\mathbf{k} \tag{29}$$

or

$$x^2 + y^2 = C^2. \tag{30}$$

The wave surfaces are cylindrical surfaces with the axis in the direction orthogonal to the rays.

Thus, we see that the toric and the cylindrical surfaces are the only ones in which both of the caustic surfaces degenerate into lines.

Theory of Image Errors of the Fifth Order in Rotationally Symmetrical Systems. I*

M. HERZBERGER
Eastman Kodak Company, Rochester, New York
(Received July 21, 1939)

THE designer of optical systems makes frequent use of the theory of third-order aberrations, the so-called Seidel theory, which, if intelligently used, gives an excellent starting point for investigating lens types and for obtaining an approximate solution of the problem in question. This approximation, however, says nothing about the useful aperture and the useful field that we might expect, and gives no hint about the size of the zonal errors. This problem becomes more and more important, however, the more we ask of an optical instrument with respect to field and aperture. Therefore, many optical designers have completely given up the use of the Seidel theory and have contented themselves with tracing a sufficient number of meridian rays through the system. This does not seem to be satisfactory when we come to high aperture lenses, because then the errors of the skew rays make their appearance. It is well known that a system can be perfectly corrected for all its meridian errors and yet the image can be poor. The calculation of the sine condition and the calculation of the sagittal image point on certain rays give a faint idea of the tendencies of these errors, but not much more. Two procedures of overcoming this difficulty are open. The first is to trace skew rays in a sufficient number, and the second is to develop a theory of the image errors of the fifth or higher order.

Neither procedure seems very promising. We can trace skew rays if we have the courage to undertake the considerable amount of work necessary, but it would not be easy to judge their real significance, since what counts is not the size of the aberrations of the single rays but their distribution and the amount of energy transported. Moreover, it will be a very difficult task to estimate the effect that a change of radius has on these skew rays.

The other method does not look more hopeful. The only attempt to attack the fifth-order errors has been made by K. Schwarzschild, in 1905, who gave a short survey of the figures of confusion in the image plane produced by the different image error coefficients. In 1908, Kohlchütter calculated Schwarzschild's coefficients for a system of spherical and aspherical surfaces, but the length of the resulting formulas seemed to discourage further application, and as far as the present author knows, they have not been applied since.

Moreover, there is a hidden inaccuracy in Schwarzschild's theory, which is insignificant as far as the third-order aberrations are concerned, but which must be taken into account in a correct theory of fifth-order aberrations. We want to calculate the coordinates, x_1', x_2', of the intersection point of a ray with the image plane, from the coordinates x_1x_2 of the object point and the coordinates x_3x_4 of the point where our ray meets the plane of the exit pupil. Therefore we like to know the coefficients of the development of x_1', x_2' into a power series of the x_i. Now, Schwarzschild, instead of taking x_3, x_4 as coordinates, took $\bar{x}_3$, $\bar{x}_4$, which are the coordinates of the intersection point of our ray with the sphere of radius m', having its center at the axial point of the Gaussian image plane, where m' is the axial distance between exit pupil and image point.

In recent years, the author has found an easier and more direct approach to Seidel's theory of image errors. This held out the hope that a fifth-order theory according to this development might not give rise to such dismaying difficulties. The main problem is to correlate the results as completely as possible.

We can expect a great deal from a theory of fifth-order aberration. It really means that, in all ray-tracing formulas for finite aperture and field, we have replaced sine and tangent by their first three members of the Taylor development.

$$\begin{aligned} \sin u &= u - u^3/6 + u^5/120, \\ \tan u &= u + u^3/3 + 2u^5/15. \end{aligned} \tag{1}$$

* Communication No. 735 from the Kodak Research Laboratories.

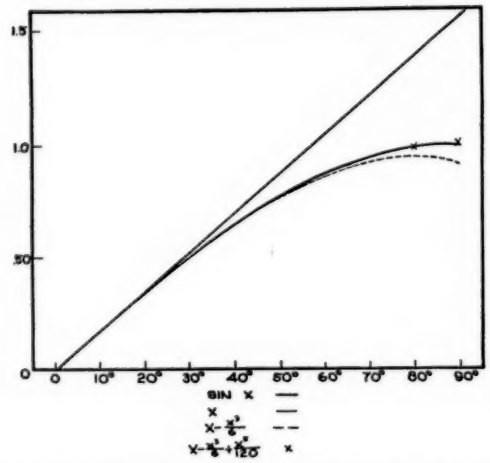

FIG. 1. The curve of sine x, and the first-, third- and fifth-order approximations.

Figures 1 and 2 show that this approximation is good enough for the sine to an angle of about 90° and for the tangent to an angle of more than 40°, which means it is quite a good approximation.

We shall now sketch the problems we want to investigate. First, we want to know the interrelations between the image error coefficients. For this purpose we assume that we know the development of the characteristics and then calculate the image error coefficients. The next step is to investigate the image errors for a curved object and a curved image surface. Another section will deal with the question of how the image errors change with a shift of the exit pupil, and how they change when we choose a different object.

I. Introduction. Image Errors and Image Coefficients

Let $\bar{x}_1$, $\bar{x}_2$ be the Cartesian coordinates of a point in the object plane (multiplied by the refractive index of the object space), and let $\bar{x}'_3$, $\bar{x}'_4$ be the coordinates of a point in the exit pupil (multiplied by the refractive index in the image space). ξ_1, ξ_2 are the direction cosines of the object ray, and ξ'_3, ξ'_4 of the image ray. Since we consider only rotationally symmetrical systems, we use as variables the following combinations of the coordinates:

$$u_1=\tfrac{1}{2}(\bar{x}_1^2+\bar{x}_2^2),\quad u_2=(\bar{x}_1\bar{x}_3+\bar{x}_2\bar{x}_4),\quad u_3=(\bar{x}_3^2+\bar{x}_4^2). \tag{I,1}$$

Hamilton's (Bruns') theory now tells us that, for a rotationally symmetrical system with its axis orthogonal to the object plane and the exit pupil, the optical path along each ray between these two planes is given by a function E of u_1, u_2, u_3 alone. (The optical path is equal to the sum of the physical lengths of the paths in each medium, multiplied by the respective indices.) If, for abbreviation, we use Einstein's notation, in which

$$A_{ik}u_iu_k=A_{11}u_1^2+2A_{12}u_1u_2+2A_{13}u_1u_3+A_{22}u_2^2+2A_{23}u_2u_3+A_{33}u_3^2, \tag{I,2}$$

we have for the characteristic function of Hamilton (the eiconal of Bruns)

$$E=E_0+\bar{A}_i\bar{u}_i+\tfrac{1}{2}\bar{A}_{ik}\bar{u}_i\bar{u}_k+\tfrac{1}{6}A_{ik\lambda}u_iu_ku_\lambda. \tag{I,3}$$

The three A_i are called the characteristic coefficients of the first order, and the $6A_{ik}$ are the characteristic coefficients of the third order. The development (I,3) shows that we have $m+3/2$ characteristic coefficients of the order $2m+1$.

According to Hamilton's theory, we now find the direction cosines of the object and image rays by setting

$$\begin{aligned}\xi_1&=-\partial E/\partial\bar{x}_1, &\quad \xi'_3&=\partial E/\partial\bar{x}'_3,\\ \xi_2&=-\partial E/\partial\bar{x}_2, &\quad \xi'_4&=\partial E/\partial\bar{x}'_4,\end{aligned} \tag{I,4}$$

or, because of (I,1)

$$\begin{aligned}-\xi_1&=\frac{\partial E}{\partial\bar{u}_1}\bar{x}_1+\frac{\partial E}{\partial\bar{u}_2}\bar{x}'_3\\ &=(\bar{A}_1+\bar{A}_{1i}\bar{u}_i+\tfrac{1}{2}\bar{A}_{1ik}\bar{u}_i\bar{u}_k)\bar{x}_1\\ &\quad+(\bar{A}_2+\bar{A}_{2i}\bar{u}_i+\tfrac{1}{2}\bar{A}_{2ik}\bar{u}_i\bar{u}_k)\bar{x}'_3,\\ \xi'_3&=\frac{\partial E}{\partial\bar{u}_2}\bar{x}_1+\frac{\partial E}{\partial\bar{u}_3}\bar{x}'_3\\ &=(\bar{A}_2+\bar{A}_{2i}\bar{u}_i+\tfrac{1}{2}\bar{A}_{2ik}\bar{u}_i\bar{u}_k)\bar{x}_1\\ &\quad+(\bar{A}_3+\bar{A}_{3i}\bar{u}_i+\tfrac{1}{2}\bar{A}_{3ik}\bar{u}_i\bar{u}_k)\bar{x}'_3.\end{aligned} \tag{I,5}$$

We need not write down in the future the equations for x_2 and x'_4, since, for reasons of rotational symmetry, they are identical with (I,5) except that we have to replace $\bar{x}_1$ by $\bar{x}_2$ and $\bar{x}'_3$ by $\bar{x}'_4$.

We can always assume that $A_2\neq 0$, because that is the condition in which to a given object ray (x_1, x_2, ξ_1, ξ_2) belongs an image ray (x'_3, x'_4,

ξ'_3, ξ'_4). That allows us to introduce new coordinates

$$x_i = \bar{A}_2 \bar{x}_i, \quad u_i = \bar{A}_2^2 \bar{u}_i \tag{I,6}$$

into (I,5). We then obtain

$$\begin{aligned} -\xi_1 &= (A_1 + A_{1i}u_i + \tfrac{1}{2}A_{1ik}u_iu_k)x_1 \\ &\quad + (1 + A_{2i}u_i + \tfrac{1}{2}A_{2ik}u_iu_k)x'_3, \\ \xi_3 &= (1 + A_{2i}u_i + \tfrac{1}{2}A_{2ik}u_iu_k)x_1 \\ &\quad + (A_3 + A_{3i}u_i + \tfrac{1}{2}A_{3ik}u_iu_k)x'_3, \end{aligned} \tag{I,7}$$

where

$$A_i = \bar{A}_i/\bar{A}_2, \quad A_{ik} = \bar{A}_{ik}/\bar{A}_2^2, \quad A_{ik\lambda} = \bar{A}_{ik\lambda}/\bar{A}_2^3. \tag{I,8}$$

Substitution of (I,6) means physically that we have replaced our system by another which has all the dimensions increased in the ratio $1 : \bar{A}_2$. But if we want to obtain the actual lengths, we must again divide by $\bar{A}_2$.

Equations (I,7) are entirely sufficient to give us all the results we want. Since we know the image ray of every object ray, Eqs. (I,7) are potentially sufficient to allow us to investigate the image of every object point.

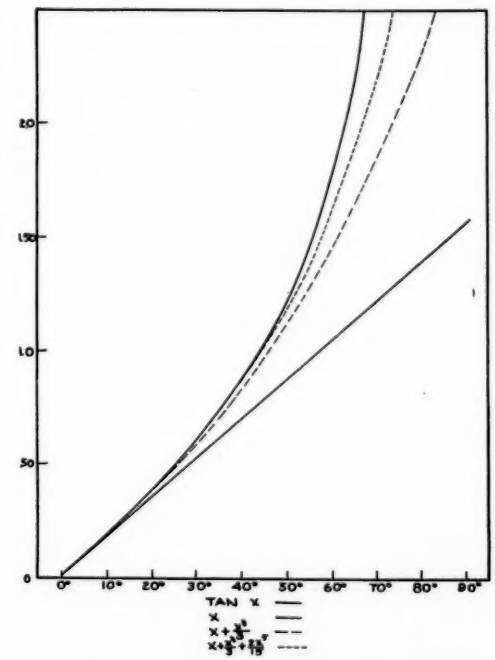

FIG. 2. The curve of tangent x, and the first-, third- and fifth-order approximations.

Now the sines and the tangents of the angles which the ray forms with the axis on object and image sides are given by

$$\begin{aligned} \sin\sigma &= (\xi_1^2 + \xi_2^2)^{\frac{1}{2}}, \quad \tan\sigma = \frac{(\xi_1^2 + \xi_2^2)^{\frac{1}{2}}}{(1 - (\xi_1^2 + \xi_2^2))^{\frac{1}{2}}}, \\ \sin\sigma' &= (\xi'^2_3 + \xi'^2_4)^{\frac{1}{2}}, \quad \tan\sigma' = \frac{(\xi'^2_3 + \xi'^2_4)^{\frac{1}{2}}}{(1 - (\xi'^2_3 + \xi'^2_4))^{\frac{1}{2}}}. \end{aligned} \tag{I,9}$$

This suggests the investigation of the expressions $\xi_1/(1-(\xi_1^2+\xi_2^2))^{\frac{1}{2}}$ and $\xi'_3/(1-(\xi'^2_3+\xi'^2_4))^{\frac{1}{2}}$ in addition to ξ'_3 and ξ'_4 (I,7). The development into a series may be represented by

$$\begin{aligned} -\Xi_1 &= \frac{\xi_1}{(1-(\xi'^2_3+\xi'^2_4))^{\frac{1}{2}}} \\ &= (B_1 + B_{1i}u_i + \tfrac{1}{2}B_{1ik}u_iu_k)x_1 \\ &\quad + (1 + B_{2i}u_i + \tfrac{1}{2}B_{2ik}u_iu_k)x'_3, \\ \Xi_3 &= \frac{\xi'_3}{(1-(\xi'^2_3+\xi'^2_4))^{\frac{1}{2}}} \\ &= (1 + B'_{2i}u_i + \tfrac{1}{2}B'_{2ik}u_iu_k)x_1 \\ &\quad + (B'_3 + B'_{3i}u_i + \tfrac{1}{2}B'_{3ik}u_iu_k)x'_3, \end{aligned} \tag{I,10}$$

where B_{ik} and B'_{ik} are functions of A_i and A_{ik}, which we must determine.

Let us now investigate the point of intersection with a plane, at the reduced distance g' from the exit pupil. We have

$$\begin{aligned} x'_{1g} &= x'_3 + \lambda\xi'_3, \qquad x'_{1g} = x'_3 + g'\Xi_3, \\ &\text{or} \\ x'_{2g} &= x'_4 + \lambda\xi'_4, \qquad x'_{2g} = x'_4 + g'\Xi_4, \\ g' &= \lambda(1-(\xi'^2_3+\xi'^2_4))^{\frac{1}{2}}. \end{aligned} \tag{I,11}$$

Substituting (I,10), we have

$$\begin{aligned} x'_{1g} &= g(1 + B'_{2i}u_i + \tfrac{1}{2}B'_{2ik}u_iu_k)x_1 \\ &\quad + g'(1/g' + B'_3 + B'_{3i}u_i + \tfrac{1}{2}B'_{3ik}u_iu_k)x'_3. \end{aligned} \tag{I,12}$$

We get the intersection point with the Gaussian image plane, if we choose $g' = -1/B'_3$. That gives

$$\begin{aligned} -B'_3x' - x_1 &= (B'_{2i}u_i + \tfrac{1}{2}B'_{2ik}u_iu_k)x_1 \\ &\quad + (B'_{3i}u_i + \tfrac{1}{2}B'_{3ik}u_iu_k)x'_3. \end{aligned} \tag{I,13}$$

Equation (I,13) shows that we have in the

first order,

$$x' = -\frac{1}{B'_3}x_1 = \beta' x_1, \tag{I,14}$$

where $\beta' = -1/B'_3$ is the object magnification. On the right side of (I,13), therefore, we find the deviation from Gaussian optics, i.e., the "image errors." We see that we have six image errors of the third order, and twelve of the fifth order: in general $(m+1)(m+2)$ errors of the $(2m+1)$ order. Since we have for each order a smaller number of characteristic coefficients than image errors, we therefore must have some relations between the B's.

In the same way, we can investigate the intersection point of our ray with an object plane in the reduced distance g' from the object-side origins. We find that

$$x_{3g} = x_1 + g'\Xi_1 = -g'[B_1 - 1/g' + B_{1i}u_i + \tfrac{1}{2}B_{1ik}u_iu_k]x_1 - g'[1 + B_{2i}u_i + \tfrac{1}{2}B_{2ik}u_iu_k]x'_3. \tag{I,15}$$

In particular, if we let $g' = 1/B_P$, we have the origin at the entrance pupil and

$$-(B_1x_3^* + x'_3) = [B_{1i}u_i + \tfrac{1}{2}B_{1ik}u_iu_k]x_1 + [B_{2i}u_i + \tfrac{1}{2}B_{2ik}u_iu_k]x'_3. \tag{I,16}$$

We see that we have in the first order

$$x'_3 = -B_1x_3^* = B'_Px_3^*, \tag{I,17}$$

where β'_P is the magnification of the entrance pupil and B_{ik} can be considered as the object-side image errors of the exit pupil. We see that there we have again $(m+1)(m+2)$ image errors of the order $(2m+1)$, all of which we must be able to express with the help of our A_{2k}.

Now, if we develop to the fifth order, we have

$$\Xi_1 = \frac{\xi_1}{(1-(\xi^2_1+\xi^2_2))^{\frac{1}{2}}} = \xi_1[1 + \tfrac{1}{2}(\xi^2_1+\xi^2_2) + \tfrac{3}{8}(\xi^2_1+\xi^2_2)^2],$$
$$\Xi'_3 = \frac{\xi'_3}{(1-(\xi'^2_3+\xi'^2_4))^{\frac{1}{2}}} = \xi'_3[1 + \tfrac{1}{2}(\xi'^2_3+\xi'^2_4) + \tfrac{3}{8}(\xi'^2_3+\xi'^2_4)^2]. \tag{I,18}$$

Eq. (I,7) gives

$$\tfrac{1}{2}(\xi^2_1+\xi^2_2) = A_1{}^2u_1 + A_1u_2 + u_3 + 2A_1A_{11}u_1{}^2 + (3A_1A_{12}+A_{11})u_1u_2 + 2(A_1A_{13}+A_{12})u_1u_3 + (A_1A_{22}+A_{12})u_2{}^2 + (A_1A_{23} + 2A_{22}+A_{13})u_2u_3 + 2A_{23}u_3{}^2 \tag{I,19}$$

and similarly for ξ'_3 and ξ'_4. Substitution in (I,18) and comparison with (I,10) gives for the first-order coefficients

$$B_1 = A_1, \quad B'_3 = A_3, \tag{I,20}$$

and for the third-order coefficients,

$$\begin{aligned} B_{11} &= A_{11} + A_1{}^3, & & \\ B_{12} &= A_{12} + A_1{}^2, & B'_{21} &= A_{12} + 1, \\ B_{13} &= A_{13} + A_1, & B'_{22} &= A_{22} + A'_3, \\ B_{21} &= A_{12} + A_1{}^2, & B'_{23} &= A_{23} + A'^2_3, \\ B_{22} &= A_{22} + A_1, & B'_{31} &= A_{13} + A'_3, \\ B_{23} &= A_{23} + 1, & B'_{32} &= A_{23} + A'^2_3, \\ & & B'_{33} &= A_{33} + A'^3_3, \end{aligned} \tag{I,21}$$

and for the fifth-order coefficients,

$$\begin{aligned} B_{111} &= A_{111} + 6A_1{}^2A_{11} + 3A_1{}^5, \\ B_{112} &= A_{112} + 4A_1{}^2A_{12} + 2A_1A_{11} + 3A_1{}^4, \\ B_{113} &= A_{113} + 3A_1{}^2A_{13} + 2A_1A_{12} + A_{11} + 3A_1{}^3, \\ B_{122} &= A_{122} + 2A_1{}^2A_{22} + 4A_1A_{12} + 3A_1{}^3, \\ B_{123} &= A_{123} + A_1{}^2A_{23} + 2A_1(A_{13}+A_{22}) + A_{12} + 3A_1{}^2, \\ B_{133} &= A_{133} + 4A_1A_{23} + 2A_{13} + 3A_1, \\ B_{211} &= A_{112} + 2A_1{}^2A_{12} + 4A_1A_{11} + 3A_1{}^4, \\ B_{212} &= A_{122} + A_1{}^2A_{22} + 4A_1A_{12} + A_{11} + 3A_1{}^3, \\ B_{213} &= A_{123} + A_1{}^2A_{23} + 2A_1A_{13} + 3A_{12} + 3A_1{}^2, \\ B_{222} &= A_{222} + 4A_1A_{22} + 2A_{12} + 3A_1{}^2, \\ B_{223} &= A_{223} + 2A_1A_{23} + (3A_{22}+A_{13}) + 3A_1, \\ B_{233} &= A_{233} + 6A_{23} + 3, \end{aligned}$$

$$\begin{aligned} B'_{211} &= A_{112} + 6A_{12} + 3, \\ B'_{212} &= A_{122} + 2A_3A_{12} + 3A_{22} + A_{13} + 3A_3, \\ B'_{213} &= A_{123} + A_3{}^2A_{12} + 2A_3A_{13} + 3A_{23} + 3A_3{}^2, \\ B'_{222} &= A_{222} + 4A_3A_{22} + 2A_{23} + 3A_3{}^2, \\ B'_{223} &= A_{223} + A_3{}^2A_{22} + 4A_3A_{23} + A_{33} + 3A_3{}^3, \\ B'_{233} &= A_{233} + 2A_3{}^2A_{23} + 4A_3A_{33} + 3A_3{}^4, \\ B'_{311} &= A_{113} + 4A_3A_{12} + 2A_{13} + 3A_3, \\ B'_{312} &= A_{123} + A_3{}^2A_{12} + 2A_3(A_{13}+A_{22}) + A_{23} + 3A_3{}^2, \\ B'_{313} &= A_{133} + 3A_3{}^2A_{13} + 2A_3A_{23} + A_{33} + 3A_3{}^3, \\ B'_{322} &= A_{223} + 2A_3{}^2A_{22} + 4A_3A_{23} + 3A_3{}^3, \\ B'_{323} &= A_{233} + 4A_3{}^2A_{23} + 2A_3A_{33} + 3A_3{}^4, \\ B'_{333} &= A_{333} + 6A_3{}^2A_{33} + 3A_3{}^5. \end{aligned} \tag{I,22}$$

We draw the attention of our readers to the fact that we cannot interchange the indices in the B' of the fifth and higher orders, whereas an interchange of indices in the A's is permitted:

$$\begin{aligned} &A_{i\kappa\lambda}=A_{\kappa i\lambda},\\ &B_{i\kappa\lambda}\text{ not necessarily}=B_{\kappa i\lambda}. \end{aligned} \qquad \text{(I,23)}$$

We can and will divide our image errors into groups according to the order of aperture and field which they contain in Eq. (I,13). There we can say,

	Order in Field	Order in Aperture
x_1	1	0
x_3	0	1
u_1	2	0
u_2	1	1
u_3	0	2

Then we can divide our third-order aberrations into four groups, and give a name to each of the errors, and the same procedure can be followed for the fifth-order aberrations.

Coefficient	Order in Field	Order in Aperture	Name
B'_{21}	3	0	Distortion
B'_{22}, B'_{31}	2	1	Field errors
B'_{23}, B'_{32}	1	2	Coma
B'_{33}	0	3	Spherical aberration

In the same way, we divide the fifth-order errors.

Coefficient	Order in Field	Order in Aperture	Name
B'_{211}	5	0	Zonal distortion
B'_{212}, B'_{311}	4	1	Zonal field
B'_{222}, B'_{213}, B'_{312}	3	2	"Asymmetry"
B'_{223}, B'_{313}, B'_{322}	2	3	"Deformation"
B'_{233}, B'_{323}	1	4	Zonal coma
B'_{333}	0	5	Zonal spherical aberration

We shall discuss in a following paper each group of errors separately, as has been done for the Seidel theory.

Let us now give the connection between the object and image side errors. For this purpose we substitute (20) in (21). We find that

$$\begin{aligned} &B_{11}=A_{11}+B_1^3, && \\ &B_{12}=A_{12}+B_1^2=B_{21}, && B'_{21}=A_{12}+1,\\ &B_{13}=A_{13}+B_1, && B'_{31}=A_{13}+B'_3,\\ &B_{22}=A_{22}+B_1, && B'_{22}=A_{22}+B'_3,\\ &B_{23}=A_{23}+1, && B'_{23}=A_{23}+B'^2_3=B'_{32},\\ & && B'_{33}=A_{33}+B'^3_3. \end{aligned} \qquad \text{(I,24)}$$

We see that for the third-order coefficients we are allowed to interchange the indices. We have

$$B'_{23}-B'_{32}=0, \quad B_{21}-B_{12}=0. \qquad \text{(I,25)}$$

Between the object and image errors there are the connecting equations

$$\begin{aligned} &B'_{23}-B_{23}=B'^2_3-1=\alpha_1,\\ &B'_{22}-B_{22}=B'_{13}-B_{13}=B'_3-B_1=\alpha_2,\\ &B'_{12}-B_{12}=1-B_1^2=\alpha_3. \end{aligned} \qquad \text{(I,26)}$$

Before we substitute (24) in (22) we shall introduce the image coefficients C_{ik} with permutable indices,

$$\begin{aligned} &C_{111}=A_{111}-3B_1^5, && && \\ &C_{112}=A_{112}-3B_1^4, && && C'_{112}=A_{112}-3,\\ &C_{113}=A_{113}-3B_1^3, && C_{122}=A_{122}-3B_1^3, && \\ & && && C'_{122}=A_{122}-3B_3, && C'_{113}=A_{113}-3B_3,\\ &C_{123}=A_{123}-3B_1^2, && C_{222}=A_{222}-3B_1^2, && C'_{222}=A_{222}-3B_3^2, && C'_{123}=A_{123}-3B_3^2,\\ &C_{133}=A_{133}-3B_1, && C_{223}=A_{223}-3B_1, && C'_{223}=A_{223}-3B_3^3, && C'_{133}=A_{133}-3B_3^3,\\ & && C_{233}=A_{233}-3, && C'_{233}=A_{233}-3B_3^4,\\ & && && C'_{333}=A_{333}-3B_3^5. \end{aligned} \qquad \text{(I,27)}$$

Substituting this in (I,22) we find that

$$\begin{aligned} &B_{111}=C_{111}+6B_1^2B_{11}, && \\ &B_{112}=C_{112}+4B_1^2B_{12}+2B_1B_{11}, && B_{211}=C_{112}+2B_1^2B_{12}+4B_1B_{11},\\ &B_{113}=C_{113}+3B_1^2B_{13}+2B_1B_{12}+B_{11}, && B_{122}=C_{122}+2B_1^2B_{22}+4B_1B_{12},\\ & && B_{212}=C_{122}+B_1^2B_{22}+4B_1B_{12}+B_{11},\\ &B_{123}=C_{123}+B_1^2B_{23}+2B_1(B_{13}+B_{22})+B_{12}, && B_{213}=C_{123}+B_1^2B_{23}+2B_1B_{13}+3B_{12},\\ & && B_{222}=C_{222}+4B_1B_{22}+2B_{12},\\ &B_{133}=C_{133}+4B_1B_{23}+2B_{13}, && B_{223}=C_{223}+2B_1B_{23}+(3B_{22}+B_{13}),\\ & && B_{233}=C_{233}+6B_{23}, \end{aligned} \qquad \text{(I,28)}$$

and on the image side

$$
\begin{aligned}
&B'_{211}=C'_{112}+6B'_{12},\\
&B'_{212}=C'_{122}+2B'_3B'_{12}+3B'_{22}+B'_{13}, \qquad B'_{311}=C'_{113}+4B'_3B'_{12}+2B'_{13},\\
&B'_{222}=C'_{222}+4B'_3B'_{22}+2B'_{23}, \qquad B'_{213}=C'_{123}+B'^2_3B'_{12}+2B'_3B'_{13}+3B'_{23},\\
&\qquad\qquad B'_{312}=C'_{123}+B'^2_3B'_{12}+2B'_3(B'_{13}+B'_{22})+B'_{23},\\
&B'_{223}=C'_{223}+B'^2_3B'_{22}+4B'_3B'_{23}+B'_{33}, \qquad B'_{322}=C'_{223}+2B'^2_3B'_{22}+4B'_3B'_{23},\\
&\qquad\qquad B'_{313}=C'_{133}+3B'^2_3B'_{13}+2B'_3B'_{23}+B'_{33},\\
&B'_{233}=C'_{233}+2B'^2_3B'_{23}+4B'_3B'_{33}, \qquad B'_{323}=C'_{233}+4B'^2_3B'_{23}+2B'_3B'_{33},\\
&\qquad\qquad B'_{333}=C'_{333}+6B'^2_3B'_{33}.
\end{aligned}
\tag{I,29}
$$

On the object and image sides we have three connecting equations each, namely,

$$
\begin{aligned}
&B_{311}-B_{112}=2B_1(B_{11}-B_1B_{12}), \qquad B'_{312}-B'_{213}=2(B'_3B'_{22}-B'_{23}),\\
&B_{212}-B_{122}=B_{11}-B_1{}^2B_{22}, \qquad B'_{322}-B'_{223}=B'^2_3B'_{22}-B'_{33},\\
&B_{213}-B_{123}=2(B_{12}-B_1B_{22}), \qquad B'_{323}-B'_{233}=2B'_3(B'_3B'_{23}-B'_{33}),
\end{aligned}
\tag{I,30}
$$

and the object and image coefficients are connected by

$$
\begin{aligned}
&C'_{112}-C_{112}=3(B_1{}^4-1) &&=\gamma_5,\\
&C'_{122}-C_{122}=C'_{113}-C_{113}=3(B_1{}^3-B'_3) &&=\gamma_4,\\
&C'_{123}-C_{123}=C'_{222}-C_{222}=3(B_1{}^2-B'^2_3) &&=\gamma_3,\\
&C'_{223}-C_{223}=C'_{133}-C_{133}=3(B_1-B'^3_3) &&=\gamma_2,\\
&C'_{233}-C_{233}=3(1-B'^4_3) &&=\gamma_1.
\end{aligned}
\tag{I,31}
$$

II. Curvature of Object and Curvature of Field

Let us now assume that both object and image surfaces are curved. The equations of both may be written in a general form (the coefficients being standardized to have the dimension of a reciprocal length) thus,

$$
\begin{aligned}
z_c&=\tfrac{1}{2}D_1(x_c{}^2+y_c{}^2)+\tfrac{1}{8}D_2{}^3(x_c{}^2+y_c{}^2)^2\\
&=D_1u_c+\tfrac{1}{2}D_2{}^3u_c{}^2, \qquad \text{(II,1)}\\
z'_c&=D_3u'_c+\tfrac{1}{2}D_4{}^3u'^2_c.
\end{aligned}
$$

In writing these equations we must keep in mind that we have divided all lengths by $\bar{A}_2$ (I,6) so that in real coordinates we have

$$
\begin{aligned}
\bar{z}_c&=(D_1/\bar{A}_2)\bar{u}_c+\tfrac{1}{2}(D_2/\bar{A}_2)^3\bar{u}_c{}^2,\\
\bar{z}'_c&=(D_3/\bar{A}_2)\bar{u}'_c+\tfrac{1}{2}(D_4/\bar{A}_2)^3\bar{u}'^2_c.
\end{aligned}
\qquad \text{(II,2)}
$$

Equation (II,1) represents a spherical object (image), if

$$D_1=D_2 \quad (D_3=D_4), \qquad \text{(II,3)}$$

with the curvature $D_1/\bar{A}_2(D_3/\bar{A}_2)$. Eq. (II,1) represents a paraboloid if $D_2=0$ ($D_4=0$). In the general case, (II,1) represents

An ellipsoid for $(D_1/D_2)>0$ $((D_3/D_4)>0)$,
A hyperboloid for $(D_1/D_2)<0$ $((D_3/D_4)<0)$, (II,4)

the main axes being

$$a=D_1{}^2/D_2{}^3, \quad b=((-)D_1/D_2{}^3)^{\frac{1}{2}}, \qquad \text{(II,5)}$$

the minus sign representing the hyperbola.

Let us now write again

$$
\begin{aligned}
-B'_3x'-x_1=&[B'_{2i}u_i+\tfrac{1}{2}B'_{2i\kappa}u_iu_\kappa]x_1\\
&+[B'_{3i}u_i+\tfrac{1}{2}B'_{3i\kappa}u_iu_\kappa]x'_3,
\end{aligned}
$$

and

$$
\begin{aligned}
-B'_3x'_c-x_c=&[B'_{2ic}u_{ic}+\tfrac{1}{2}B'_{2i\kappa c}\,u_{ic}\,u_{\kappa c}]x_c\\
&+[B'_{3ic}u_{ic}+\tfrac{1}{2}B'_{3i\kappa c}\,u_{ic}\,u_{\kappa c}]x'_{3c}.
\end{aligned}
\qquad \text{(II,6)}
$$

We obtain easily

$$x_c=x_1+z_c\Xi_1, \quad x'_c=x'+z'_c\Xi_3. \qquad \text{(II,7)}$$

In substituting Ξ_1 and Ξ_3 from (I,10), and using (II,1), we can express x_c and x'_c in terms of x alone. The evaluation gives finally

$$
\begin{aligned}
x_c=&x_1-(D_1B_1u_1x_1+D_1u_1x'_3)\\
&-\tfrac{1}{2}[(2D_1B_{11}-4D_1{}^2B_1{}^2+D_2{}^3B_1)u_1{}^2\\
&+2(D_1B_{12}-D_1{}^2B_1)u_1u_2+2D_1B_{13}u_1u_3]x_1\\
&-\tfrac{1}{2}[(2D_1B_{12}-4D_1{}^2B_1+D_2{}^3)u_1{}^2\\
&+2(D_1B_{22}-D_1{}^2)u_1u_2+2D_1B_{23}u_1u_3]x'_3,
\end{aligned}
\qquad \text{(II,8)}
$$

and

$$\begin{aligned} u_{1c} &= u_1 - 2B_1D_1u_1^2 - D_1u_1u_2, \\ u_{2c} &= u_2 - D_1B_1u_1u_2 - 2D_1u_1u_3, \\ u_{3c} &= u_3. \end{aligned} \tag{II,9}$$

In the same way, using the first equations (II,6), (II,1) and the second equation, (I,10), we can evaluate x'_{1c} and obtain after a not-too-difficult computation

$$\begin{aligned} -B'_3x'_c - x_c = &\left[\left(B'_{21} - \frac{D_3}{B'_3}\right)u_1 + B'_{22}u_2 + B'_{23}u_3\right]x_1 \\ &+ [(B'_{13} - D_3)u_1 + B'_{23}u_2 + B'_{33}u_3]x'_3 \\ &+ \left\{\frac{1}{2}\left[B'_{212} - \frac{D_3}{B'_3}\left(6B'_{12} - 4\frac{D_3}{B'_3}\right) - \frac{D_4}{B'^2_3}\right]u_1^2\right. \\ &+ \left[B'_{212} - \frac{D_3}{B'_3}(3B'_{22} + B'_{13} - D_3)\right]u_1u_2 \\ &+ \left[B'_{213} - 3\frac{D_3}{B'_3}B'_{23}\right]u_1u_3 + \tfrac{1}{2}\left[B'_{222} - 2\frac{D_3}{B'_3}B'_{23}\right]u_2^2 \\ &+ \left.\left[B'_{223} - \frac{D_3}{B'_3}B'_{33}\right]u_2u_3 + \tfrac{1}{2}B'_{233}u_3^2\right\}x_1 \\ &+ \left\{\frac{1}{2}\left[B'_{311} - \frac{D_3}{B'_3}(2B'_{13} + 4B'_3B'_{12} - 4D_3)\right]u_1^2\right. \\ &+ \left[B'_{312} - \frac{D_3}{B'_3}(B'_{23} + B'_3(2B'_{22} + B'_{13}) - D_3)\right]u_1u_2 \\ &+ \left[B'_{313} - \frac{D_3}{B'_3}(B'_{33} + 2B'_3B'_{23})\right]u_1u_3 \\ &+ \tfrac{1}{2}[B'_{322} - D_3B'_{23}]u_2^2 + [B'_{323} - D_3B'_{33}]u_2u_3 \\ &\left. + \tfrac{1}{2}B'_{333}u_3^2]\right\}x'_3. \end{aligned} \tag{II,10}$$

Let us substitute (II,8, 9, and 10) in the second equation, (II,6), and compare it member by member with the first equation, (II,6). We then obtain the following equations which give the image errors for both curved object and image.

We find for the third-order terms:

$$\begin{aligned} B'_{12c} &= B'_{12} + D_1B_1 - D_3/B'_3, \\ B'_{13c} &= B'_{13} + D_1 - D_3, \\ B'_{22c} &= B'_{22}, \\ B'_{23c} &= B'_{23}, \\ B'_{33c} &= B'_{33}, \end{aligned} \tag{II,11}$$

and for the fifth-order terms

$$\begin{aligned} B'_{211c} = &B'_{211} + 2D_1B_4 + 6B'_{12}\left(B_1D_1 - \frac{D_3}{B'_3}\right) \\ &+ \left(B_1D_2{}^3 - \frac{D_4{}^3}{B'^3_3}\right) \\ &+ 2\left(B_1D_1 - \frac{D_3}{B'_3}\right)\left(B_1D_1 - \frac{2D_3}{B'_3}\right), \\ B'_{212c} = &B'_{212} + D_1B_{12} + D_1(B'_{12} + 2B_1B'_{22}) \\ &- \frac{D_3}{B'_3}(B'_{13} + 3B'_{22}) + \frac{D_3}{B'_3}(D_3 - D_1), \\ B'_{311c} = &B'_{311} + 2D_1B_{12} + 2D_1(B'_{12} + 2B_1B'_{13}) \\ &- 2\frac{D_3}{B'_3}(B'_{13} + 2B'_3B'_{12}) + \left(D_2{}^3 - \frac{D_4{}^3}{B'^2_3}\right) \\ &+ 2\left(\frac{D_3}{B'_3} - B_1D_1\right)(2D_3 - D_1), \\ B'_{213c} = &B'_{213} + D_1B_{13} + D_1(2B'_{22} + B_1B'_{23}) \\ &- 3D_3B'_{23}/B'_3, \\ B'_{222c} = &B'_{222} - 2D_3B'_{23}/B'_3, \\ B'_{312c} = &B'_{312} + D_1B_{22} + D_1(B'_{13} + B'_{22} + B_1B'_{23}) \\ &- (D_3/B'_3)(B'_{23} + B'_3(B'_{13} + 2B'_{22})) \\ &+ D_3(D_3 - D_1), \\ B'_{223c} = &B'_{223} - D_3B'_{33}/B'_3, \\ B'_{313c} = &B'_{313} + D_1B_{23} + 3D_1B'_{23} \\ &- (D_3/B'_3)(B'_{33} + 2B'_3B'_{23}), \\ B'_{322c} = &B'_{322} - 2D_3B'_{23}, \\ B'_{233c} = &B'_{233}, \\ B'_{323c} = &B'_{323} - D_3B'_{33}, \\ B'_{333c} = &B'_{333}. \end{aligned} \tag{II,12}$$

Sometimes the question has been raised whether a curved diaphragm would be of any service. We assume that

$$z^* = \tfrac{1}{2}E_3(x^*{}_3{}^2 + y^*{}_3{}^2) = E_3u^*{}_3. \tag{II,13}$$

We find that

$$\begin{aligned} x^*_3 &= x'_3 + E_3u_3\Xi_3 = E_3u_3x_1 + (1+E_3B'_3u_3)x'_3), \\ u^*_1 &= u_1, \\ u^*_2 &= 2E_3u_3u_1 + (1+E_3B'_3u_3)u_2, \\ u^*_3 &= u_3 + E_3u_2u_3 + 2E_3B'_3u_3^2. \end{aligned} \tag{II,14}$$

Substituting

$$\begin{aligned} -B'_3x' - x_1 = &[B^{*\prime}_{2i}u^*_i + \tfrac{1}{2}B^{*\prime}_{2i\kappa}u^*_iu^*_\kappa]x_1 \\ &+[B^{*\prime}_{3i}u^*_i + \tfrac{1}{2}B^{*\prime}_{3i\kappa}u^*_iu^*_\kappa]x^*_3, \end{aligned} \tag{II,15}$$

and comparison with (II,6) gives

$$\begin{aligned} &B^{*\prime}_{12} = B'_{12}, \quad B^{*\prime}_{23} = B'_{23}, \\ &B^{*\prime}_{22} = B'_{22}, \quad B^{*\prime}_{33} = B'_{33}. \\ &B^{*\prime}_{13} = B'_{13}, \end{aligned} \tag{II,16}$$

That means that curvature of the diaphragm has no influence on the Seidel aberrations. However, in the fifth order we obtain

$$\begin{aligned} &B^{*\prime}_{211} = B'_{211}, && B^{*\prime}_{212} = B'_{212}, && B^{*\prime}_{311} = B'_{311}, \\ &B^{*\prime}_{213} = B'_{213} - E_3(2B'_{22} + B'_{13}), && B^{*\prime}_{222} = B'_{222}, && B^{*\prime}_{312} = B'_{312}, \\ &B'_{223} = B'_{223} - E_3(2B'_{23} + B'_3B'_{22}), && B^{*\prime}_{313} = B'_{313} - E_3(2B'_{23} + B'_3B'_{13}), && B^{*\prime}_{322} = B'_{322}, \\ &B^{*\prime}_{233} = B'_{233} - 2E_3(B'_{33} + 2B'_3B'_{23}), && B^{*\prime}_{323} = B'_{323} - E_3(B'_{33} + 2B'_3B'_{23}), && B^{*\prime}_{333} = B'_{333} - 6E_3B'_3B'_{33}. \end{aligned} \tag{II,17}$$

III. Shifting of Object and Stop

In this section, we want to investigate how our image errors change as we shift object and stop, and thus find for the fifth-order expressions corresponding to the change of Seidel aberrations with this shift.

First, we investigate the effect of shifting the diaphragm. Let us express the coordinates for the new diaphragm by a boldface Roman letter.

If we shift the diaphragm the optical distance k', we have

$$\bar{x}_1 = \mathring{x}_1, \quad \bar{x}_3 = \mathring{x}_3 + k'\Xi'_3 \tag{III,1}$$

or, considering (I,6)

$$x_3/A_2 = \mathbf{x}_3/\mathbf{A}_2 + k'\Xi'_3, \quad x_1/A_1 = \mathbf{x}_1/\mathbf{A}_2. \tag{III,2}$$

Let us put, for abbreviation,

$$\kappa_3 = A_2/\mathbf{A}_2, \quad \lambda_3 = k'A_2, \tag{III,3}$$

and we find, using (I,10), that

$$\begin{aligned} x_3 &= \kappa_3\mathbf{x}_3 + \lambda_3\Xi'_3 = \kappa_3\mathbf{x}_3 + \lambda_3(1 + \mathbf{B}'_{2i}\mathbf{u}_i + \tfrac{1}{2}\mathbf{B}'_{2i\kappa}\mathbf{u}_i\mathbf{u}_\kappa)\mathbf{x}_1 + \lambda_3(\mathbf{B}'_3 + \mathbf{B}'_{3i}\mathbf{u}_i + \tfrac{1}{2}\mathbf{B}'_{3i\kappa}\mathbf{u}_i\mathbf{u}_\kappa)\mathbf{x}_3 \\ &= \lambda_3x_1 + (\kappa_3 + \mathbf{B}'_3\lambda_3)\mathbf{x}_3 + \lambda_3(\mathbf{B}'_{2i}\mathbf{u}_i + \tfrac{1}{2}\mathbf{B}'_{2i\kappa}\mathbf{u}_i\mathbf{u}_\kappa)x_1 + \lambda_3(\mathbf{B}'_3 + \mathbf{B}'_{3i}\mathbf{u}_i + \tfrac{1}{2}\mathbf{B}'_{3i\kappa}\mathbf{u}_i\mathbf{u}_\kappa)\mathbf{x}_3 \\ x_1 &= \kappa_3\mathbf{x}_1. \end{aligned} \tag{III,4}$$

In the first order we have, therefore

$$x_3 = \lambda_3\mathbf{x}_1 + (\kappa_3 + \mathbf{B}'_3\lambda_3)\mathbf{x}_3, \quad x_1 = \kappa_3\mathbf{x}_{13}, \tag{III,5}$$

and, moreover,

$$\Xi_3 = x_1 + B'_3x_3 = \mathbf{x}_1 + \mathbf{B}'_3\mathbf{x}_3. \tag{III,6}$$

Substituting (III,5) in (6) gives

$$\mathbf{B}'_3 = B'_3, \quad \kappa_3 + B'_3\lambda_3 = 1. \tag{III,7}$$

The first equation is obvious, since the magnification of the object cannot depend on shifting the stop. If we substitute (III,5) in the first equation, (I,10),

$$-\Xi_1 = B_1x_1 + x'_3 = \mathbf{B}_1\mathbf{x}_1 + \mathbf{x}'_3, \tag{III,8}$$

we find that

$$B_1\kappa_3 + \lambda_3 = \mathbf{B}_1. \tag{III,9}$$

Eqs. (III,9) and (III,7) allow us to calculate κ and λ if the change of B_1, or geometrically speaking, the change of stop magnification, is known, thus

$$\kappa_3 = \frac{1 - \mathbf{B}_1B'_3}{1 - B_1B'_3}, \quad \lambda_3 = \frac{\mathbf{B}_1 - B_1}{1 - B_1B'_3}. \tag{III,10}$$

If we now substitute (III,7) in (III,4), we obtain finally

$$x_1 = \kappa_3 \mathbf{x}_1, \quad x_3 = \lambda_3 \mathbf{x}_1 + \mathbf{x}_3 + \lambda_3(\mathbf{B}'_{2i}\mathbf{u}_i + \tfrac{1}{2}\mathbf{B}'_{2i\kappa}\mathbf{u}_i\mathbf{u}_\kappa)\mathbf{x}_1 + \lambda_3(\mathbf{B}'_{3i}\mathbf{u}_i + \tfrac{1}{2}\mathbf{B}'_{3i\kappa}\mathbf{u}_i\mathbf{u}_\kappa)\mathbf{x}'_3 \qquad \text{(III,11)}$$

and

$$\begin{aligned} u_1 &= \kappa_3^2 \mathbf{u}_1, \\ u_2 &= 2\kappa_3\lambda_3\mathbf{u}_1 + \kappa_3\mathbf{u}_2 + \kappa_3\lambda_3(2\mathbf{B}'_{2i}u_i u_1 + \mathbf{B}'_{3i}\mathbf{u}_i\mathbf{u}_2), \\ u_3 &= \lambda_3^2\mathbf{u}_1 + \lambda_3\mathbf{u}_2 + \mathbf{u}_3 + \lambda_3[\mathbf{B}'_{2i}u_i(2\lambda_3\mathbf{u}_1 + \mathbf{u}_2) + \mathbf{B}'_{3i}u_i(\lambda_3\mathbf{u}_2 + 2\mathbf{u}_3)]. \end{aligned} \qquad \text{(III,12)}$$

Let us substitute this in

$$\begin{aligned} \Xi'_3 &= [1 + B'_{2i}u_i + \tfrac{1}{2}B'_{2i\kappa}u_i u_\kappa]x_1 + [B'_3 + B'_{3i}u_i + \tfrac{1}{2}B'_{3i\kappa}u_i u_\kappa]x'_3 \\ &= [1 + \mathbf{B}'_{2i}\mathbf{u}_i + \tfrac{1}{2}\mathbf{B}'_{2i\kappa}\mathbf{u}_i\mathbf{u}_\kappa]\mathbf{x}_1 + [\mathbf{B}'_3 + \mathbf{B}'_{3i}\mathbf{u}_i + \tfrac{1}{2}\mathbf{B}'_{3i\kappa}\mathbf{u}_i\mathbf{u}_\kappa]\mathbf{x}'_3 \end{aligned} \qquad \text{(III,13)}$$

and compare them member by member. We obtain, for the Siedel errors, the well-known formulas

$$\begin{aligned} \kappa_3\mathbf{B}'_{12} &= \kappa_3^3 B'_{12} + \kappa_3^2\lambda_3(2B'_{22} + B'_{13}) + 3\kappa_3\lambda_3^2 B'_{23} + \lambda_3^3 B'_{33}, \\ \kappa_3\mathbf{B}'_{13} &= \kappa_3^2 B'_{13} + 2\kappa_3\lambda_3 B'_{23} + \lambda_3^2 B'_{33}, \\ \kappa_3\mathbf{B}'_{22} &= \kappa_3^2 B'_{22} + 2\kappa_3\lambda_3 B'_{23} + \lambda_3^2 B'_{33}, \\ \kappa_3\mathbf{B}'_{23} &= \kappa_3 B'_{23} + \lambda_3 B'_{33}, \\ \kappa_3\mathbf{B}'_{33} &= B'_{33}, \end{aligned} \qquad \text{(III,14)}$$

and for the fifth-order errors, we find

$$\begin{aligned}
\kappa_3\mathbf{B}'_{211} &= \kappa_3^5 B'_{211} + \kappa_3^4\lambda_3(B'_{311} + 4B'_{212}) + 2\kappa_3^3\lambda_3^2[B'_{213} + 2(B'_{222} + B'_{312})] \\
&\quad + 2\kappa_3^2\lambda_3^3[2(B'_{223} + B'_{322}) + B'_{313}] + \kappa_3\lambda_3^4(B'_{233} + 4B'_{323}) + \lambda_3^5 B'_{333} + 2\kappa_3\lambda_3\mathbf{B}'_{12}(\mathbf{B}'_{13} + 2B'_{22}), \\
\kappa_3\mathbf{B}'_{212} &= \kappa_3^4 B'_{212} + \kappa_3^3\lambda_3(B'_{213} + 2B'_{222} + B'_{312}) + \kappa_3^2\lambda_3^2(3B'_{223} + B'_{313} + 2B'_{322}) + \kappa_3\lambda_3^3(B'_{233} + 3B'_{323}) \\
&\quad + \lambda_3^4 B'_{333} + 2\kappa_3\lambda_3[\mathbf{B}'_{12}\mathbf{B}'_{23} + \mathbf{B}'_{22}(\mathbf{B}'_{13} + \mathbf{B}'_{22})], \\
\kappa_3\mathbf{B}'_{311} &= \kappa_5^4 B'_{311} + 4\kappa_3^3\lambda_3 B'_{312} + 2\kappa_3^2\lambda_3^2(B'_{313} + 2B'_{322}) + 4\kappa_3\lambda_3^3 B'_{323} \\
&\quad + \lambda_3^4 B'_{333} + 2\kappa_3\lambda_3(\mathbf{B}'^2_{13} + 2\mathbf{B}'_{12}\mathbf{B}'_{23}), \\
\kappa_3\mathbf{B}'_{213} &= \kappa_3^3 B'_{213} + \kappa_3^2\lambda_3(2B'_{223} + B'_{313}) + \kappa_3\lambda_3^2(B'_{233} + 2B'_{323}) \\
&\quad + \lambda_3^3 B'_{333} + \kappa_3\lambda_3[\mathbf{B}'_{12}\mathbf{B}'_{33} + \mathbf{B}'_{22}(3\mathbf{B}'_{13} + 2\mathbf{B}'_{22})], \\
\kappa_3\mathbf{B}'_{222} &= \kappa_3^3 B'_{222} + \kappa_3^2\lambda_3(2B'_{223} + B'_{322}) + \kappa_3\lambda_3^2(B'_{233} + 2B'_{323}) + \lambda_3^3 B'_{333} + 6\kappa_3\lambda_3\mathbf{B}'_{22}\mathbf{B}'_{23}, \\
\kappa_3\mathbf{B}'_{312} &= \kappa_3^3 B'_{312} + \kappa_3^2\lambda_3(B'_{313} + 2B'_{322}) + 3\kappa_3\lambda_3^2 B'_{323} + \lambda_3^3 B'_{333} + \kappa_3\lambda_3[\mathbf{B}'_{12}\mathbf{B}'_{33} + \mathbf{B}'_{23}(2\mathbf{B}'_{22} + 3\mathbf{B}'_{13})], \\
\kappa_3\mathbf{B}'_{223} &= \kappa_3^2 B'_{223} + \kappa_3\lambda_3(B'_{233} + B'_{323}) + \lambda_3^2 B'_{333} + 2\kappa_3\lambda_3[2\mathbf{B}'^2_{23} + \mathbf{B}'_{22}\mathbf{B}'_{33}], \\
\kappa_3\mathbf{B}'_{313} &= \kappa_3^2 B'_{313} + 2\kappa_3\lambda_3 B'_{323} + \lambda_3^2 B'_{333} + 2\kappa_5\lambda_3(\mathbf{B}'^2_{23} + 2\mathbf{B}'_{13}\mathbf{B}'_{33}), \\
\kappa_3\mathbf{B}'_{322} &= \kappa_3^2 B'_{322} + 2\kappa_3\lambda_3 B'_{323} + \lambda_3^2 B'_{333} + 2\kappa_3\lambda_3(2\mathbf{B}'^2_{23} + \mathbf{B}'_{22}\mathbf{B}'_{33}), \\
\kappa_3\mathbf{B}'_{233} &= \kappa_3 B'_{233} + \lambda_3 B'_{333} + 6\kappa_3\lambda_3\mathbf{B}'_{23}\mathbf{B}'_{33}, \\
\kappa_3\mathbf{B}'_{323} &= \kappa_3 B'_{323} + \lambda_3 B'_{333} + 6\kappa_3\lambda_3\mathbf{B}'_{23}\mathbf{B}'_{32}, \\
\kappa_3\mathbf{B}'_{333} &= B'_{333} + 6\kappa_3\lambda_3\mathbf{B}'^2_{33}.
\end{aligned} \qquad \text{(III,15)}$$

From (III,15) we can obtain formulas for the change of our image coefficients. We have only to substitute (I,29) in (III,15), which gives

$$\begin{aligned}
\kappa_3\mathbf{C}'_{112} &= \kappa_3^5 C'_{112} + \kappa_3^4\lambda_3(3C'_{122} + C'_{113}) + 2\kappa_3^3\lambda_3^2(3C'_{123} + 2C'_{222}) + 2\kappa_3^2\lambda_3^3(C'_{133} + 4C'_{223}) \\
&\quad + 5\kappa_3\lambda_3^4 C'_{233} + \lambda_3^5 C'_{333} + 2\kappa_3\lambda_3\mathbf{B}'_{12}(\mathbf{B}'_{13} + 2\mathbf{B}'_{22}), \\
\kappa_3\mathbf{C}'_{122} &= \kappa_3^4 C'_{122} + 2\kappa_3^3\lambda_3(C'_{123} + C'_{222}) + \kappa_3^2\lambda_3^2(C'_{133} + 5C'_{223}) + 4\kappa_3\lambda_3^3 C'_{223} + \lambda_3^4 C'_{333} \\
&\quad + 2\kappa_3\lambda_3[\mathbf{B}'_{12}\mathbf{B}'_{23} + \mathbf{B}'_{22}(\mathbf{B}'_{13} + \mathbf{B}'_{22})], \\
\kappa_3\mathbf{C}'_{113} &= \kappa_3^4 C'_{113} + 4\kappa_3^3\lambda_3 C'_{123} + 2\kappa_3^2\lambda_3^2(C'_{133} + 2C'_{223}) + 4\kappa_3\lambda_3^3 C'_{233} + \lambda_3^4 C'_{333} \\
&\quad + 2\kappa_3\lambda_3[\mathbf{B}'^2_{13} + 2\mathbf{B}'_{12}\mathbf{B}'_{23}], \\
\kappa_3\mathbf{C}'_{123} &= \kappa_3^3 C'_{123} + \kappa_3^2\lambda_3(2C'_{223} + C'_{133}) + 3\kappa_3\lambda_3^2 C'_{233} + \lambda_3^3 C'_{333} + \kappa_3\lambda_3[\mathbf{B}'_{12}\mathbf{B}'_{33} + \mathbf{B}'_{23}(3\mathbf{B}'_{13} + 2\mathbf{B}'_{22})], \\
\kappa_3\mathbf{C}'_{222} &= \kappa_3^3 C'_{222} + 3\kappa_3^2\lambda_3 C'_{223} + 3\kappa_3\lambda_3^2 C'_{233} + \lambda_3^3 C'_{333} + 6\kappa_3\lambda_3\mathbf{B}'_{22}\mathbf{B}'_{23}, \\
\kappa_3\mathbf{C}'_{133} &= \kappa_3^2 C'_{133} + 2\kappa_3\lambda_3 C'_{233} + \lambda_3^2 C'_{333} + 2\kappa_3\lambda_3[\mathbf{B}'^2_{23} + 2\mathbf{B}'_{13}\mathbf{B}'_{33}], \\
\kappa_3\mathbf{C}'_{223} &= \kappa_3^2 C'_{223} + 2\kappa_3\lambda_3 C'_{233} + \lambda_3^2 C'_{333} + 2\kappa_3\lambda_3[2\mathbf{B}'^2_{23} + \mathbf{B}'_{22}\mathbf{B}'_{33}], \\
\kappa_3\mathbf{C}'_{233} &= \kappa_3 C'_{233} + \lambda_3 C'_{333} + 6\kappa_3\lambda_3\mathbf{B}'_{23}\mathbf{B}'_{33}, \\
\kappa_3\mathbf{C}'_{333} &= C'_{333} + 6\kappa_3\lambda_3\mathbf{B}'^2_{33}.
\end{aligned} \qquad \text{(III,16)}$$

Let us now investigate how the image errors change if we shift the object. Let us designate the magnitudes for a changed object by a boldface italic letter.

Corresponding to (III,4) we have

$$x_1 = \kappa_1 \boldsymbol{x}_1 - \lambda_1 \Xi_1, \quad x'_3 = \kappa_1 \boldsymbol{x}_3. \tag{III,17}$$

In the first order we find

$$-\Xi_1 = B_1 x_1 + x'_3 = \boldsymbol{B}_1 \boldsymbol{x}_1 + \boldsymbol{x}_3, \quad \Xi_3 = x_1 + B'_3 x'_3 = \boldsymbol{x}_1 + \boldsymbol{B}_3 \boldsymbol{x}_3, \tag{III,18}$$

and

$$\begin{matrix} x_1 \\ x_3 \end{matrix} = \begin{matrix} (\kappa_1 + \lambda_1 \boldsymbol{B}_1) \boldsymbol{x}_1 + \lambda_1 \boldsymbol{x}_3, \\ \kappa_1 \boldsymbol{x}_3. \end{matrix} \tag{III,19}$$

Substituting (II,19) in (II,18) and comparing them member by member, we obtain

$$\boldsymbol{B}_1 = B_1, \quad \kappa_1 + \lambda_1 B_1 = 1, \quad \lambda_1 + \kappa_1 B'_3 = \boldsymbol{B}_3, \tag{III,20}$$

or

$$\kappa_1 = \frac{1 - B_1 \boldsymbol{B}_3}{1 - B_1 B'_3}, \quad \lambda_1 = \frac{\boldsymbol{B}_3 - B'_3}{1 - B_1 B'_3}. \tag{III,21}$$

Substituting (III,20) in (III,17) we have

$$x_1 = \boldsymbol{x}_1 + \lambda_1 \boldsymbol{x}_3 + \lambda_1 (\boldsymbol{B}_{1i} \boldsymbol{u}_i + \tfrac{1}{2} \boldsymbol{B}_{1i\kappa} \boldsymbol{u}_i \boldsymbol{u}_\kappa) \boldsymbol{x}_1 + \lambda_1 (\boldsymbol{B}_{2i} \boldsymbol{u}_i + \tfrac{1}{2} \boldsymbol{B}_{2i\kappa} \boldsymbol{u}_i \boldsymbol{u}_\kappa) \boldsymbol{x}_3 \tag{III,22}$$

and

$$x'_3 = \kappa_1 \boldsymbol{x}_3.$$

We now insert (III,22) into

$$\begin{aligned} -\Xi_1 &= (B_1 + B_{1i} u_i + \tfrac{1}{2} B_{1i\kappa} u_i u_\kappa) x_1 + (1 + B_{2i} u_i + \tfrac{1}{2} B_{2i\kappa} u_i u_\kappa) x'_3 \\ &= (\boldsymbol{B}_1 + \boldsymbol{B}_{1i} \boldsymbol{u}_i + \tfrac{1}{2} \boldsymbol{B}_{1i\kappa} \boldsymbol{u}_i \boldsymbol{u}_\kappa) \boldsymbol{x}_1 + (1 + \boldsymbol{B}_{2i} \boldsymbol{u}_i + \tfrac{1}{2} \boldsymbol{B}_{2i\kappa} \boldsymbol{u}_i \boldsymbol{u}_\kappa) \boldsymbol{x}_3, \end{aligned} \tag{III,23}$$

$$\begin{aligned} \kappa_1 \boldsymbol{B}'_{12} &= \kappa_1 B'_{12} + \lambda_1 B_{11}, \\ \kappa_1 \boldsymbol{B}'_{13} &= \kappa_1^2 B'_{13} + \kappa_1 \lambda_1 (2B'_{12} - \alpha_3) + \lambda_1^2 B_{11}, \\ \kappa_1 \boldsymbol{B}'_{22} &= \kappa_1^2 B'_{22} + \kappa_1 \lambda_1 (2B'_{12} - \alpha_3) + \lambda_1^2 B_{11}, \\ \kappa_1 \boldsymbol{B}'_{23} &= \kappa_1^3 B'_{23} + \kappa_1^2 \lambda_1 (B'_{13} + 2B'_{22} - \alpha_2) + \kappa_1 \lambda_1^2 (3B'_{12} - 2\alpha_1) + \lambda_1^3 B_{11}, \\ \kappa_1 \boldsymbol{B}'_{33} &= \kappa_1^4 B'_{33} + \kappa_1^3 \lambda_1 (4B'_{23} - \alpha_1) + \kappa_1^2 \lambda_1^2 [2(2B'_{22} + B'_{13}) - 3\alpha_2] + \kappa_1 \lambda_1^5 (4B'_{12} - 3\alpha_1) + \lambda_1^4 B_{11}. \end{aligned} \tag{III,24}$$

We see that the third-order errors for another object point can be found if we know the third-order members for the given point and in addition B_{11}, the spherical aberration of the exit pupil.

In the same way, by comparing the fifth-order members of (III,23), we get from Ξ_1 and Ξ_3 the following equations (III,25) and (III,26), respectively, for our fifth-order errors:

$$\begin{aligned} \kappa_1 \boldsymbol{B}_{111} &= B_{111} + 6\kappa_1 \lambda_1 \boldsymbol{B}_{11}^2, \\ \kappa_1 \boldsymbol{B}_{112} &= \kappa_1 B_{112} + \lambda_1 B_{111} + 6\kappa_1 \lambda_1 \boldsymbol{B}_{11} \boldsymbol{B}_{12}, \\ \kappa_1 \boldsymbol{B}_{211} &= \kappa_1 B_{211} + \lambda_1 B_{111} + 6\kappa_1 \lambda_1 \boldsymbol{B}_{11} \boldsymbol{B}_{12}, \\ \kappa_1 \boldsymbol{B}_{113} &= \kappa_1^2 B_{113} + 2\kappa_1 \lambda_1 B_{112} + \lambda_1^2 B_{111} + \kappa_1 \lambda_1 (4\boldsymbol{B}_{11} \boldsymbol{B}_{13} + 2\boldsymbol{B}_{12}^2), \\ \kappa_1 \boldsymbol{B}_{122} &= \kappa_1^2 B_{122} + 2\kappa_1 \lambda_1 B_{112} + \lambda_1^2 B_{111} + \kappa_1 \lambda_1 (2\boldsymbol{B}_{11} \boldsymbol{B}_{22} + 4\boldsymbol{B}_{12}^2), \\ \kappa_1 \boldsymbol{B}_{212} &= \kappa_1^2 B_{212} + \kappa_1 \lambda_1 (B_{211} + B_{112}) + \lambda_1^2 B_{111} + \kappa_1 \lambda_1 (2\boldsymbol{B}_{11} \boldsymbol{B}_{22} + 4\boldsymbol{B}_{12}^2), \\ \kappa_1 \boldsymbol{B}_{123} &= \kappa_1^3 B_{123} + \kappa_1^2 \lambda_1 (B_{113} + 2B_{112}) + 3\kappa_1 \lambda_1^2 B_{112} + \lambda_1^3 B_{111} + \kappa_1 \lambda_1 [\boldsymbol{B}_{11} B_{23} + \boldsymbol{B}_{12} (3\boldsymbol{B}_{13} + 2\boldsymbol{B}_{22})], \\ \kappa_1 \boldsymbol{B}_{213} &= \kappa_1^3 B_{213} + \kappa_1^2 \lambda_1 (B_{113} + 2B_{212}) + \kappa_1 \lambda_1^2 (B_{211} + 2B_{112}) + \lambda_1^3 B_{111} + \kappa_1 \lambda_1 [\boldsymbol{B}_{11} \boldsymbol{B}_{23} + \boldsymbol{B}_{12} (3\boldsymbol{B}_{13} + 2\boldsymbol{B}_{22})], \\ \kappa_1 \boldsymbol{B}_{222} &= \kappa_1^3 B_{222} + \kappa_1^2 \lambda_1 (B_{122} + 2B_{212}) + \kappa_1 \lambda_1^2 (B_{211} + 2B_{112}) + \lambda_1^3 B_{111} + 6\kappa_1 \lambda_1 \boldsymbol{B}_{12} \boldsymbol{B}_{22}, \\ \kappa_1 \boldsymbol{B}_{133} &= \kappa_1^4 B_{133} + 4\kappa_1^3 \lambda_1 B_{123} + 2\kappa_1^2 \lambda_1^2 (B_{113} + 2B_{122}) + 4\kappa_1 \lambda_1^3 B_{112} + \lambda_1^4 B_{111} + \kappa_1 \lambda_1 [2\boldsymbol{B}_{13}^2 + 4\boldsymbol{B}_{12} \boldsymbol{B}_{23}], \\ \kappa_1 \boldsymbol{B}_{223} &= \kappa_1^4 B_{223} + \kappa_1^3 \lambda_1 (2B_{222} + B_{213} + B_{123}) + \kappa_1^2 \lambda_1^2 (3B_{212} + 2B_{122} + B_{113}) + \kappa_1 \lambda_1^3 (B_{211} + 3B_{112}) \\ &\qquad + \lambda_1^4 B_{111} + 2\kappa_1 \lambda_1 [\boldsymbol{B}_{12} \boldsymbol{B}_{23} + \boldsymbol{B}_{22} (\boldsymbol{B}_{13} + \boldsymbol{B}_{22})], \\ \kappa_1 \boldsymbol{B}_{233} &= \kappa_1^5 B_{233} + \kappa_1^4 \lambda_1 (4B_{223} + B_{133}) + \kappa_1^3 \lambda_1^2 (4B_{222} + 2B_{213} + 4B_{123}) + \kappa_1^2 \lambda_1^3 (4B_{112} + 4B_{122} + 2B_{113}) \\ &\qquad + \kappa_1 \lambda_1^4 (B_{211} + 4B_{112}) + \lambda_1^5 B_{111} + 2\kappa_1 \lambda_1 \boldsymbol{B}_{23} (\boldsymbol{B}_{13} + 2\boldsymbol{B}_{22}) \end{aligned} \tag{III,25}$$

and

$$
\begin{aligned}
B'_{211} &= \lambda_1 B_{111} + B'_{211} + 6\lambda_1 B'_{12} B_{11},\\
B'_{212} &= \lambda_1 B_{112} + \lambda_1 B'_{211} + \kappa_1 B'_{212} + 2\lambda_1 B_{11}(\kappa_1 B'_{22} + \lambda_1 B'_{12}) + 4\lambda_1 B_{12} B'_{12},\\
B'_{311} &= \lambda_1 B_{211} + \lambda_1 B'_{211} + \kappa_1 B'_{311} + 4\lambda_1 B_{11}(\kappa_1 B'_{13} + \lambda_1 B'_{12}) + 2\lambda_1 B_{12} B'_{12},\\
B'_{213} &= \lambda_1 B_{113} + \lambda_1{}^2 B'_{211} + 2\kappa_1\lambda_1 B'_{212} + \kappa_1{}^2 B'_{213} + \lambda_1 B_{11}(\kappa_1{}^2 B'_{23} + 2\kappa_1\lambda_1 B'_{22} + \lambda_1{}^2 B'_{12})\\
&\qquad + 2\lambda_1 B_{12}(\kappa_1 B'_{22} + \lambda_1 B'_{12}) + 3\lambda_1 B_{13} B'_{12},\\
B'_{222} &= \lambda_1 B_{122} + \lambda_1{}^2 B'_{211} + 2\kappa_1\lambda_1 B'_{212} + \kappa_1{}^2 B'_{222} + 4\lambda_1 B_{12}(\kappa_1 B'_{22} + \lambda_1 B'_{12}) + 2\lambda_1 B_{22} B'_{12},\\
B'_{312} &= \lambda_1 B_{212} + \lambda_1{}^2 B'_{211} + \kappa_1\lambda_1(B'_{212} + B'_{311}) + \kappa_1{}^2 B'_{312} + \lambda_1 B_{11}[\kappa_1{}^2 B'_{23} + \kappa_1\lambda_1(B'_{13} + B'_{22}) + \lambda_1{}^2 B'_{12}]\\
&\qquad + \lambda_1 B_{12}[\kappa_1(3B'_{13} + B'_{22}) + 4\lambda_1 B'_{12}] + \lambda_1 B_{22} B'_{12},\\
B'_{223} &= \lambda_1 B_{123} + \lambda_1{}^3 B'_{211} + 3\kappa_1\lambda_1{}^2 B'_{212} + \kappa_1{}^2\lambda_1(B'_{213} + 2B'_{222}) + \kappa_1{}^3 B'_{223} + \lambda_1 B_{12}(\kappa_1{}^2 B'_{23} + 2\kappa_1\lambda_1 B'_{22}\\
&\qquad + \lambda_1{}^2 B'_{12}) + 2\lambda_1(B_{22} + B_{13})(\kappa_1 B'_{22} + \lambda_1 B'_{12}) + \lambda_1 B_{23} B'_{12}, \qquad \text{(III,26)}\\
B'_{313} &= \lambda_1 B_{213} + \lambda_1{}^3 B'_{211} + \kappa_1\lambda_1{}^2(2B'_{212} + B'_{311}) + \kappa_1{}^2\lambda_1(B'_{213} + 2B'_{312}) + \kappa_1{}^3 B'_{313}\\
&\qquad + \lambda_1 B_{12}[3\kappa_1{}^2 B'_{23} + 2\kappa_1\lambda_1(B'_{13} + 2B'_{22}) + 3\lambda_1{}^2 B'_{12}] + 2\lambda_1 B_{13}(\kappa_1 B'_{13} + \lambda_1 B'_{12}) + \lambda_1 B_{23} B'_{12},\\
B'_{322} &= \lambda_1 B_{222} + \lambda_1{}^3 B'_{211} + \kappa_1\lambda_1{}^2(2B'_{212} + B'_{311}) + \kappa_1{}^2\lambda_1(B'_{222} + 2B'_{312}) + \kappa_1{}^3 B'_{322}\\
&\qquad + 2\lambda_1 B_{12}[\kappa_1{}^2 B'_{23} + \kappa\lambda(B'_{13} + B'_{22}) + \lambda_1{}^2 B'_{12}] + 2\lambda_1 B_{22}[\kappa_1(B'_{13} + B'_{22}) + 2\lambda_1 B'_{12}],\\
B'_{233} &= \lambda_1 B_{133} + \lambda_1{}^4 B'_{211} + 4\kappa_1\lambda_1{}^3 B'_{212} + 2\kappa_1{}^2\lambda_1{}^2(B'_{213} + 2B'_{222}) + 4\kappa_1{}^3\lambda_1 B'_{223} + \kappa_1{}^4 B'_{233}\\
&\qquad + 2\lambda_1 B_{13}(\kappa_1{}^2 B'_{23} + 2\kappa_1\lambda_1 B'_{22} + \lambda_1{}^2 B'_{12}) + 4\lambda_1 B_{23}(\kappa_1 B'_{22} + \lambda_1 B'_{12}),\\
B'_{323} &= \lambda_1 B_{223} + \lambda_1{}^4 B'_{211} + \kappa_1\lambda_1{}^3(3B'_{212} + B'_{311}) + \kappa_1{}^2\lambda_1{}^2(B'_{213} + 2B'_{222} + 3B'_{312})\\
&\qquad + \kappa_1{}^3\lambda_1(B'_{223} + B'_{313} + 2B'_{322}) + \kappa_1{}^4 B'_{323} + \lambda_1 B_{22}[3\kappa_1{}^2 B'_{23} + 2\kappa_1\lambda_1(B'_{13} + 2B'_{22}) + 3\lambda_1{}^2 B'_{12}]\\
&\qquad + \lambda_1 B_{23}[\kappa_1(B'_{13} + B'_{22}) + 2\lambda_1 B'_{12}] + \lambda_1 B_{13}[\kappa_1{}^2 B'_{23} + \kappa_1\lambda_1(B'_{13} + B'_{22}) + \lambda_1{}^2 B'_{12}],\\
B'_{333} &= \lambda_1 B_{233} + \lambda_1{}^5 B'_{211} + \lambda_1{}^4\kappa_1(4B'_{212} + B'_{311}) + 2\kappa_1{}^2\lambda_1{}^3(2B'_{232} + B'_{213} + 2B'_{312})\\
&\qquad + 2\kappa_1{}^3\lambda_1{}^2(2B'_{223} + B'_{313} + 2B'_{322}) + \kappa_1{}^4\lambda_1(B'_{233} + 4B'_{322}) + \kappa_1{}^5 B'_{333}\\
&\qquad + 2\lambda_1 B_{23}[3\kappa_1{}^2 B'_{23} + 2\kappa_1\lambda_1(B'_{13} + 2B'_{22}) + 3\lambda_1{}^2 B'_{12}].
\end{aligned}
$$

If we combine (III,25) and (III,26), we have finally

$$
\begin{aligned}
\kappa_1 B'_{211} &= \kappa_1 B'_{211} + \lambda_1 B_{111} + 6\kappa_1\lambda_1 B_{11} B'_{12},\\
\kappa_1 B'_{212} &= \kappa_1{}^2 B'_{212} + \kappa_1\lambda_1(B'_{211} + B_{112}) + \lambda_1{}^2 B_{111} + 2\kappa_1\lambda_1[B_{11} B'_{22} + 2B_{12} B'_{12}],\\
\kappa_1 B'_{311} &= \kappa_1{}^2 B'_{311} + \kappa_1\lambda_1(B'_{211} + B_{211}) + \lambda_1{}^2 B_{111} + 2\kappa_1\lambda_1[2B_{11} B'_{13} + B_{12} B'_{12}],\\
\kappa_1 B'_{213} &= \kappa_1{}^3 B'_{213} + \kappa_1{}^2\lambda_1(B_{113} + 2B'_{212}) + \kappa_1\lambda_1{}^2(2B_{112} + B'_{211}) + \lambda_1{}^3 B_{111}\\
&\qquad + \kappa_1\lambda_1[B_{11} B'_{23} + 2B_{12} B'_{22} + 3B_{13} B'_{12}],\\
\kappa_1 B'_{222} &= \kappa_1{}^3 B'_{222} + \kappa_1{}^2\lambda_1(B_{122} + 2B'_{212}) + \kappa_1\lambda_1{}^2(2B_{112} + B'_{211}) + \lambda_1{}^3 B_{111} + 2\kappa_1\lambda_1[2B_{12} B'_{22} + B_{22} B'_{12}],\\
\kappa_1 B'_{312} &= \kappa_1{}^3 B'_{312} + \kappa_1{}^2\lambda_1(B_{212} + B'_{212} + B'_{311}) + \kappa_1\lambda_1{}^2(B_{211} + B_{112} + B'_{211}) + \lambda_1{}^3 B_{111}\\
&\qquad + \kappa_1\lambda_1[B_{11} B'_{23} + B_{12}(B'_{22} + 3B'_{13}) + B_{22} B'_{12}],\\
\kappa_1 B'_{223} &= \kappa_1{}^4 B'_{223} + \kappa_1{}^3\lambda_1(B_{123} + 2B'_{222} + B'_{213}) + \kappa_1{}^2\lambda_1{}^2(2B_{122} + B_{113} + 3B'_{212})\\
&\qquad + \kappa_1\lambda_1{}^3(3B_{112} + B'_{211}) + \lambda_1{}^4 B_{111} + \kappa_1\lambda_1[B_{12} B'_{23} + 2(B_{13} + B_{22}) B'_{22} + B_{23} B'_{12}],\\
\kappa_1 B'_{313} &= \kappa_1{}^4 B'_{313} + \kappa_1{}^3\lambda_1(B_{213} + B'_{213} + 2B'_{312}) + \kappa_1{}^2\lambda_1{}^2(2B_{212} + 2B'_{212} + B_{113} + B'_{311})\\
&\qquad + \kappa_1\lambda_1{}^3(2B_{112} + B_{211} + B'_{211}) + \lambda_1{}^4 B_{111} + \kappa_1\lambda_1[3B_{12} B'_{23} + 2B_{13} B'_{13} + B_{23} B'_{12}],\\
\kappa_1 B'_{322} &= \kappa_1{}^4 B'_{322} + \kappa_1{}^3\lambda_1(B_{222} + B'_{222} + 2B'_{312}) + \kappa_1{}^2\lambda_1{}^2(B_{122} + 2B_{212} + 2B'_{212} + B'_{311})\\
&\qquad + \kappa_1\lambda_1{}^3(2B_{112} + B_{211} + B'_{211}) + \lambda_1{}^4 B_{111} + 2\kappa_1\lambda_1[B_{12} B'_{23} + B_{22}(B'_{13} + B'_{22})], \qquad \text{(III,27)}\\
\kappa_1 B'_{233} &= \kappa_1{}^5 B'_{233} + \kappa_1{}^4\lambda_1(B_{133} + 4B'_{223}) + \kappa_1{}^3\lambda_1{}^2(4B_{123} + 2B'_{213} + 4B'_{222}) + \kappa_1{}^2\lambda_1{}^3(4B_{122} + 2B_{113} + 4B'_{212})\\
&\qquad + \kappa_1\lambda_1{}^4(4B_{112} + B'_{211}) + \lambda_1{}^5 B_{111} + 2\kappa_1\lambda_1[B_{13} B'_{23} + 2B_{23} B'_{22}],\\
\kappa_1 B'_{323} &= \kappa_1{}^5 B'_{323} + \kappa_1{}^4\lambda_1(B_{223} + B'_{223} + B'_{313} + 2B'_{322}) + \kappa_1{}^3\lambda_1{}^2(B_{123} + 2B_{222} + B_{213} + B'_{213} + 2B'_{222} + 3B'_{312})\\
&\qquad + \kappa_1{}^2\lambda_1{}^3(B_{113} + 2B_{122} + 3B_{212} + 3B'_{212} + B'_{311}) + \kappa_1\lambda_1{}^4(3B_{112} + B_{211} + B'_{211})\\
&\qquad + \lambda_1{}^5 B_{111} + \kappa_1\lambda_1[B_{13} B'_{23} + 3B_{22} B'_{23} + B_{23}(B'_{13} + B'_{22})],\\
\kappa_1 B'_{333} &= \kappa_1{}^6 B'_{333} + \kappa_1{}^5\lambda_1(B_{233} + B'_{233} + 4B'_{323}) + \kappa_1{}^4\lambda_1{}^2(B_{133} + 4B_{223} + 4B'_{223} + 2B'_{313} + 4B'_{322})\\
&\qquad + 2\kappa_1{}^3\lambda_1{}^3(2B_{123} + B_{213} + 2B_{222} + B'_{213} + 2B'_{222} + 2B'_{312}) + \kappa_1{}^2\lambda_1{}^4(4B_{122} + 2B_{113} + 4B_{212}\\
&\qquad + 4B'_{212} + B'_{311}) + \kappa_1\lambda_1{}^5(4B_{112} + B_{211} + B'_{211}) + \lambda_1{}^6 B_{111} + 6\kappa_1\lambda_1 B_{23} B'_{23}.
\end{aligned}
$$

We could try here to substitute for all the $B_{i\kappa\lambda}$ the $B'_{i\kappa\lambda}$'s, but the connections become a little clearer if we consider besides the change of the image errors, the change of the image coefficients

$C_{i\varkappa\lambda}$. Substitution of (I,28) and (I,29) and consideration of (III,24) give now, if we replace the $C_{i\varkappa\lambda}$, according to (I,31)

$$
\begin{aligned}
\kappa_1 \boldsymbol{C}'_{112} &= \kappa_1 C'_{112} + \lambda_1 C_{111} + 6\kappa_1\lambda_1 \boldsymbol{B}_{11}\boldsymbol{B}_{12},\\
\kappa_1 \boldsymbol{C}'_{113} &= \kappa_1^2 C'_{113} + \kappa_1\lambda_1(2C'_{112} - \gamma_5) + \lambda_1^2 C_{111} + 2\kappa_1\lambda_1(\boldsymbol{B}_{12}^2 + 2\boldsymbol{B}_{11}\boldsymbol{B}_{13}),\\
\kappa_1 \boldsymbol{C}'_{122} &= \kappa_1^2 C'_{122} + \kappa_1\lambda_1(2C'_{112} - \gamma_5) + \lambda_1^2 C_{111} + 2\kappa_1\lambda_1(2\boldsymbol{B}_{12}^2 + \boldsymbol{B}_{11}\boldsymbol{B}_{22}),\\
\kappa_1 \boldsymbol{C}'_{123} &= \kappa_1^3 C'_{123} + \kappa_1^2\lambda_1(C'_{113} + 2C'_{122} - \gamma_4) + \kappa_1\lambda_1^2(3C'_{112} - 2\gamma_5) + \lambda_1^3 C_{111}\\
&\qquad + \kappa_1\lambda_1[\boldsymbol{B}_{11}\boldsymbol{B}_{23} + \boldsymbol{B}_{12}(3\boldsymbol{B}_{13} + 2\boldsymbol{B}_{22})],\\
\kappa_1 \boldsymbol{C}'_{222} &= \kappa_1^3 C'_{222} + \kappa_1^2\lambda_1(3C'_{122} - \gamma_4) + \kappa_1\lambda_1^2(3C'_{112} - 2\gamma_5) + \lambda_1^3 C_{111} + 6\kappa_1\lambda_1 \boldsymbol{B}_{12}\boldsymbol{B}_{22},\\
\kappa_1 \boldsymbol{C}'_{133} &= \kappa_1^4 C'_{133} + \kappa_1^3\lambda_1(4C'_{123} - \gamma_3) + \kappa_1^2\lambda_1^2(2C'_{113} + 4C'_{122} - 3\gamma_4) + \kappa_1\lambda_1^3(4C'_{112} - 3\gamma_5) + \lambda_1^4 C_{111}\\
&\qquad + 2\kappa_1\lambda_1(\boldsymbol{B}_{13}^2 + 2\boldsymbol{B}_{12}\boldsymbol{B}_{23}), \qquad \text{(III,28)}\\
\kappa_1 \boldsymbol{C}'_{223} &= \kappa_1^4 C'_{223} + \kappa_1^3\lambda_1(2C'_{123} + 2C'_{222} - \gamma_3) + \kappa_1^2\lambda_1^2(C'_{113} + 5C'_{122} - 3\gamma_4)\\
&\qquad + \kappa_1\lambda_1^3(4C'_{112} - 3\gamma_5) + \lambda_1^4 C_{111} + 2\kappa_1\lambda_1[\boldsymbol{B}_{12}\boldsymbol{B}_{23} + \boldsymbol{B}_{22}(\boldsymbol{B}_{13} + \boldsymbol{B}_{22})],\\
\kappa_1 \boldsymbol{C}'_{233} &= \kappa_1^5 C'_{233} + \kappa_1^4\lambda_1(4C'_{223} + C'_{133} - \gamma_2) + \kappa_1^3\lambda_1^2(8C_{123} + 4C'_{222} - 6\gamma_3)\\
&\qquad + \kappa_1^2\lambda_1^3(2C'_{113} + 8C'_{122} - 6\gamma_4) + \kappa_1\lambda_1^4(5C'_{112} - 4\gamma_5) + \lambda_1^5 C_{111} + 2\kappa_1\lambda_1 \boldsymbol{B}_{23}[\boldsymbol{B}_{13} + 2\boldsymbol{B}_{22}],\\
\kappa_1 \boldsymbol{C}'_{333} &= \kappa_1^6 C'_{333} + \kappa_1^5\lambda_1(6C'_{233} - \gamma_1) + \kappa_1^4\lambda_1^2(12C'_{223} + 3C'_{133} - 5\gamma_2)\\
&\qquad + \kappa_1^3\lambda_1^3(12C'_{123} + 8C'_{222} - 10\gamma_3) + \kappa_1^2\lambda_1^4(12C'_{122} + 3C'_{113} - 10\gamma_4)\\
&\qquad + \kappa_1\lambda_1^5(6C'_{112} - 5\gamma_5) + \lambda_1^6 C_{111} + 6\kappa_1\lambda_1 \boldsymbol{B}_{23}^2.
\end{aligned}
$$

Now we have formulas which allow us to calculate the image errors for every object and stop, if we know the image errors for a given object and stop, and the values B_{11}, and B_{111} or C_{111}. In a similar way, we can calculate from them the image errors for an object situated on the image side. We then have only to investigate $B_{i\varkappa\lambda}$ instead of $B'_{i\varkappa\lambda}$.

The formulas above do not cover the important case when the object is at infinity (photographic objective). It is, however, easy to develop the corresponding theory if we take into account the fact that we must start with the mixed characteristic and replace everywhere ξ by Ξ.

In a second paper we shall discuss the separate groups of image errors, show their geometrical significance, and investigate the properties of systems where one or all of the image errors are corrected for the maximum number of object points.